1-1-2011

Pamam dendrimer-based therapeutic and diagnostic nanodevices

Admira Bosnjakovic
Wayne State University,

PAMAM DENDRIMER-BASED THERAPEUTIC AND DIAGNOSTIC NANODEVICES

by

ADMIRA BOSNJAKOVIC

DISSERTATION

Submitted to Graduate School

of Wayne State University,

Detroit, Michigan

in partial fulfillment of the requirements

for the degree of

DOCTOR OF PHILOSOPHY

2011

MAJOR: MATERIALS SCIENCE AND
ENGINEERING

Aproved by:

_____
Advisor   Date

_____

_____

_____

_____

DEDICATION

To my son Haris Tabaković.

ACKNOWLEDGEMENTS

TABLE OF CONTENTS

LIST OF TABLES

LIST OF FIGURES

CHAPTER 1 "DENDRIMER–BASED NANODEVICES"

1.1 Dendrimers in Nanomedicine: The Rationale

Due to their unique properties dendrimers have exceptional potential for the application in the emerging field of nanomedicine. The goal of nanomedicine is to control and manipulate biomacromolecular constructs and supramolecular assemblies such as proteins, DNA/RNA, viruses, cellular lipid bilayers, cellular receptor sites and antibody variable regions that are critical to living cells in order to improve the quality of human health. The nanotherapeutics and diagnostic devices will allow a deeper understanding of human life and illnesses such as cancer, cardiovascular disease, genetic disorders, and trauma.[1] Detection of a disease in its earliest stage is the ultimate goal.

Dendrimers are polymers having highly branched structures and globular shapes with the nanosize ranging from 2 to 10 nm. Due to their exceptional structural properties such as monodispersity, controllable size and structure, modifiable surface functionalities, and multivalency they have become prominent synthetic macromolecules in the field of biomedical science. Dendrimers are widely utilized as drug delivery systems, antiviral agents and magnetic resonance imaging contrast agents.[2-7] In the past decades dendrimers have been investigated as novel diagnostic nanodevices.[8,9] They have been utilized in dip-pen nanolithography,[10] DNA and protein arrays,[11,12] nanocatalyst-based electro-chemical immunosensor,[13] biosensor-based on dendrimer encapsulated Pt nanoparticles[14] and regenerable affinity biosensing surfaces.[15] Research in antibody-based diagnostics has been focused on improving the specificity and sensitivity of immunoassay techniques. The most important steps in the development of immunosensors are the immobilization of antibodies onto a substrate at high density with

uniform distribution, retaining their specific antigen-binding activities, maintaining accessibility to the antigens,[16] and minimizing nonspecific adsorptions of extraneous cellular proteins onto the modified surfaces, which can reduce the sensitivity during detection steps. Based on their properties, dendrimers could play an essential role in each of these steps. Dendrimers can form stable, dense, well-organized, and close-packed arrays on substrate surfaces and they have ability to incorporate multiple branch ends available for conjugation reactions.[8] Recently Kannan's group has reported a dendrimer based ELISA assay for IL-6 and IL-1β cytokines capture that are found in infected intraamniotic fluid.[17] The dendrimer modified plate provides assays with significantly enhanced sensitivity, lower nonspecific adsorption, and significantly higher detection limits compared to traditional ELISA.

Controlled delivery of drugs can sustain blood level of the drug over a long period of time, decrease side effects, and lead the drug through the body without degradation, increase drug solubility, and decrease dose. The functional surface groups on dendrimers can affect their physicochemical properties. It is known that these functional groups make dendrimers very hydrophilic and highly water soluble.[18] Drug molecules can be either encapsulated, complexed, or covalently attached to the dendrimers through their functional groups.[19,20] The most common covalently linkage of the drugs to surface functional groups of dendrimers can be achieved by a coupling reaction through the ester or amide bonds. If the drug does not have a reactive group, a spacer or linker molecules are very often used to provide the drug with reactive group, which is required for coupling reaction with dendrimer. These ester or amide bonds, can be cleaved either hydrolytically or enzymatically.[21] The drug release due to hydrolysis will be governed by the pH of the media and ester bonds are more liable towards the hydrolysis compared to amide bonds.[22]

The study has showed that ester linked conjugates in human plasma can be hydrolyzed by esterase enzymes, while amide bonds are relatively stable.[23,24] Disulfide bonds have also been demonstrated to be cleaved in the presence of intracellular glutathione (GSH).[25] Targeting ligands can be linked to the functional groups of dendrimers too, and used for targeted drug delivery.[20]

The key issues in the design of dendrimer-drug nanodevices include improving drug payload, overcoming cytotoxicity especially in the case of cationic dendrimers, understanding the mechanism and dynamics of intracellular transport, and engineering of the drug release at the appropriate tissue. This can be achieved by optimizing biodistrubution, passive targeting – mediated via EPR (enhanced permeability retention) effect involving organ-specific targeting, and active targeting – receptor-mediated cell-specific targeting involving receptor-specific targeting groups.[1,22] Cellular uptake of dendrimers is affected by their size, type and the charge of surface groups.[26,27] Although there has been a significant success of attaching a multiple drug molecules on dendrimers, optimal release of drugs is still a challenge. Presence or absence of linker can greatly affect the drug release from dendrimers.[21] High stability of the conjugate or release of the drug before reaching its target will make the dendrimer-drug-delivery system ineffective.

1.2 Introduction to Dendrimers

Dendrimers are well-defined polymeric macromolecules having nanometer size and unique properties. The structure of dendrimers consists of a repetitive sequence of monomers, called branching units (dendrons). These units are growing from a core in a radial iterative fashion giving rise to higher generations (Figure 1). Beside the branching units, dendrimers

always have core units, and surface groups located at their peripheries.[28] Due to controlled step by step synthesis dendrimers are nearly monodisperse architectures (polydispersity indexes close to 1),[29] in contrast to traditional polymers. One of the most attracting aspects reletad to dendrimers is that it is relatively easily to control their size, composition, and physicochemical properties in a very precise manner.
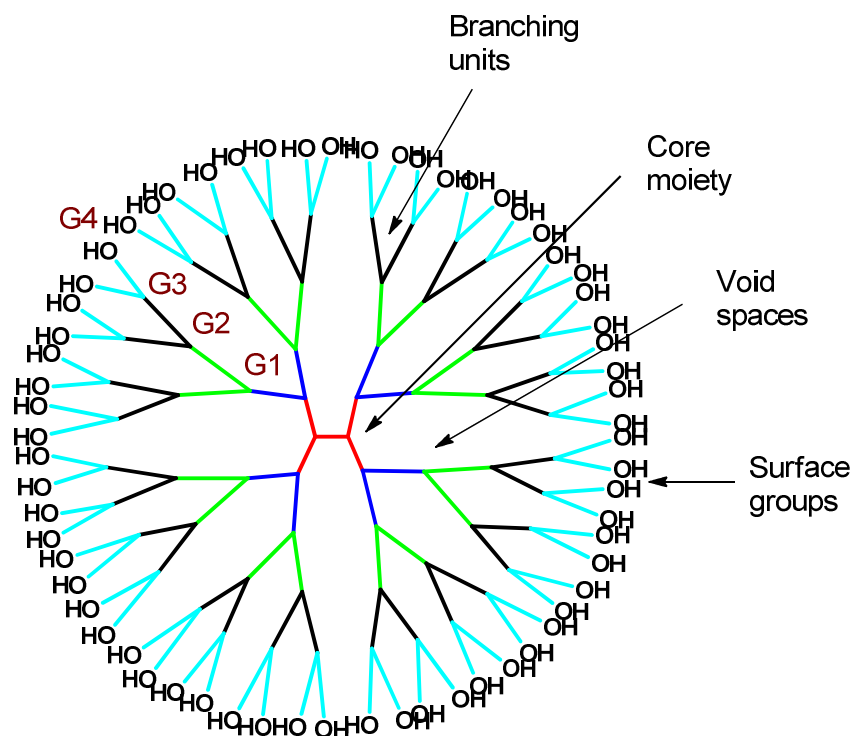
Figure 1. Schematic representation of generation four hydroxyl PAMAM dendrimer.

This type of molecules were first time synthesized by Vögtle in 1978 and called cascade.[30] The synthesis involves two steps; first step is an exhaustive Michael-type addition of acrylonitrile to an amine, and second step is reduction of nitrile groups to primary amines. These steps could be theoretically repeated to give highly branched macromolecules, but there are difficulties due to loss of substrate catalytic activity and poor yields. In early 1980s Denkewalter

and co-workers patented the synthesis of polylysine dendrimers.[31] Then in 1985, similar type of molecules were synthesized independently by Newkome and Tomalia groups.[32,33] Newkome named his molecules as arbosols, while Tomalia dendrimers, based on two greek words, 'dendros' meaning tree and 'meros' meaning part.

1.3 Synthesis of Dendrimers

There are two approaches for dendrimer synthesis. First approach is called divergent method that was developed by Tomalia. Tomalia synthesized poly(amidoamine) (PAMAM) dendrimers by this method, in which the growth of dendrimer starts from a core as the root and goes outward building up generation by generation. The second approach, developed by Hawker and Fréchet, is convergent method, which proceeds from the dendron surface inward to a reactive focal point at the root.

1.3.1 Divergent Method

The name of divergent method originates from the way how dendrimers grow starting from the core and going outwards, i.e. diverging into space (Figure 2). The synthesis consists of two steps: the core is reacted with two or more moles of reagent containing at least two protected branching sites, followed by removal of the protecting groups. The subsequent deprotected reactive sites lead to the zero generation dendrimers. This process can be repeated until the dendrimer with desired size and nuber of terminal groups is obtained. Usually ethylene diamine, ammonia, or cystamine may be used as cores.[34] relatively large dendrimers can be prepared using this method. However, the isolation and characterization can be hard due to incomplete growth steps and side reactions.
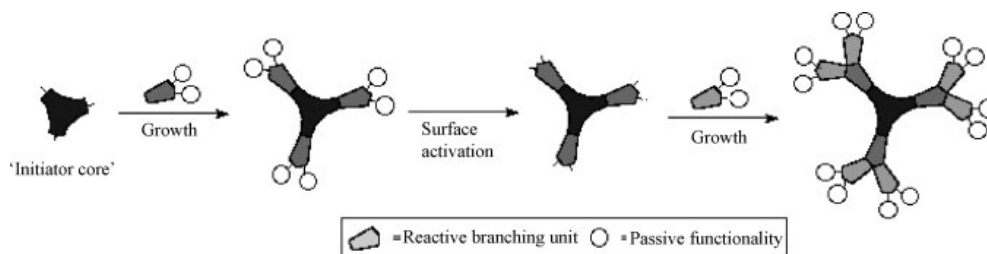
Figure 2. Dendrimer synthesis by divergent growth method [Adopted from Ref. 28]

1.3.2 Convergent Method

In response to the disadvantages of divergent method convergent method was developed by Hawker and Fréchet in 1990 (Figure 3).[35] The synthesis involves two steps: the first is a reiterative coupling of protected/deprotected branching units to obtain a focal point functionalized dendron and the second is the reaction of several dendrons leading to formation of dendrimer. Basically, the convergent growth starts at the surface of the dendrimer and proceeds inwards by progressively linking surface units with other monomers. When the growing blocks, called dendrons, are large enough, several of them are attached to an appropriate core to give a complete dendritic structure. Compared to divergent method the convergent method requires only two simultaneous reactions for any-adding step, it has lower number of side reactions and purification of dendrimers is simpler.
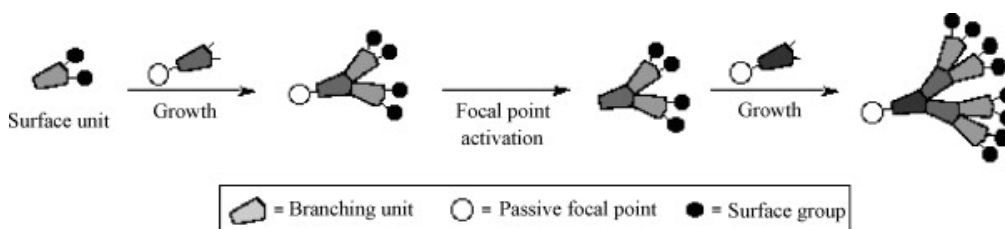
Figure 3. Dendrimer synthesis by convergent growth method [Adopted from Ref. 28]

1.4 Properties of Dendrimers

Dendrimers have crucial properties required for fabrication of the synthetic nanostructures with size, shape, surface chemistry similar to nanobiological constracts. They are nearly monodisperse, nanoscale size, well-defined molecular structures. Their size is similar to globular proteins. Generation 4 PAMAM dendrimer has size comparable to cytochrome c (4 nm), generation 5 PAMAM dendrimer has size comparable to hemoglobin (5 nm), and so on. Based on their systematic, dimensional length scaling, narrow size distribution, and biomimetic properties dendrimers are like 'artificial proteins'.[36] On the contrary to proteins, dendrimers are known to be robust, covalently fixed, three-dimensional structures possessing both solvent-filled interior hollowness and defined surface functionality.

Dendrimers are multivalent ligands due to presence of high number of reactive terminal groups. Dendritic scaffolds, compared to the other multivalent ligands such as polymers, proteins, and liposomes, exhibit advantageous controllable synthesis pathway. They have the ability of linking different chemical moieties on the surface, and in the interior. Dendrimer surface may be functionally designed to enhance or reduce *trans*-cellular, epithelial or vascular biopermeability. They also have a void space within the structure of the scaffold suitable for encapsulation of small-molecule drugs, metals (e.g. gold, silver) or signalling groups. These features make dendrimers ideal drug carriers with high drug payload capacities.[37] Complexation of the drug to the dendrimers can lead to enhanced permeation and retention (EPR) of the drug in the targeted sites.[1]

The properties of dendrimrs are tailored by the functional groups on their surface. They can be water-soluble when their end-groups are hydrophilic such as hydroxyl, amino, and carboxyl

groups as seen in PAMAM dendrimers. Dendrimer conformations are determined by dendrimer growth, the nature of building blocks, end-group functionalities, and the external environment.[29] Hydrogen bonding of terminal groups makes outer shell of dendrimers more rigid. Conforamtion of dendrimers stricktly depends on pH. At low pH (~3), all primary amine groups of PAMAM dendrimers are protonated leading to an extended conformation due to electrostatic repulsion between the positively charged NH_3^+ groups. At neutral pH back folding occurs which is due to the hydrogen bonding between the uncharged tertiary amines in the interior and the positively charged surface amines. At basic pH the dendrimer is completely neutralized and repulsive interactions between the wedges and end-groups reach a minimum leading to a conformation with a higher degree of back folding so dendrimer acquires a more spherical (globular) structure. The conformation of dendrimers is also affected by the polarity of the solvent as well as the ionic strength (high concentration of salts).[28]

In order to use dendrimers for drug design or as drug delivery devices *in vivo*, dendrimers have to be non-toxic, non-immunogenic (except for vaccines), and able to cross biobarriers (biopermeable) such as, the intestines, the blood–tissue barriers, cell membranes, and so on. They also have to be capable of staying in circulation for the time needed to target specific organs and exhibit clinical effects. The cytotoxicity of dendrimers is related to their size and surface groups which are directly interacting to cells' membrane. It has been reported that cationic dendrimers show heamolitic and cytotoxic effect at even relatively low concentration, while anionic and hydroxyl terminated dendrimers are not toxic. The studies showed that amino-terminated PAMAM dendrimers are weakly immunogenic, which can be eliminated by

pegylation with polyethylene glycol (PEG) chains. It also extends dendrimers lifetime in the blood stream compared to unmodified dendrimers.[38]

1.5 PAMAM Dendrimers

Polyamidoamine (PAMAM) dendrimers were synthesized by Tomalia.[33] They are known to be first commercialized dendrimers family, which are the most extensively characterized and widely used. PAMAM dendrimers have ethylene diamine (EDA) core and an amidoamine repeat branching structure. They are synthesized via Michael addition of amino groups of EDA with methyl acrylate, followed by amidation of the resulting esters with EDA, and generation 0 is formed (Figure 4). A repetition of these two synthetic steps adds another layer of branching units and produces next generation. The size of dendrimer grows linearly in diameter as a function of added generations, approximately 1 nm per generation (Table 1). Each new generation also doubles the number of terminal groups and approximately doubles the molecular weight of the previous generation. Figure 4 shows the synthesis of amine (NH_2) terminated PAMAM dendrimers that are cationic; however there are also neutral hydroxyl (OH) and anionic carboxyl (COOH) terminated PAMAM dendrimers. Due to half completion of the monomer addition the carboxyl terminated dendrimers are called half generations. These active terminal groups make dendrimers multivalent and they can be used to covalently attach several drug molecules, targeting groups, and other agent to the periphery of dendrimers in a well-defined manner. To avoid sterical hindrance and to provide drug with reactive group, a variety of spacer molecules can be linked to the drug and as such used for conjugation reaction with dendrimers. The presence of hydrophilic terminal groups makes dendrimers highly water soluble. The solubility

increases with the generation number; the higher generation, the higher number of terminal groups, leads to increased surface charge and polarity.
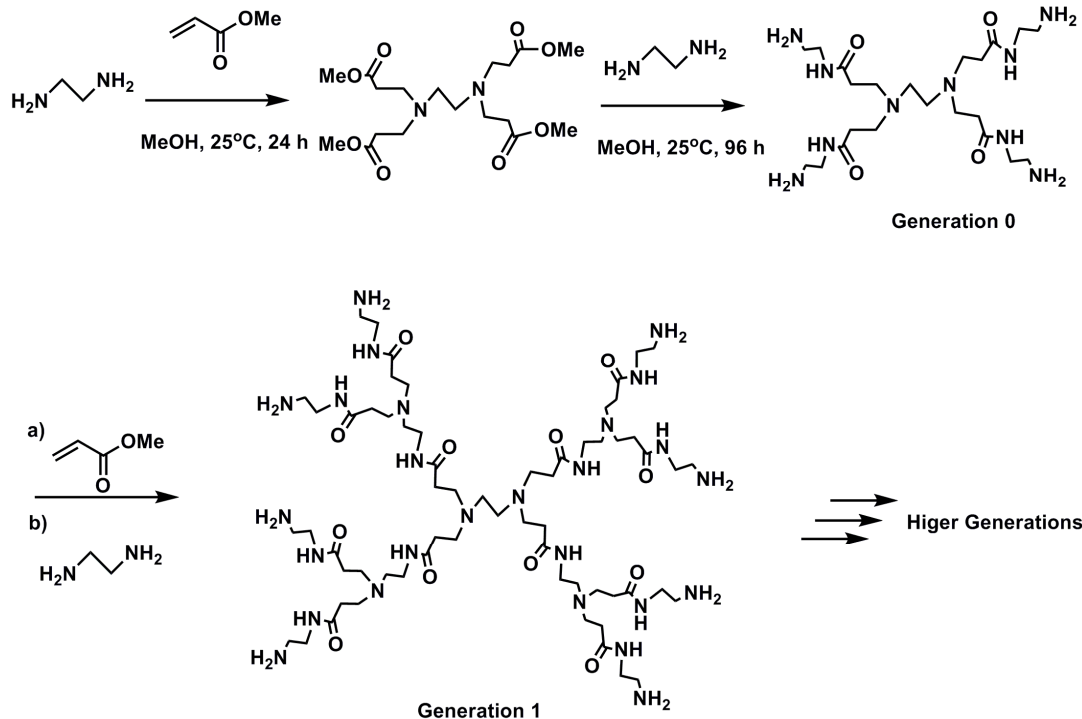
Figure 4. Synthesis of PAMAM dendrimer by Tomalia et al[33]

Table 1. Physicochemical characteristics of amine terminated PAMAM dendrimers

Generation	Number of surface groups	Molecular weight	Diameter (nm)
0	4	517	1.5
1	8	1,430	2.2
2	16	3,256	2.9
3	32	6,909	3.6
4	64	14,215	4.5
5	128	28,826	5.4
6	256	58,048	6.7
7	512	116,493	8.1
8	1024	233,383	9.7
9	2048	467,162	11.4
10	4096	934,720	13.5

1.6 Research Objectives

Over the past several decades, a great number of dendrimer structures with various chemical compositions have been developed and investigated for a variety of applications in physics, chemistry, biology, and medicine. Among them, poly(amidoamine) (PAMAM) dendrimers are the most extensively characterized and widely used. Even though many different surface end functionalities are available on these dendrimers, $-NH_2$, $-OH$, and $-COOH$ end groups are the most commonly studied. Of these, the hydroxyl-terminated ethylenediamine core generation 4 poly(amidoamine) dendrimers (G4-OH PAMAM) that are highly biocompatible, and have low protein interactions are explored here as vehicles for targeted intracellular drug delivery. The overall scientific goal of this research is to tailor the G4-OH PAMAM dendrimer surface, linking chemistry, and other physicochemical properties for enabling covalent linking with drugs, imaging agents and antibodies, to impact the improved functionality in the resultant nanodevices. Two specific goals are pursued: (1) development of G4-OH PAMAM dendrimer – drug nanodevices, and (2) development of G4-OH PAMAM dendrimer-based multipurpose novel diagnostic platforms. As mentioned dendrimers have multiple terminal functional groups available for further conjugation between dendrimer functionalities and guest molecules. The most common covalent linkages of the guest molecules to surface functional groups of dendrimers are ester or amide that are usually obtained by coupling reactions. Recently our group has been used disulfide bond to link the drug molecules to dendrimers.[25] In the case of the development of dendrimer-drug nanodevices choosing the right linkage and/or putting the proper spacer between the dendrimer and drug molecules the drug payload can be increased, the cytotoxicity especially in the case of cationic dendrimers will be avoided, and the drug will

release at the appropriate tissue. The development of dendrimer-based diagnostic nanodevices includes dendrimer-linked antibody assays. The design involves various linking chemistries between solid support and dendrimer, and between dendrimer and antibody such as amide, sulfide, and hydrazone bonds. Introducing the dendrimer as a spacer between antibody and solid support reduces non-specific interactions between immobilized antibody and analyte which will improve the detection limits.

In this thesis four chapters are discussed. In Chapter 1 an overview of dendrimers evolution and their role in nanomedicine is summarized. The synthesis, characterization, and *in vitro* study of dendrimer-Erythromycin (D-EM) nanodevice for *sustained* treatment of orthopedic inflammation are described in Chapter 2. In Chapter 3 the G4-OH PAMAM dendrimer is used to develop an immunoassay for detection of TNF-α cytokine. Chapter 4 describes the synthesis, characterization, and *in vitro* studies of dendrimer-allopregnanolone isomer and dendrimer-allopregnanolone nanodevices for traumatin brain injury (TBI) treatment.

CHAPTER 2 "SYNTHESIS, CHARACTERIZATION, DRUG RELEASE PROFILE, AND *IN VITRO* EFFICACY OF PAMAM DENDRIMER-ERYTHROMYCIN NANODEVICES"

2.1 Abstract

Erythromycin (EM), an antibiotic that has been used for infectious diseases, is now gaining attention because of its novel *anti-inflammatory* effects. A dendrimer-EM nanodevice is explored for *sustained* treatment of orthopedic inflammation. To sustain pharmacological activity, EM has been conjugated to poly(amidoamine) dendrimer (PAMAM) through an ester bond. Hydroxyl-terminated poly(amidoamine) dendrimer (G4-OH) was reacted to a protected amine linker followed by deprotection to obtain a bifunctional dendrimer that contains 10-15 % amine groups. EM was modified to EM-glutarate then conjugated to the bifunctional dendrimer through an amide bond. The cytotoxicity and activity of this EM-dendrimer conjugate was evaluated on RAW 264.7 cells *in vitro* by lactate dehydrogenase (LDH) assay and nitric oxide (NO) assay, respectively. From LDH assay dendrimer-EM conjugate and free EM were found to be non-cytotoxic within the dose range 0.1-1 µg/mL after 48 hours. Dendrimer-EM conjugate showed significant nitrite inhibition activity, reducing the nitrite levels by 42 % as compared to those in untreated cells. Dendrimer-EM conjugate has better efficacy than free EM for dose concentration of 1-10 µg/mL. The improvement in the *in vitro* efficacy of EM by dendrimer conjugation was the strongest within the dosage range of (5-10) µg/mL. The zone of inhibition of dendrimer-EM conjugate on bacterial growth at different concentrations showed similar activity compared to free EM treatment with equivalent dose. Furthermore, free dendrimer did not show any effect of bacterial inhibition at the concentration up to 0.2 mg/mL.

2.2 Introduction

Dendrimers are polymers with highly branched structures and globular shapes with the size range 2-10 nm. Due to their properties such as monodispersity, controllable size and structure, tailorable surface functionality, and multivalency, they are extensively investigated for various biomedical applications[2,36] such as drug delivery systems,[5-7] antiviral agents, and as magnetic resonance imaging contrast agents.[3,4] PAMAM dendrimers have also been studied in isolation as topical antibacterial agents to treat intrauterine infections.[39] In the past decades dendrimers have been investigated as novel diagnostic nanodevices.[8,9] Recently our group has reported a dendrimer based ELISA assay for IL-6 cytokine detection that is found in infected intraamniotic fluid.[17]

Controlled delivery of drugs can sustain blood level of a drug over a longer period of time, limit side effects, and lead the drug through the body without degradation, increase drug solubility, and decrease dose frequency. It is well known that the functional surface groups on dendrimers can affect their physicochemical properties, making them hydrophilic. Conjugation of poorly water-soluble drugs to PAMAM dendrimers increases the bioavailability as well as drug solubility and decreases the dose frequency.[18,40,41] Drug molecules can either be encapsulated and complexed, or covalently attached to the dendrimers through their functional groups.[19,20] The most common covalent linkage of the drugs to the surface functional groups of dendrimers can be achieved through the ester or amide bond which can be cleaved hydrolytically or enzymatically.[21] In the recent past disulfide bonds have also been demonstrated to be cleaved in presence of intracellular glutathione (GSH).[25] Ligand can be attached to the dendrimer to increase the accumulation of drug at the targeted site.[20] Neutral PAMAM dendrimers with no

targeting ligands have been shown to have an intrinsic ability to localize in cells associated with neuroinflammation in a rabbit model of cerebral palsy.[42] The key issues in the design of dendrimer-drug conjugates include improving drug payload; overcoming cytotoxicity especially in the case of cationic dendrimers; understanding the mechanism and dynamics of intracellular transport; and engineering the drug release at the appropriate tissue. The cellular uptake of dendrimer is also affected by their size, construct, surface functional groups and their charge.[26,43] Premature or lack of drug release from the dendrimer-drug conjugate before the appropriate time can decrease the *in vivo* effectiveness.

Total joint replacement (TJR) has been very successful in restoring function and mobility to millions of patients worldwide since its advent more than thirty years ago. With improvements in prophylaxis against infection, the fatigue strength of the components, and skeletal fixation, wear debris- induced periprosthetic membrane inflammation has become the primary limitation to TJR longevity.[44] There is currently no cure for aseptic loosening (AL) patients with osteolysis except revision surgery, primarily due to a lack of safe or effective drug candidate(s).[45] A recent approach to limiting osteolysis has focused on reducing periprosthetic inflammation and enhancing periprosthetic bone quality.[45-47] Erythromycin (EM) has been used for infectious disease for over 50 years.[48] For the last decade, EM has attracted a great deal of attention because of its novel anti-inflammatory effects far beyond antibiotics.[49,50] EM demonstrates a unique "phagocyte targeted delivery" property, favorable concentrating in monocyte/macrophages.[51-54] There are accumulating evidence,[55] that EM exerts its anti-inflammatory effects through targeting to NF-κB signaling.[56-58] Data from previous studies showed that EM inhibits wear debris-induced inflammation and osteolysis (both *in vitro* and *in*

vivo),[55,59-62] suggesting that EM represents an appropriate drug candidate to prevent or treat periprosthetic membrane inflammation. However, delivering adequate levels of EM to the site of periprosthetic inflammation, without undesirable systemic side effects, presents a considerable challenge. The goal of this work is to develop and validate intravenously dendrimer-EM delivery nanodevices that can target the periprosthetic tissue and reduce local inflammation in a sustained manner.

In this Chapter the synthesis and characterization of hydroxyl terminated generation four PAMAM dendrimer-Erythromycin conjugate (dendrimer-EM) and its *in vitro* activity and cytotoxicity is described. First, PAMAM G4-OH was partially functionalized with amine groups using amino-valeric acid as linker and then conjugated to EM-2′-glutarate via EM-glutarate-N-succinimidyl ester intermediate. The cell toxicity was determined by measuring the release of lactate dehydrogenase (LDH) from dead or dying cells into the culture medium using a Cytotoxity Detection Kit. A zone of inhibition study was performed using the modified Kirby-Bauer Method to determine the levels of Staphylococcus aureus (*S. aureus*) activity inhibited by dendrimer-EM conjugate release in the sample eluents. The effect of dendrimer-EM conjugate on LPS-induced nitrite production in RAW 264.7 cells was demonstrated. The cell studies were done at the Biomedical Engineering by our collaborator, Dr. Ren's lab.

2.3 Materials and Methods

2.3.1 Materials

Generation four hydroxyl terminated PAMAM dendrimer (G4-OH) with ethylendiamine core and 64 surface groups (MW 14,279) in methanol solution was purchased from Dendritech Inc. (Midland, MI, USA). N-(3-dimethylaminopropyl)-N-ethylcarbodiimide (EDC), 4-

(dimethylamino) pyridine (DMAP), glutaric anhydride, 5-(tert-butoxycarbonyl-amino)valeric acid, N,N-dimethylacetamide (DMA), diphenyl chlorophosphate and lipopolysaccharide (LPS, Escherichia coli O55:B5) were purchased from Sigma-Aldrich Chemical Company (St. Louis, USA). Triethylamine (TEA) and N-hydroxysuccinimide (NHS) were purchased from Thermo Scientific. Trifluoroacetic acid (TFA), dimethylformamide (DMF), and dimethyl sulfoxide (DMSO) were purchased from EMD. All anhydrous solvents DMSO, DMF, acetonitrile (ACN), and dichloromethane (DCM) were purchased from Acros Organics, USA. Fluorescein isothiocyanate (FITC) was obtained from Alfa Aesar, MA, USA. All other solvents and chemicals used were purchased from Fisher Scientific. Regenerated cellulose (RC) dialysis membrane with molecular weight cut-off of 1000 Da was obtained from Spectrum Laboratories. DMEM medium was purchased from Gibco-BRL Life Technologies, USA. FBS (fetal bovine serum) was purchased from HyClone Laboratories (Utah, USA).

All reactions were carried out under nitrogen conditions. The anhydrous solvents and other reagents that are commercially available were directly used without further purification. Thin layer chromatography (TLC) was performed on silica gel GF$_{254}$ plates (Watmann) and the spots were visualized with UV light and 2% H$_2$SO$_4$ in EtOH.

2.3.2 Characterization

NMR spectra were recorded on a Varian INOVA 400 spectrometer using commercially available deuterated solvents. Proton chemical shifts are reported in ppm (δ) and tetramethylsilane (TMS) used for internal standard. Coupling constants (*J*) are reported in hertz (Hz). ESI mass spectra were recorded on Waters Micromass ZQ spectrometer. Matrix-assisted laser desorption ionization-time of flight (MALDI-TOF) mass spectra were recorded on a Bruker

Ultraflex system equipped with a pulsed nitrogen laser (337 nm), operating in positive ion reflector mode, using 19 kV acceleration voltage and a matrix of 2,5-dihydroxybenzoic acid. Cytochrome C (MW 12,361 g/mol), and Apomyoglobin (MW 16,952 g/mol) were used as external standards. A dendrimer solution was prepared by dissolving 2 mg of dendrimer in 1 mL of DMSO. The matrix solution was prepared by dissolving 20 mg of matrix in 1 mL of the 1:1 mixture of deionized water and acetonitrile (0.1% TFA). Analytical samples were prepared by mixing 10 μL of dendrimer solution with 100 μL of matrix solution, followed by deposition of 1 μL of sample mixture onto a 384-well aluminum plate. This mixture was allowed to air dry at room temperature.

2.3.3 HPLC Characterization

High performance liquid chromatography (HPLC) characterization was carried out using Waters HPLC instrument equipped with dual pumps, an auto-sampler and dual UV detector interfaced to Breeze software. The HPLC chromatogram was monitored at 210 and 238 nm simultaneously using the dual UV absorbance detector. H_2O:ACN (0.14 % TFA) was used as mobile phase. Both phases were freshly prepared, filtered, and degassed prior to use. Symmetry300 C_{18} reverse-phase column (5 μm particle size, 25 cm × 4.6 mm length × I.D.) equipped with a Supelguard Cartridges (5 μm particle size, 2.0 cm ×3.9 mm length × I.D.) was used for characterization of the conjugates. HPLC analysis was done using 90:10 to 30:70 (H_2O:ACN) gradient flow in 30 minutes with flow rate of 1 mL/min.

2.3.4 Release Study Protocol

The release studies were performed in 0.1M PBS buffer solution (pH = 7.4). The conjugate was added into 3 mL preheated buffer solutions in triplicates. All the release solutions

containing 2.5 mg/mL dendrimer drug conjugate were stirred continuously and maintained at 37ºC. At appropriate time intervals samples were withdrawn and immediately analyzed by HPLC to determine the EM concentrations.

2.3.5 Dynamic Light Scattering and ζ-Potential

The particle size and ζ-potential of G4-OH and dendrimer conjugates were determined by dynamic light scattering (DLS) using a Malvern Instruments Zetasizer Nano ZEN3600 instrument (Westborough, MA). The samples were dissolved in DI water (18.2 Ω) and filtered using AccuSpin Micro 17/17R ultracentrifuge (Fisher Scientific). DLS measurements were performed at a 173° scattering angle at 25°C.

2.3.6 RAW 264.7 Cell Culture Stimulation, and Dendrimer Treatment

Murine RAW 264.7 macrophage cell line was obtained from the American Type Culture Collection (ATCC, Rockville, MD). RAW 264.7 cells were maintained in Dulbecco's modified Eagle's medium (DMEM) (Gibco BRL, MD) containing 10% fetal bovine serum (FBS) and antibiotics (100 units/mL of penicillin-G and 100 µg/mL of streptomycin) at 37°C in a humidified incubator with 5% CO_2. RAW 264.7 cells were plated at a density of 1×10^5 cells/well, in 96-well plates in the presence of LPS (1 µg/mL) with or without dendrimer-EM conjugate at different concentrations for 48 hours.

2.3.7 Cell Toxicity Assay

Cell toxicity was determined by measuring the release of lactate dehydrogenase (LDH) from dead or dying cells into the culture medium using a Cytotoxity Detection Kit (Roche Diagnostics BmbH) following the manufacturer's instruction. 48 hours after treatment of dendrimer-EM conjugates at different concentrations, the conditioned media were collected and

used for the measurement of LDH activity. Briefly, 100 μL of culture medium was added into a plate of 96 wells, mixed with 100 μL working solution and incubated at room temperature for 30 minutes in the dark. Then, the plate was read under the UVmax colorimeter (Molecular Devices) at OD 490 nm. Blank culture medium was used as a blank control and the total cell lysate was used as a positive control as well. LDH activity was expressed as absorbance (OD) per mg protein.

2.3.8 Detection of Nitrite Production

RAW 264.7 cells (passage 10) (5×10^5 cells per well) were cultured in triplicate in 24-well plates and stimulated with 1 μg/mL LPS (positive control), and 1 μg/mL LPS [+EM, +dendrimer, or +D-EM] for 48 hours. The concentrations of free EM were 0.1, 1.0, 5.0, and 10.0 μg. They corresponded to the concentration of EM in the dendrimer-EM conjugate. The production of nitric oxide (NO) was determined by assaying culture supernatant for nitrite (NO_2^-), a stable reaction product of NO. In brief, 100 μL of culture supernatant was mixed with an equal volume of Griess reagent (Cayman) (1% sulfanilamide and 0.1% *N*-[naphthyl] ethylenediamine dihydrochloride in 2.5% H_3PO_4) at room temperature for 10 min. Absorbance was measured at 540 nm in a microplate reader. Nitrite concentration was calculated from a $NaNO_2$ standard curve.

2.3.9 Antibacterial Assay

Staphylococcus aureus (*S. Aureus*) strain was used for the present study. A zone of inhibition study was performed using the modified Kirby-Bauer Method to determine the levels of *S. aureus* activity inhibited by dendrimer-EM conjugate release in the sample eluents. Growth of the organism and diffusion of the EM commence simultaneously resulting in a circular zone

of inhibition in which the amount of dendrimer-EM conjugate exceeds inhibitory concentrations. The diameter of the inhibition zone reflects the function of the dendrimer-EM conjugate amount in the eluents. A disk paper soaked with the dendrimer-EM/PBS solution with known concentration was put into a bacterial agar plate, inoculated with the bacteria strain of *S. aureus*, for the zone of inhibition test. This strain of *S. aureus* is the main bacteria causing bone infection. The bacteria plates were incubated for 24 hours, and then the diameter of the zone of growth inhibition around each disk to the nearest whole mm were measured. The results were expressed as the size of zone of inhibition. All the tests were performed in triplicate, and repeated two times.

2.3.10 Preparation of Bifunctional PAMAM Dendrimer (G4-OH-Link-NH$_2$, 2)

The reaction scheme for the preparation of the conjugate **2** is outlined in Figure 5. The 5-(Boc-amino)valeric acid (168.9 mg, 0.7774 mmole) was dissolved in DMSO (10 mL). EDC (447 mg, 2.33 mmole) and DMAP (10.0 mg, 0.0818 mmole) each dissolved in DMSO (5 mL) were added under nitrogen atmosphere. The mixture was allowed to stir for 1 hour at room temperature and PAMAM G4-OH (370.0 mg, 0.0259 mmole) dissolved in DMSO (5 mL) was added to the reaction mixture. The reaction was stirred for 48 hrs at room temperature. The resulting solution was dialyzed extensively with DMSO (dialysis membrane of molecular weight cutoff = 1000 Da) for 24 h and with deionized water for 6 h. The obtained reaction mixture was then lyophilized yielding 328.0 mg (0.0194 mmole) of intermediate **1** (G4-OH-Link-Boc). The intermediate **1** contains Boc protected amino groups on the surface and it was characterized by proton NMR. ^{1}H NMR (DMSO-d_6, 400 MHz): δ (ppm) 8.04 (bs, CO-N*H*, Boc), 7.92 (bs, CO-N*H*, G4-OH), 7.77 (bs, CO-N*H*, G4-OH), 4.69 (bs, O*H*, G4-OH), 3.96 (m, C*H$_2$*OCO), 3.37-2.18

(986H, m, aliphatic protons of G4-OH and CH_2 of linker), 2.01 (m, CH_2, methylene protons of linker), 1.45 (m, 2 × CH_2, methylene protons of linker), 1.34 (s, 3 × CH_3, methyl groups of Boc).

To obtain free amine groups, 6.0 mL of TFA:DCM (1:1) was added to 328.0 mg G4-OH conjugate containing Boc groups at 0°C. The reaction was carried out for 1 h at 0°C, and then the solvent was removed at reduced pressure. The mixture was re-dissolved in DMSO and dialyzed with DMSO for 24 h and deionized water for 6 h. The reaction mixture was then lyophilized yielding 220 mg of bifunctional dendrimer **2**. The conjugate **2** was characterized by proton NMR. ^{1}H NMR (DMSO-d_6, 400 MHz): δ (ppm) 7.92 (bs, CO-NH, G4-OH), 7.77 (bs, CO-NH, G4-OH), 4.69 (bs, OH, G4-OH), 3.99 (t, CH_2OCO), 3.40-2.47 (986 H, m, aliphatic protons of G4-OH and CH_2 of linker), 2.31 (m, CH_2, methylene protons of linker), 1.53 (m, 2 × CH_2, methylene protons of linker).
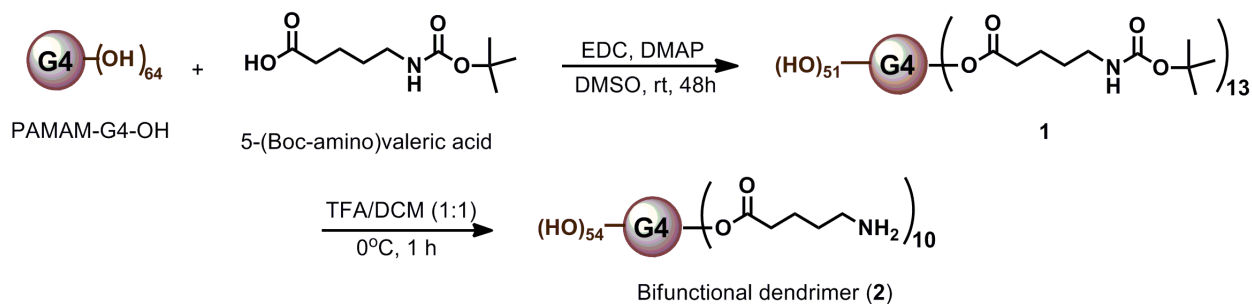
Figure 5. Synthesis of bifunctional PAMAM dendrimer (G4-OH-Link-NH$_2$, **2**).

2.3.11 Synthesis of Erythromycin-2′-Glutarate (EM-2′-glutarate, 3)

The reaction scheme is shown in Figure 6. Glutaric anhydride (31.09 mg, 0.272 mmole) and TEA (30 μL) were added to a solution of EM (100 mg, 0.136 mmole) in 80:20 (v/v) anhydrous DMF/DMA (10 mL). The reaction mixture was allowed to stir for 24 h under N$_2$ and additional 15.54 mg (0.136 mmole) of glutaric anhydride and TEA (30 μL) was added. The

reaction mixture was continued to stir and was monitored with TLC. After 3 days of stirring, TLC (methanol/ethyl acetate/DCM = 5:2:2, R_f = 0.4) showed that reaction was complete. The reaction mixture was evaporated under reduced pressure and pure EM-2′-glutarate was isolated by flash column chromatography on silica gel using methanol/ethyl acetate/hexanes (5:2:2) as mobile phase (100 mg, yield 86%).
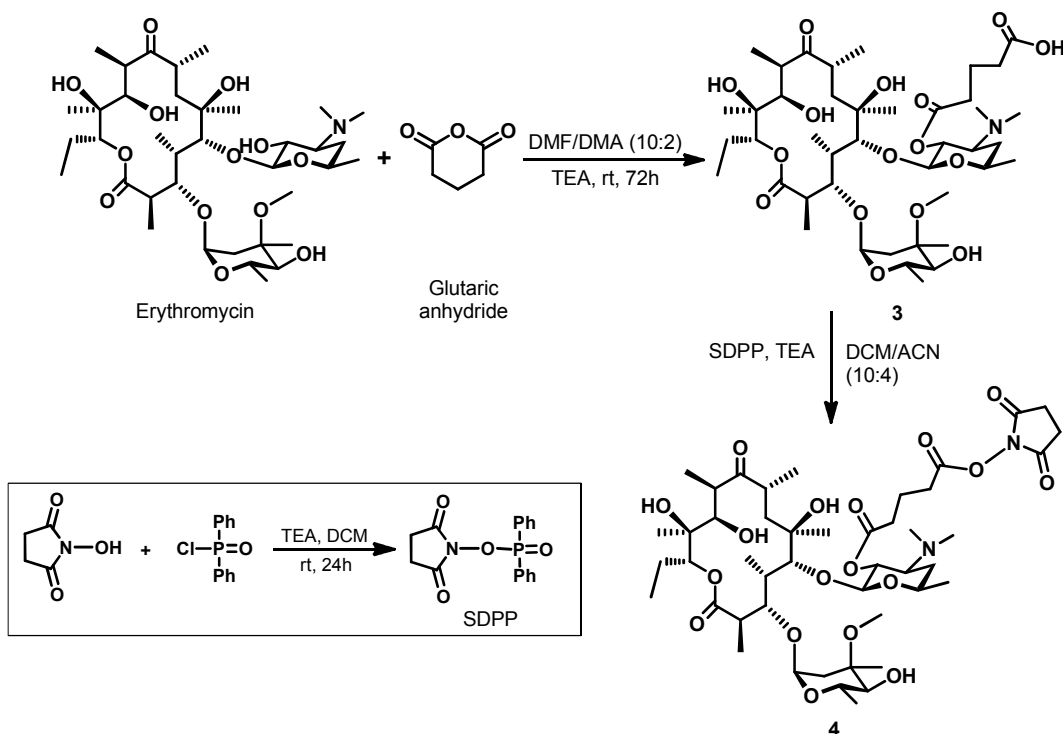
Figure 6. Synthesis of EM-2'-glutarate **3** and Erythromycin-2′-glutarate-N-succinimidyl ester **4**.

EM-2′-glutarate was characterized by proton NMR, HPLC, and ESI MS. ^{1}H NMR (DMSO-d$_6$, 400 MHz): δ (ppm) 5.07 (dd, J_1=11.6 Hz, J_2=2.4 Hz, 1H), 4.72 (dd, J_1=4.8 Hz, J_2=0.9 Hz, 1H), 4.60 (d, J=7.6, 1H), 4.52-4.49 (m, 2H), 4.01-3.96 (m, 2H), 3.88 (d, J=9.6 Hz, 1H), 3.69 (s, 1H), 3.67 (dd, 1H), 3.44-3.36 (m, 2H), 3.22 (s, 3H), 2.89 (d, J=8.8 Hz, 1H), 2.84 (d, J=7.6 Hz, 1H), 2.61 (dd, J_1=11.2 Hz, J_2=3.2 Hz, 1H), 2.287-2.13 (m, 8H), 2.11 (s, 6 H), 1.86 (t,

J=6.8 Hz, 1H), 1.80-1.74 (m, 1H), 1.71-1.63 (m, 4H), 1.59-1.46 (m, 2H), 1.39-1.31 (m, 1H), 1.23 (s, 3H), 1.15-0.97 (m, 21 H), 0.81 (d, *J*=7.2 Hz, 3H), 0.72 (t, *J*=7.2 Hz, 3H). ESI MS (*m/z*): calcd for $C_{42}H_{72}NO_{16}$ [M-H]$^+$ 846.4, found 846.8.

2.3.12 Synthesis of Erythromycin-2′-Glutarate-N-Succinimidyl Ester, 4

The synthetic scheme is shown in Figure 6. EM-2′-glutarate (70.00 mg, 0.0825 mmole) was dissolved in 70:30 (v/v) anhydrous ACN:DCM (5 mL) and TEA (50 μL) and N-hydroxysuccinimido-phosphate (SDPP) (39.00 mg, 0.1238 mmole) were added to the solution at 0°C. SDPP was synthesized following the literature procedure.[63] After 6 hours of stirring the TLC (MeOH:EtOAc:DCM = 1:3:2, R$_f$ = 0.48) showed that reaction was complete.. The reaction mixture was concentrated under vacuum and the pure product was isolated by flash column chromatography on silica gel using methanol/ethyl acetate/hexanes (1:5:1) as a mobile phase (67 mg, yield 85%). The ester (**4**) was characterized by proton NMR. ^{1}H NMR (CDCl$_3$, 400 MHz): δ (ppm) 5.00 (dd, *J₁*=11.2 Hz, *J₂*=1.6 Hz, 1H), 4.84 (d, *J*=4.0 Hz, 1H), 4.82-4.76 (m, 1H), 4.56 (d, *J*=7.2 Hz, 1H), 3.95-3.92 (m, 1H), 3.88 (d, *J*=9.2 Hz, 1H), 3.76 (s, 1H), 3.54-3.50 (m, 1H), 3.46 (d, *J*=7.2 Hz, 1H), 3.29 (s, 3H), 3.04 (d, *J*=7.2 Hz, 1H), 3.00 (d, *J*=9.6 Hz, 1H), 2.90-2.84 (m, 2H), 2.83-2.78 (m, 3H), 2.75-2.67 (m, 1H), 2.63 (bs, 4H), 2.57-2.49 (m,1H), 2.41-2.38 (m, 1H), 2.32 (s, 6H), 2.54-1.99 (m, 2H), 1.93-1.86 (m, 2H), 1.82-1.69 (m, 2H), 1.61-1.50 (m, 3H), 1.42 (s, 3H), 1.25-1.09 (m, 21 H), 0.86 (d, *J*=7.6 Hz, 3H), 0.80 (t, *J*=7.6 Hz, 3H).

2.3.13 Preparation of G4-PAMAM Dendrimer-EM Conjugate (Dendrimer - EM, 5)

The reaction scheme for the preparation of dendrimer-EM conjugate (**5**) is outlined in Figure 7. To a stirring solution of bifunctional dendrimer **2** (64 mg, 0.0041 mmole) in anhydrous DMSO (6.5 mL), TEA (10 μL) was added under nitrogen condition. To this solution EM-2′-

glutarate-N-succinimidyl ester (67 mg, 0.0708 mmole) dissolved in anhydrous DMSO (5 mL) was added and the reaction mixture was allowed to stir for overnight at room temperature. After completion of the reaction, the reaction mixture was subjected to dialysis in DMSO (membrane MW cut off = 1000 Da) for 24 hours and in deionized water for 6 hours. The obtained reaction mixture was lyophilized to get final dendrimer-EM conjugate **5**. The conjugate **5** was characterized by proton NMR. ^{1}H NMR (DMSO-d_6, 400 MHz): δ (ppm) 8.05 (bs, CO-N*H*, linker), 7.94 (bs, CO-N*H*, G4-OH), 7.79 (bs, CO-N*H*, G4-OH), 5.07 (d, *J*=12.4Hz, 1H, Ery), 4.9-4.5 (m, O*H*, G4-OH; 3H, Ery), 4.11 (m, 2H, Ery), 3.97 (m, C*H$_2$*OCO, G4-OH), 3.88 (d, *J*=12.4Hz, 1H, Ery), 3.70 (bs, 1H, Ery), 3.37-2.16 (m, 986 H aliphatic protons, G4-OH; C*H$_2$*, linker; 24H, Ery), 2.06-1.28 (m, 4H, linker; 9H, Ery), 1.22 (s, 3H, Ery-C*H$_3$*), 1.14-0.96 (m, 21 H, Ery-C*H$_3$*), 0.80 (m, 3H, Ery-C*H$_3$*),, 0.72 (m, 3H, Ery-C*H$_3$*).
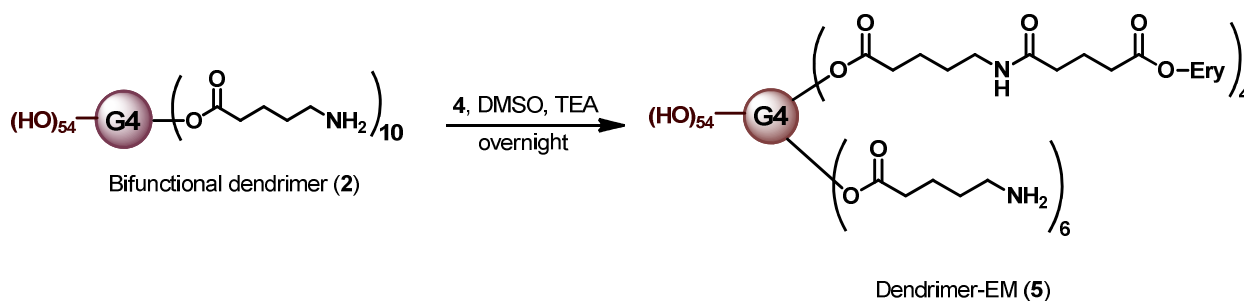
Figure 7. Synthesis of PAMAM G4-OH-Erythromycin (Dendrimer-EM, **5**).

2.4 Results

2.4.1 Synthesis and Characterization of Bifunctional PAMAM Dendrimer, 2

Due to better reactivity of amine groups compared to hydroxyl groups, a bifunctional dendrimer was prepared. The reaction scheme is shown in Figure 5. 5-Boc-amino-valeric acid was used as a linker to provide protected NH$_2$ groups. Generation four hydroxy-terminated PAMAM dendrimer (G4-OH) was reacted with activated 5-Boc-amino-valeric acid in presence

of EDC and catalytic amount of DMAP to yield intermediate **1**. The intermediate was confirmed by proton NMR chemical shift and integration of Boc protected groups (s, 1.34 ppm, 9H), as well as chemical shifts of methylenes that belong to the linker (m, 1.45 ppm, 4H) and dendrimer ester methylenes (m, 3.96 ppm, CH_2OCO) that appear after conjugation (Figure 8). The integration of characteristic peaks for Boc groups and amide peaks of dendrimer obtained from NMR spectrum suggested that 13 molecules of Boc-linker were conjugated to the dendrimer.
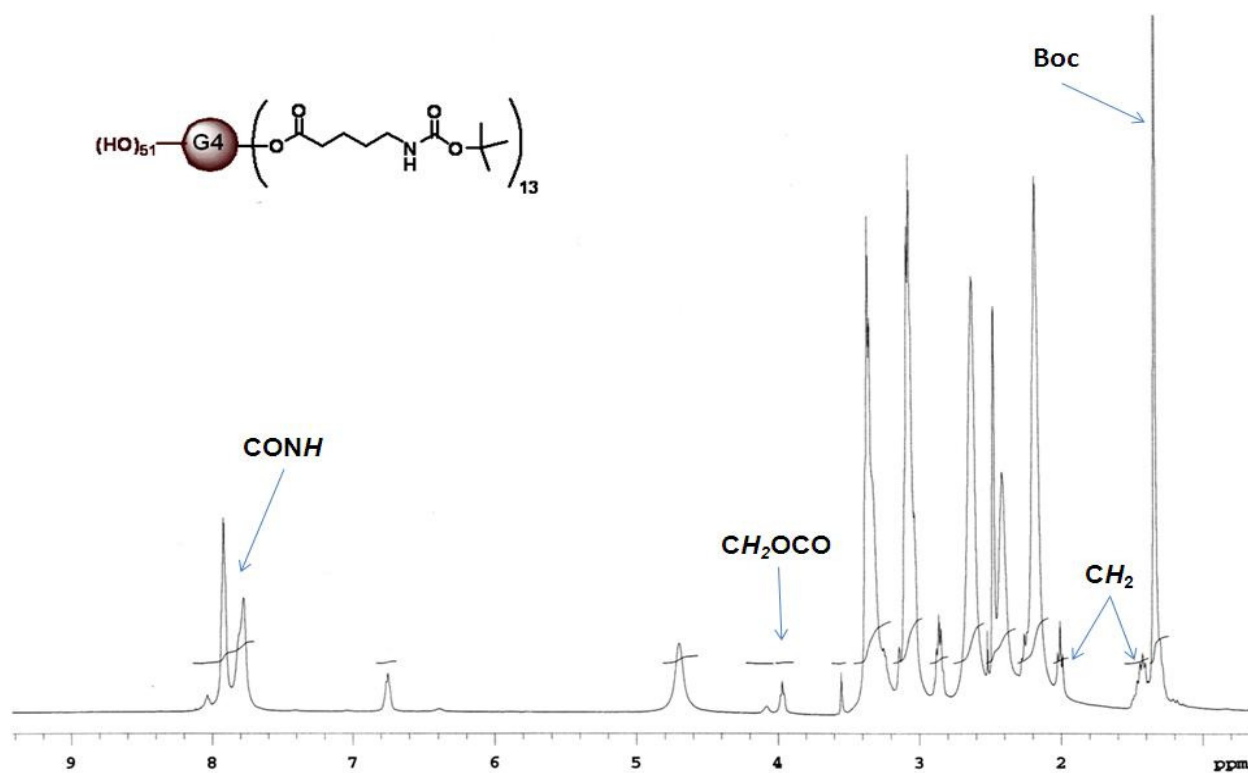
Figure 8. Proton NMR of intermediate **1** (G4-OH-Link-Boc).

The deprotection of Boc-protected amino groups in mild condition, TFA:DCM (1:1), gave bifunctional dendrimer **2** which consists of 54 hydroxyl and 10 amine groups. The slightly lower number of NH$_2$ groups (10 instead 13) are most probably due to hydrolysis of ester bond. The number of amine groups was determined based on proton NMR from integration of

characteristic peaks for methylene protons that belong to the linker (m, 1.45 ppm, 4H) and amide

protons of dendrimer (Figure 9).
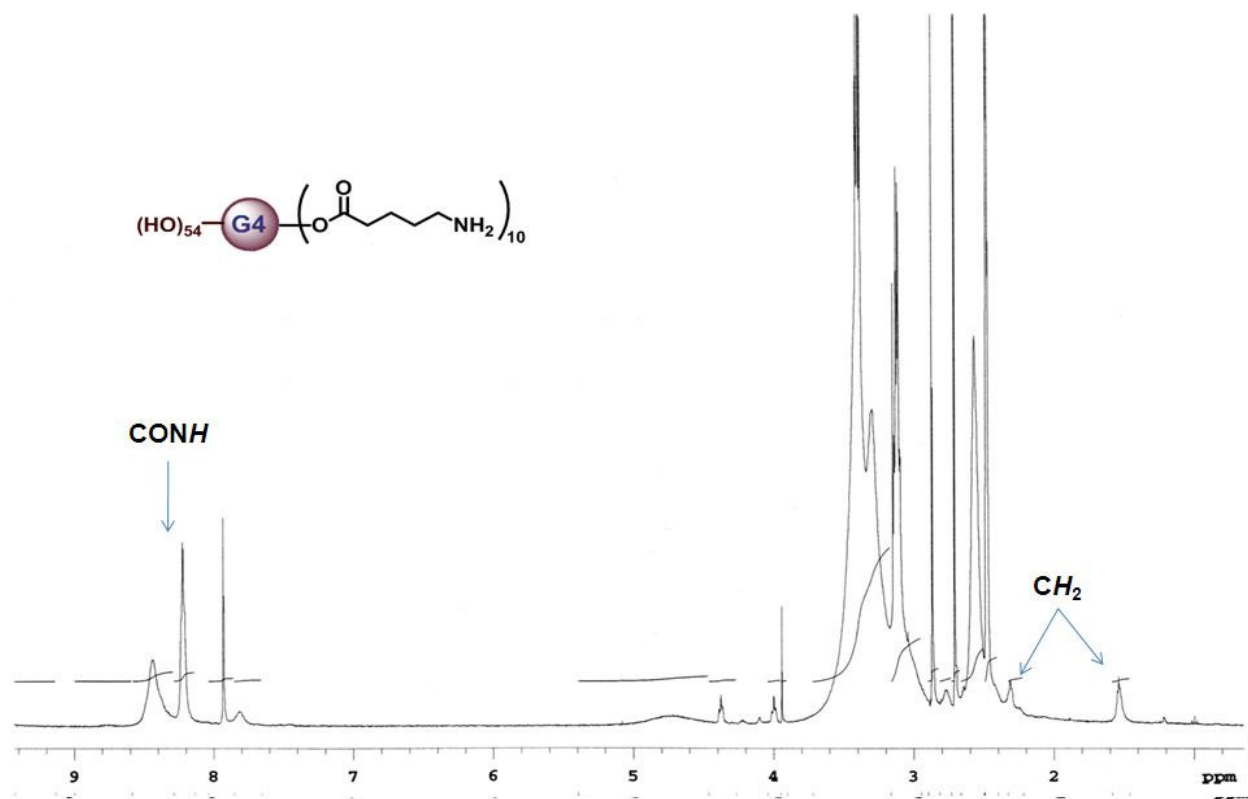
Figure 9. Proton NMR of bifunctional PAMAM dendrimer (G4-OH-Link-NH$_2$, **2**).

2.4.2 Synthesis of G4-PAMAM Dendrimer-EM Conjugate, 5

The amino groups of bifunctional dendrimer were conjugated to EM-2′-glutarate through

stable amide bond (Figure 7). Prior to conjugation of dendrimer with EM-2′-glutarate, EM-

glutarate-N-succinimidyl ester was prepared.[63] EM consists of a 14-membered lactone ring with

ten asymmetric centers, and glycosylated in two positions by desosamine and cladinose sugars.[64]

Cladinose is linked to the 4-position while desosamine to the 6-position of the lactone ring. EM

also contains four hydroxyl groups that differ in their reactivities. The order of reactivity was

established by acetylation. The most reactive hydroxyl group is at 2′-position where acetylation

occurs first due to vicinity of tertiary amine that acts as an autocatalyst.[65,66] When limiting amount of acetic anhydride is used, the 2′-monoacetate would be the only product, and it can be obtained without any catalyst. The tertiary amine group also increases the rate of 2′-monoacetate hydrolysis, which can be achieved by quenching the reaction with methanol. The second most reactive hydroxyl group is at 4″-position, while the third one is at 11-position. The reaction of EM with glutaric anhydride in the presence of triethylamine occurred at 2′-position which gave EM-2′-glutarate **3** and was characterized by HPLC, proton NMR, and mass spectroscopy. The molecular weight of **3** from mass spectrum [M-H]$^+$ was found to be 846.8 which is in agreement with calculated one, 846.4 (Figure 10).
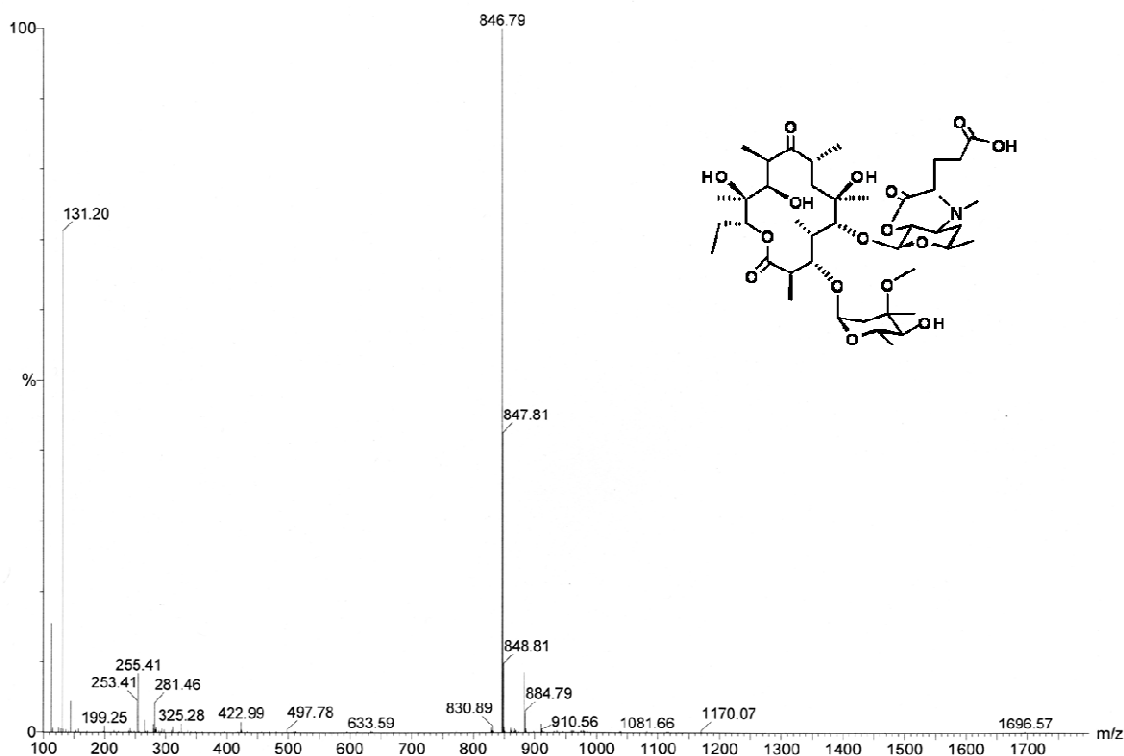
Figure 10. ESI MS of Erythromycin-2′-glutarate (EM-2'-glutarate) **3**, (*m/z*): calc. for $C_{42}H_{72}NO_{16}$ [M-H]$^+$ 846.49, found 846.79.

Analysis of proton NMR spectrum showed that th chemical shifts of H-1′ (d, 4.60 ppm, J=7.6 Hz), H-2′ and H-3′ (m, 4.52-4.49 ppm) of desosamine as well as overlapping signals for methylene protons that belong to the glutarate moiety and EM (m, 1.71-1.63 ppm and m, 2.28-2.13 ppm) confirmed the formation of EM-2′-glutarate (Figure 11).
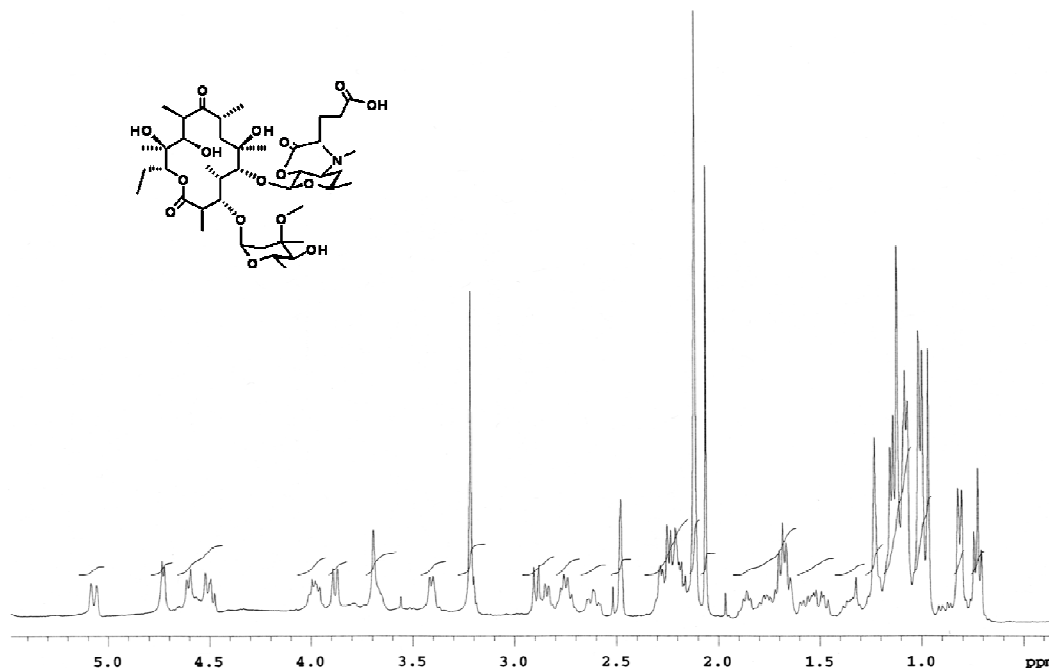
Figure 11. Proton NMR of Erythromycin-2′-glutarate (EM-2′-glutarate) **3**.

The HPLC chromatograms showed that the retention times for EM and EM-2′-glutarate were 22.08 and 23.66 min respectively (Figure 12). EM-2′-glutarate was then reacted with SDPP in the presence of triethylamine to obtain activated ester of Erythromycin **4**. The ester was characterized by proton NMR showing characteristic peak for methylene protons of succinimide ester (s, 2.63 ppm, 4H) (Figure 13). We achieved better yield when SDPP was used compared to N-hydroxysuccinimide. The activated ester of EM was coupled with bifunctional dendrimer to yield dendrimer-EM conjugate.
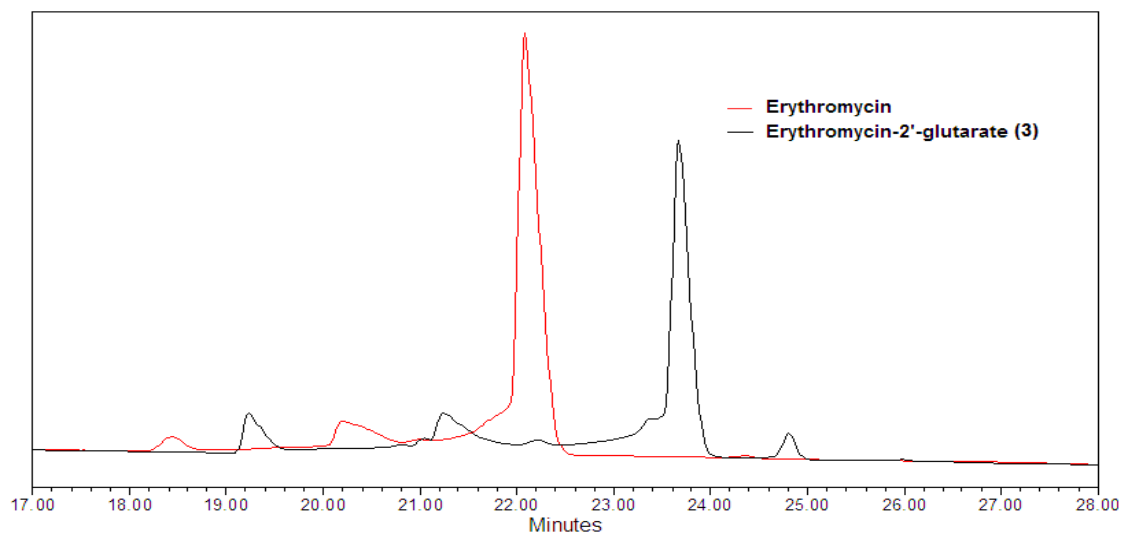
Figure 12. HPLC chromatograms of Erythromycin, and Erythromycin-2′-glutarate (**3**) at 210 nm.
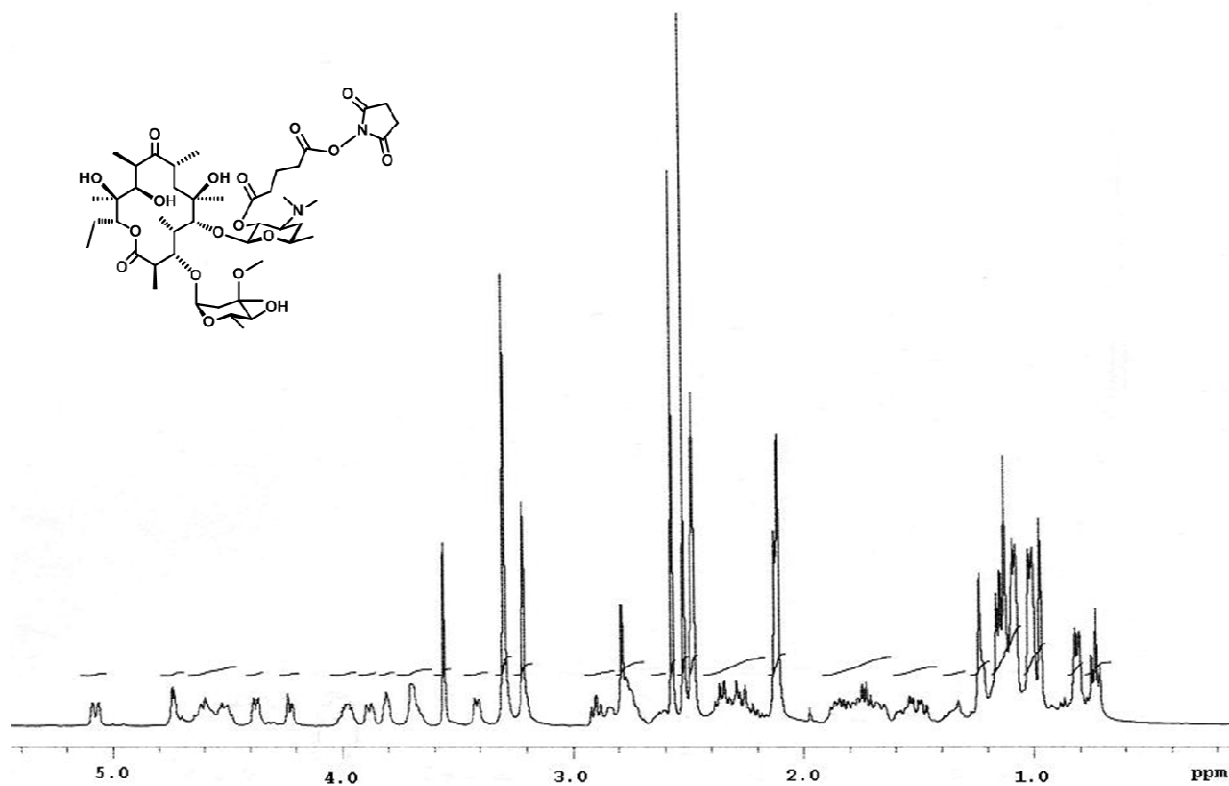
Figure 13. Proton NMR of Erythromycin-2′-glutarate-N-succinimidyl ester **4**.

Dendrimer-EM conjugate was characterized by HPLC and compared to bifuctional dendrimer and G4-OH as shown in Figure 14. The analysis of HPLC spectra showed that the retention time of G4-OG (7.96 min) was very close to bifunctional dendrimer (8.13 min), since there is no significant difference in chemical structure. However, the dendrimer-EM and G4-OH-Link-Boc intermediate gave very distinct broad peaks at 11.69 and 13.13 min, respectively. The broad peaks are due to larger size and non-polar character of conjugates compared to G4-OH and bifunctional dendrimer.
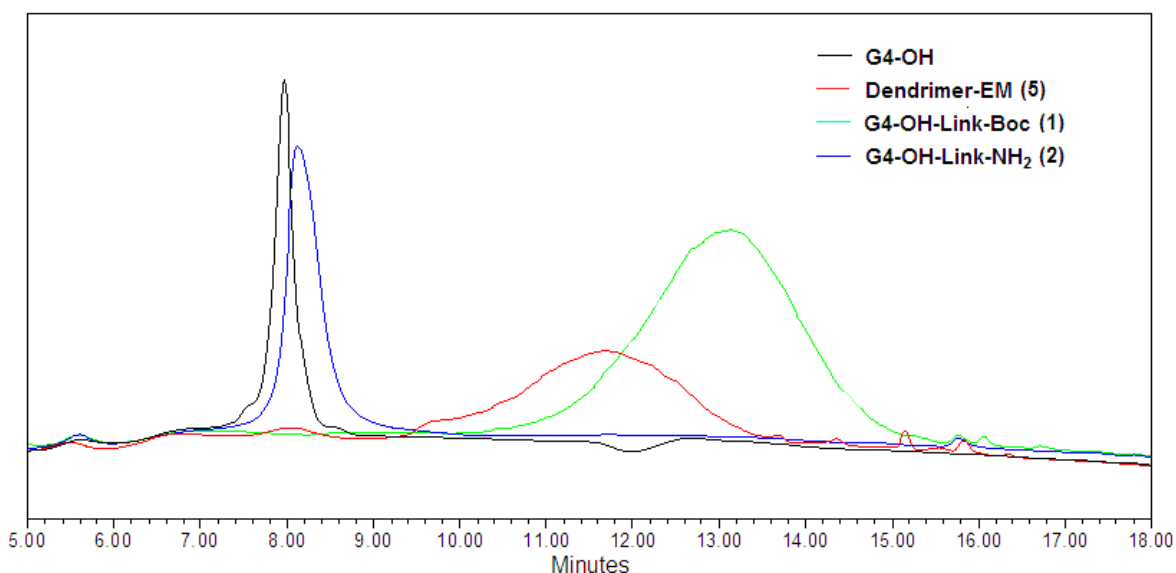
Figure 14. HPLC chromatograms of G4-OH, bifunctional dendrimer G4-OH-Link-NH$_2$ (**2**), Dendrimer-EM conjugate (**5**), and G4-OH-Link-Boc (**1**) at 210 nm.

The proton NMR of dendrimer-EM conjugate is shown in Figure 15. Comparison of the integration of amide peaks of dendrimer and methyl groups of EM revealed that four molecules of EM were attached to the surface of the dendrimer.
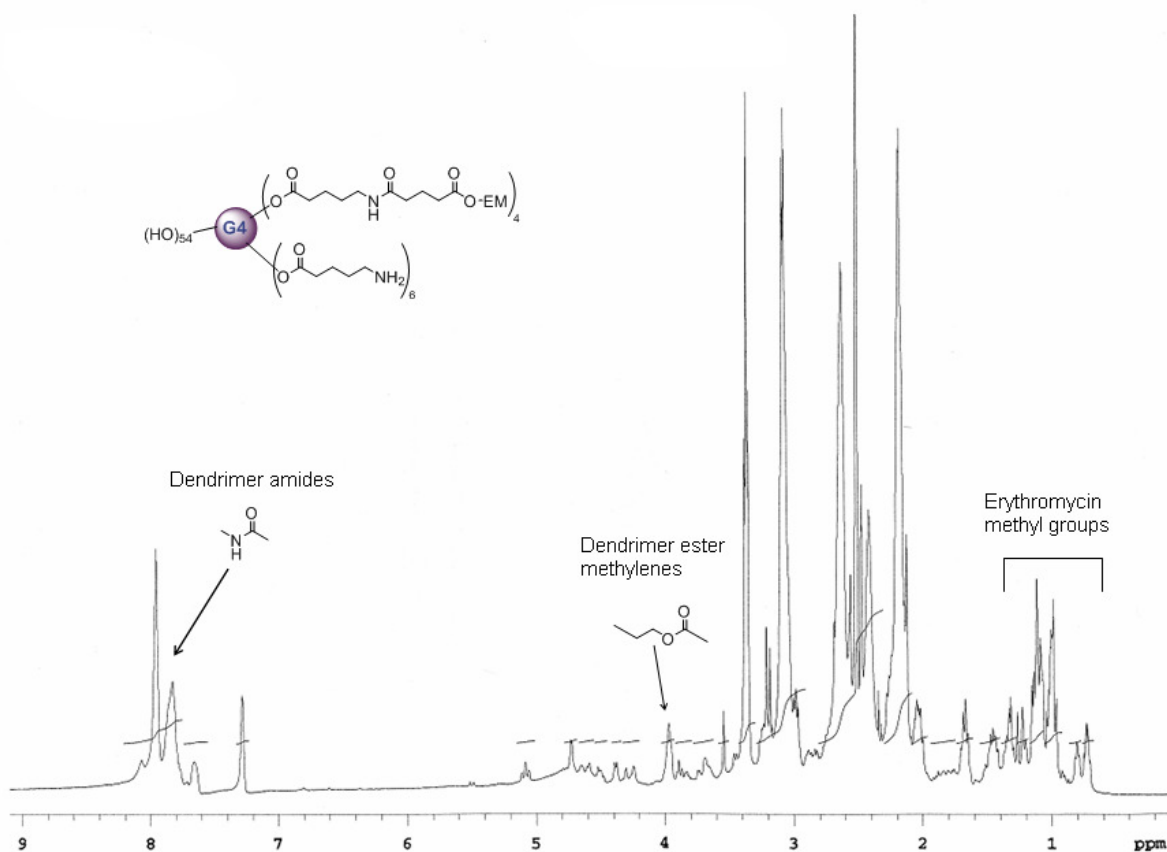
Figure 15. Proton NMR spectrum of dendrimer-EM (5) in DMSO-*d₆*.

MALDI-TOF MS spectra of dendrimer-EM were evaluated and compared with G4-OH which is shown in Figure 16. The obtained molecular weight of dendrimer-EM conjugate (18,203.6), also suggests that a payload of approximately four molecules of EM was achieved. This represents a drug payload in the conjugate of ~16% by weight, which is relatively high for a polymer-drug conjugate. The conjugate was soluble in PBS buffer pH 7.4, in contrast to the free drug.
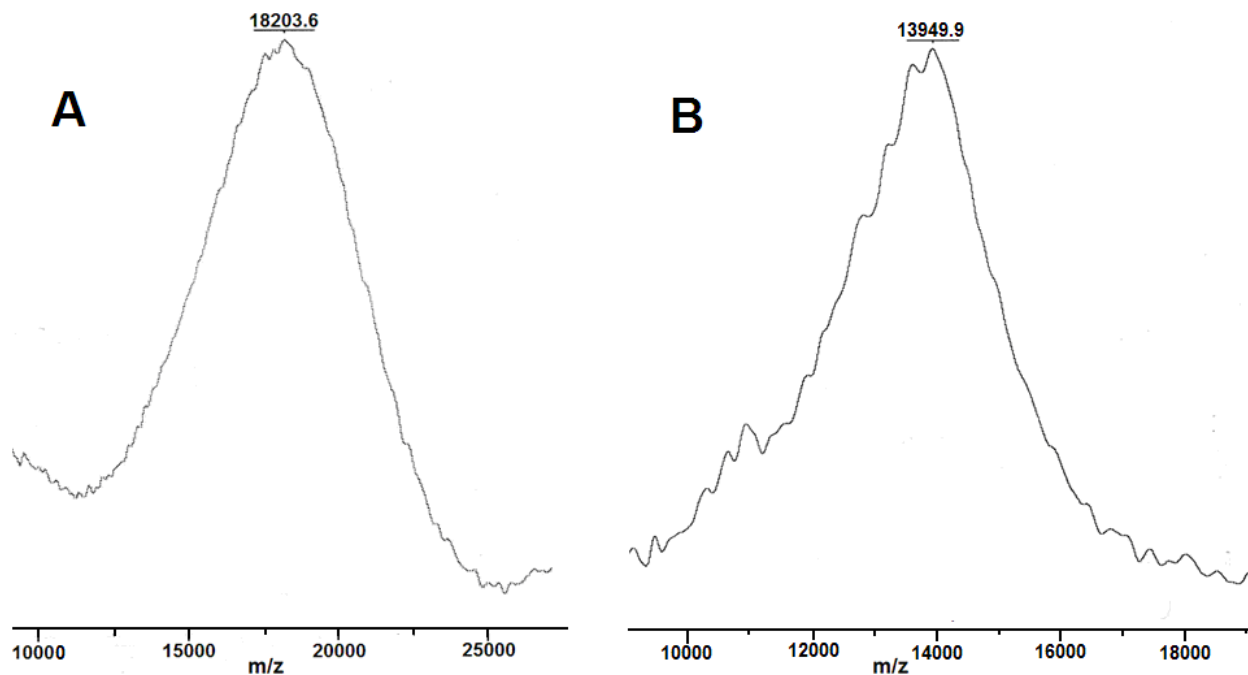
Figure 16. MALDI-TOF MS spectra of (a) dendrimer-EM (**5**), and (b) G4-OH dendrimer.

2.4.3 Particle Size and ζ-Potential

Zeta potential and size of the nanoparticle or drug molecule plays a major role in targeting and delivery to the specific site. It is also influences the binding properties of the drug and dendrimer/nanoparticle to the receptor. We have investigated particle size and zeta potential of G4-OH, bifunctional dendrimer (**2**) and dendrimer-EM conjugate (**5**) which are shown in Table 2. We did not find much difference in size between G4-OH, G4-OH-Link-Boc and bifunctional dendrimer (**2**); this may be due to minimal difference in molecular weight of these molecules. The dendrimer-EM conjugate has slight larger size (4.98 nm) compared to others. The G4-OH has less cytotoxicity due to its neutral surface charge. It has slightly positive zeta potential (4.54 mV) which is due to the presence of tertiary amines in its core even though it

suppose to have neutral value. We did not find any difference between G4-OH and G4-OH-Link-Boc, but there is a difference between G4-OH and G4-OH-Link-NH$_2$ (2). This is due to an increase in number of primary amine (12-13 groups) on the surface of the dendrimer after deprotection of Boc groups (6.29 mV). The zeta potential of dendrimer-EM conjugate is 8.08 mV. The tertiary nitrogen groups of erythromycin are responsible for slightly higher value of dendrimer-EM compared to G4-OH and bifunctional dendrimer.

Table 2. Particle size and ζ-potential of dendrimer conjugates

Compound	Diameter (nm)	ζ-potential (mV)
G4-OH	4.28±0.24	+4.54±0.10
G4-OH-Link-Boc	4.53±0.30	+4.92±1.20
G4-OH-Link-NH$_2$	4.22±0.28	+6.29±2.50
Dendrimer-EM	4.98±0.50	+8.08±0.90

2.4.4 Release Studies

The drug release rate of the conjugate was carried out in PBS buffer at pH 7.4 and analyzed by HPLC. The ester linkage used for conjugation of EM was susceptible to hydrolysis and about 90% of the EM was released within 10 hours (Figure 17). EM release from the conjugate was completed within 20 hours. There are two ester links in the dendrimer-EM conjugate, and the release study clearly showed that ester bond on the 2′-position releases preferentially. This is consistent with the previous studies where EM-2′-monoacetate easily hydrolyzes when the reaction quenched with methanol due to vicinity of tertiary amine group. This tertiary amine group acts as an autocatalyst for the hydrolysis of ester bond.[65,66]
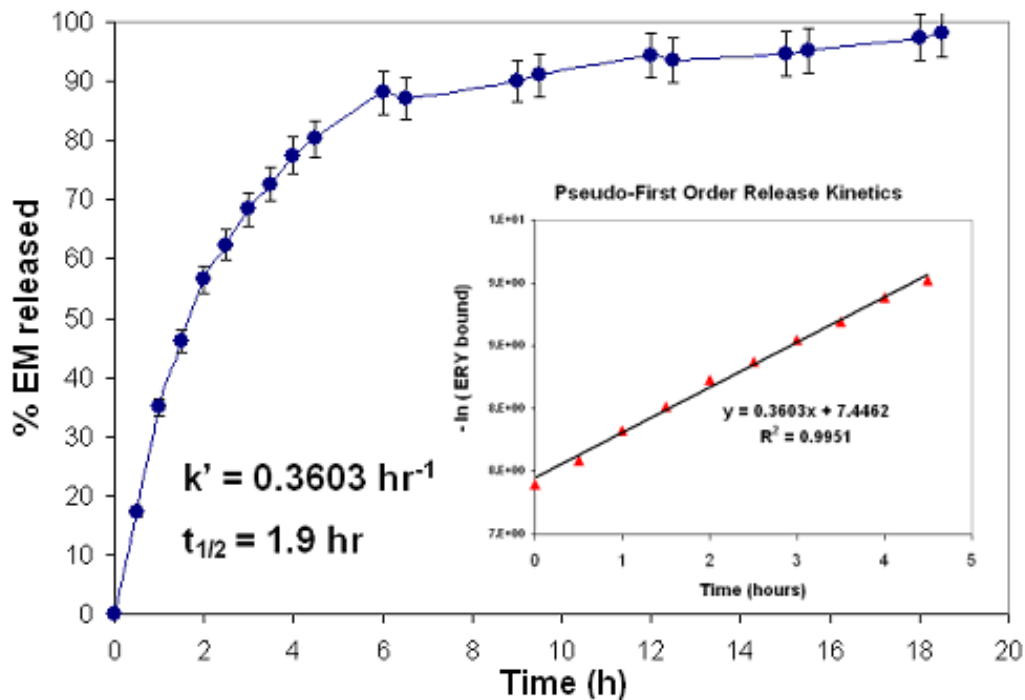
Figure 17. Drug release profile of dendrimer-EM conjugate (**5**) in PBS buffer pH 7.4.

To confirm that the EM release was due to hydrolysis of the ester linkage another control experiment was carried out. The conjugate was dissolved in anhydrous DMSO and the stability was analyzed for 24 hours. The conjugate was completely stable in anhydrous condition and did not release any EM. The drug release from the conjugate followed pseudo-first order reaction kinetics (k' = 0.36 h^{-1}, t$_{1/2}$ = 1.9 hrs) as determined by plotting natural logarithm of ester linked EM against time (Figure 17). The rate constant was determined from the linear regression of this graph where the slope of the line is the reaction rate constant. This release profile is very appropriate for the present application and it is anticipated that the dendrimer will transport the drug inside cells and release it over a period of several hours.

2.4.5 The Cytotoxicity of Dendrimer-EM Conjugates on RAW 264.7 Macrophages

In order to assess the efficacy, it was important to show that the conjugate was non cytotoxic. The concentrations of EM in the X-axis are on drug basis (Figure 18). The free dendrimer concentration was based on the amount of dendrimer present in the dendrimer-drug conjugate, at the indicated EM concentration. For example, at the highest concentration of EM (10 µg/mL), is equivalent to ~60 µg/mL of dendrimer-EM conjugate. Therefore, 50 µg/mL of the free dendrimer was used as control.
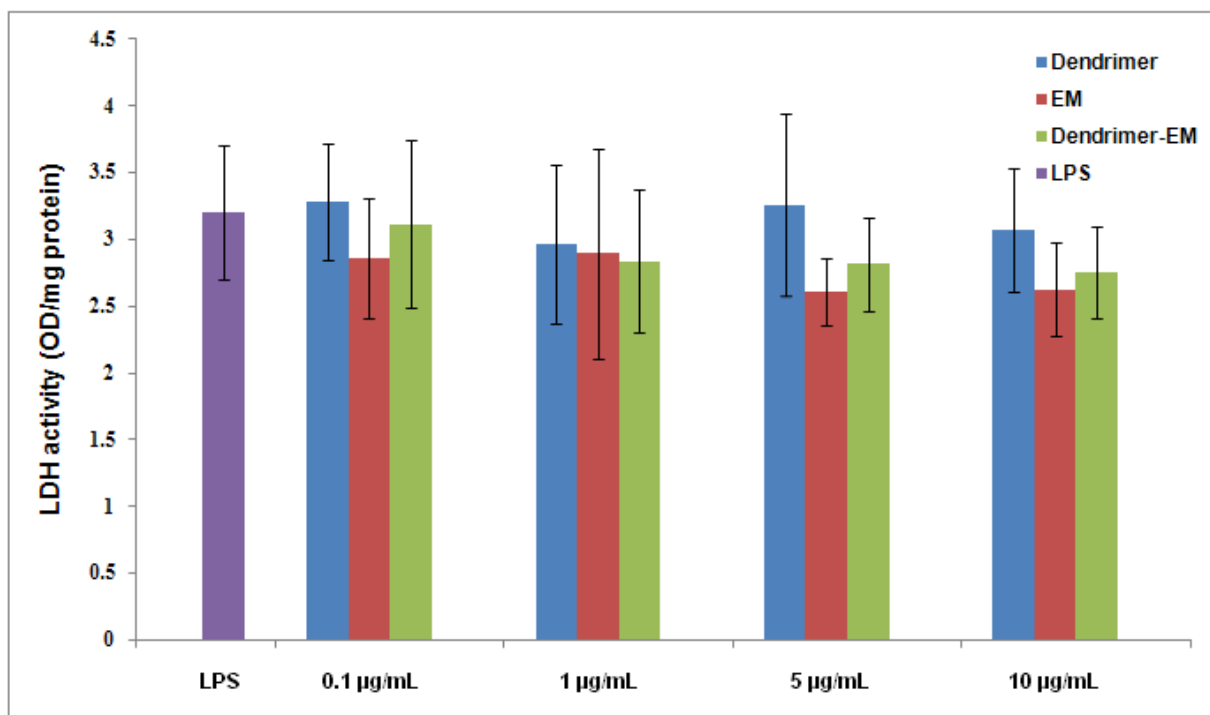
Figure 18. Effect of dendrimer-EM conjugate (**5**) on the release of LDH in LPS-stimulated RAW 264.7 cells. Three independent experiments were performed, and data are mean ± SD of six samples per group.

As shown in Figure 18, free dendrimer, EM and dendrimer-EM conjugate did not show appreciable cytotoxicity in LPS activated RAW 264.7 cells at the concentrations up to 10 µg/mL

for a treatment period of 48 hours, based on the LDH assay. Since these are the same activated

cells on which the efficacy is tested, the non-cytotoxic behavior of the compounds suggests that

the efficacy reported is primarily due to the anti-inflammatory activity.

2.4.6 Dendrimer-EM Conjugate Inhibited NO Production

RAW 264.7 cells were cultured with LPS (1 µg/mL) in the presence of dendrimer-EM for

48 hours, a concentration-dependent inhibition of NO^{2-} generation was observed (Figure 19).

These macrophages are the *in vivo* targets in the orthopedic applications envisages for these

conjugates. The stimulation by LPS causes the macrophages to release the inflammatory

markers, suppression of which would be a measure of efficacy. As shown in Figure 19,

dendrimer-EM significantly inhibited NO^{2-} release, as compared with untreated cells, and

EM-treated cells at the concentration of 1-10 µg/mL. Interestingly, we also noticed that

dendrimer-EM demonstrated much stronger NO^{2-} production inhibition than free EM at the

dosage range of 5-10 µg/mL. The improved *in vitro* activity of the dendrimer-EM conjugate

where the drug and the dendrimer are ester-linked is significant, since polymer-drug conjugates

for cancer applications typically show lower activity *in vitro*, compared to free drug.[18,31] This

suggests that enabling an effective intracellular drug release profile (as shown in Figure 17) is

crucial for improved efficacy. The improved anti-inflammatory activity of the conjugate is

qualitatively comparable to the improvements in the activity of dendrimer-N-acetyl cysteine

conjugates with glutathione sensitive linkers.[25]
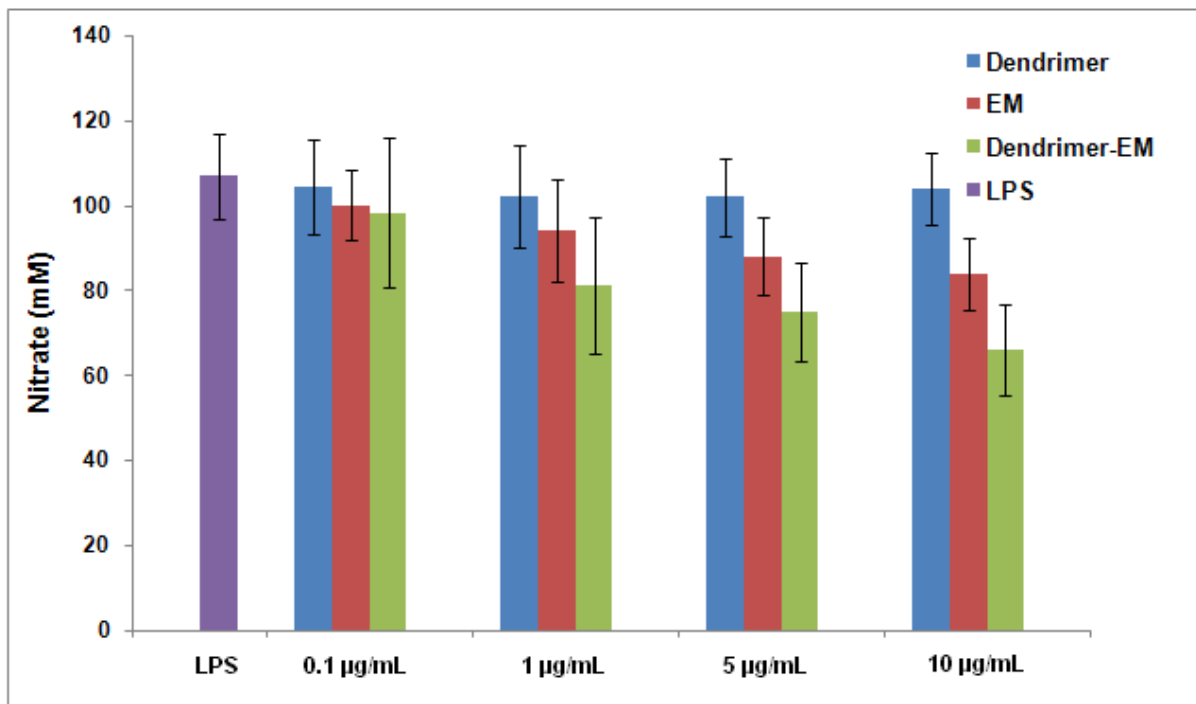
Figure 19. Effect of dendrimer-EM conjugate (**5**) on LPS-induced nitric oxide production in RAW 264.7 cells. Five independent experiments were performed, and data are mean ± SD of six samples per group. * $p < 0.05$ EM vs. dendrimer-EM, ** $p < 0.05$ EM, and dendrimer-EM vs. LPS group.

2.4.7 Dendrimer-EM Conjugate Still Preserves Its Antibacterial Activity

The antibacterial activity of the dendrimer-EM conjugate at different concentrations is shown in Figure 20. Based on a zone of inhibition evaluation, the dendrimer-EM conjugate showed similar activity, as compared to free EM with the same concentration. Furthermore, free dendrimer did not show any effect of bacterial inhibition at the concentration up to 0.2 mg/mL. This suggests that, either conjugation to dendrimers did not affect the antibacterial activity of EM, or free EM was released from the conjugate within the 24 hour period. It is most likely the latter, since the drug releases from the conjugate appreciably over this period (as shown in the release data). Of course, it is not clear if the EM is released outside the bacteria and is taken up

as free EM, or if the conjugate is internalized and the drug is released inside the cell. The results suggest that the conjugation to dendrimer did not negatively affect the antibacterial activity, while producing a superior anti-inflammatory activity.
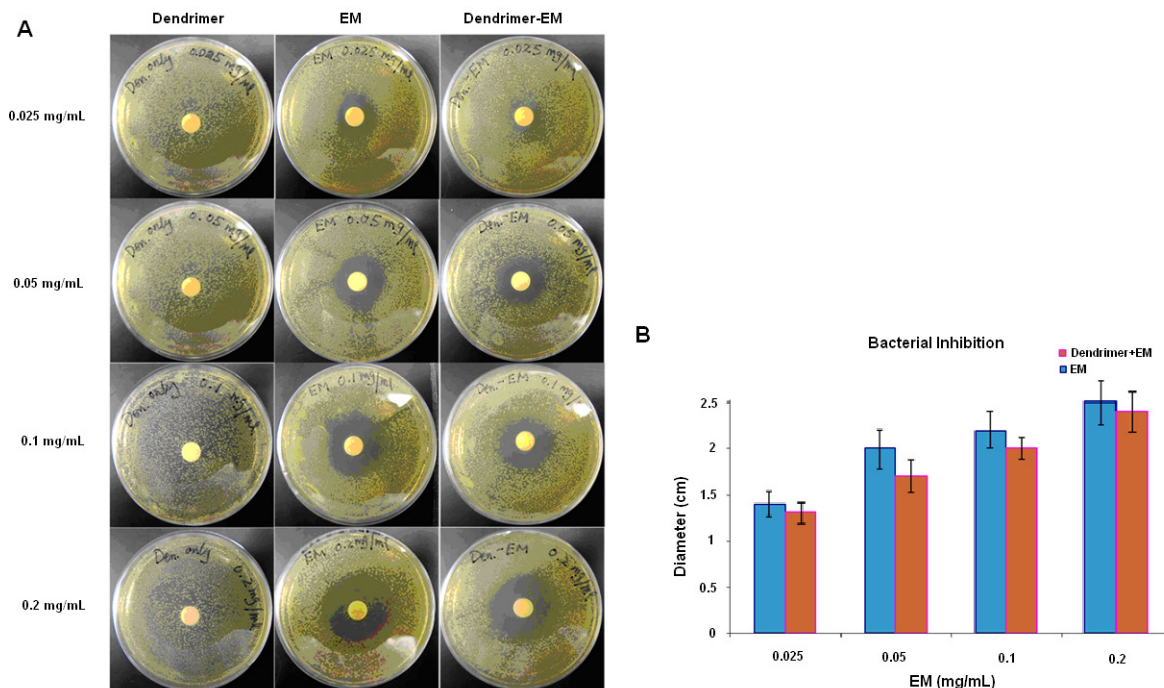
Figure 20. Zone inhibition induced by EM at different concentration. (**A**) Disk papers soaked with the PBS solution containing different concentration of dendrimer, EM and dendrimer-EM conjugate were put into a bacterial agar plate (inoculated with the bacteria strain of *S. aureus* for the zone of inhibition test. The bacteria plates were incubated for 24 hours, and then the diameter of the zone of growth inhibition around each disk to the nearest whole mm were measured. (**B**) Quantitative analysis of the size of zone of inhibition (mm) among different compounds. All the tests were performed in triplicate, and repeated two times.

2.5 Discussion

In recent years, dendrimer-based nanocarriers have been extensively used for drug and gene delivery. The drugs are attached to dendrimer surface functional groups either directly or via spacers, and very often with targeting moiety (ligand to receptor). The most common bonds are ester and amide, which can be hydrolyzed inside the cell by endosomal or lysosomal enzymes. The drug release due to hydrolysis is governed by the pH, and ester bonds are more labile towards the hydrolysis compared to amide bonds.[22] Studies have shown that ester-linked conjugates can be hydrolyzed by esterase enzymes in human plasma, while amide bonds are quite stable.[23,24] A key challenge for dendrimer-drug conjugates is to engineer systems where the drug is released over a time scale appropriate for the application.

In this study, a neutral PAMAM dendrimer-EM conjugate was prepared and evaluated for its anti-inflammatory and antibacterial activity. The hydroxy-terminated PAMAM dendrimers are more biocompatible and significantly less cytotoxic than the amine-terminated counterparts.[67] PAMAM G4-OH was reacted to a protected amine linker followed by deprotection to obtain a bifunctional dendrimer that contains 10-15% amine groups. EM was modified to EM-2'-glutarate and conjugated to the bifunctional dendrimer through an amide bond. A combination of HPLC, proton NMR and MALDI-TOF analyses showed that the conjugates were 'pure' with a drug payload of ~16% by weight, which is relatively high for polymer conjugates, yet was very soluble in PBS buffer. The conjugate released the drug effectively, with more than 90% of free drug over a period of 10 h. The efficient release of drug from 2'-position of EM preferentially is due to tertiary amine group present in the vicinity of 2′-position in EM. The conjugate was non cytotoxic to RAW 264.7 macrophages (the target cells

for anti-inflammatory activity), and showed improved efficacy over free drug. In LPS activated macrophages, the conjugate was more effective in reducing nitrite production (a measure of anti-inflammatory activity) compared to free drug. The antibacterial activity of the conjugate was comparable to free drug.

Our study indicated that the dendrimer-EM conjugates have a high drug payload (16%), and improve the solubility of the drug, and could lead to improved activity. These are especially important in delivering sufficient amount of EM to the site of periprosthetic inflammation and reducing local inflammation in a sustained manner.

2.6 Future Work

2.6.1 *In Vivo* Efficacy of Dendrimer-EM Conjugate

Since dendrimer-EM showed an improved efficacy *in vitro* compared to free EM, an *in vivo* study can be demonstrated using BALB/C mouse osteolysis model. Dr. Ren and his group used this model to evaluate *in vivo* efficacy of free EM.[59] It is created by introducing the ultrahigh molecular-weight polyethylene (UHMWPE) into established air pouches on BALB/c mice where UHMWPE debris induces tissue inflammation. A preliminary study was done by Dr. Ren in collaboration with our group where these mice were treated with dendrimer-FITC conjugates (Figure 21). As it can be seen from the images dendrimers showed to have an affinity for preferential accumulation in areas associated with periprosthetic inflammation. Based on these results we can expect that dendrimer-EM nanodevices can lead to improved *in vivo* efficacy that is the delivering of sufficient amount of EM using dendrimer as a vehicle to the site of periprosthetic inflammation and the local inflammation could be reduced in a sustained manner.
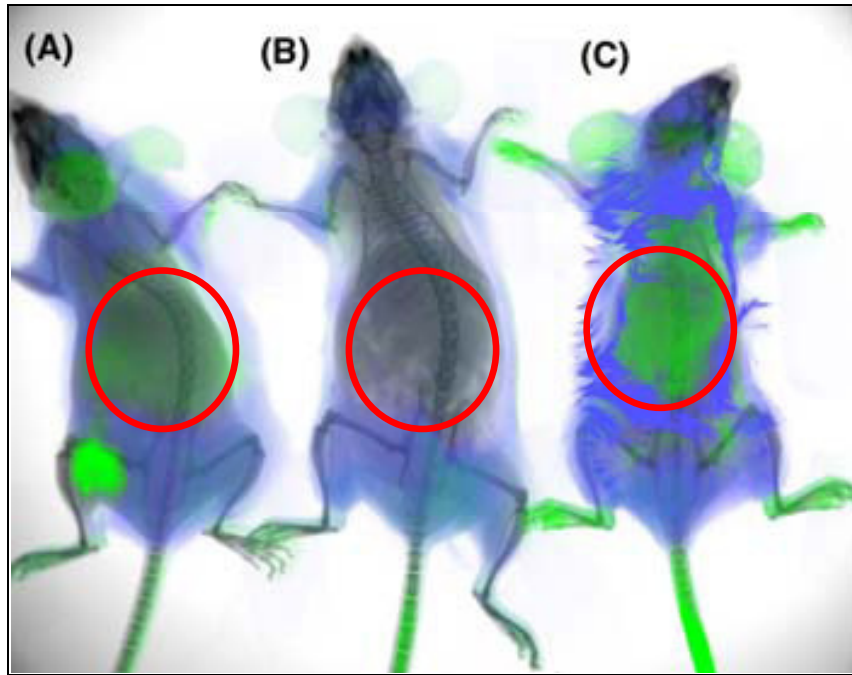
Figure 21. BALB/C mice, osteolysis model, treated with: (**A**) PAMAM dendrimer-FITC (green) - intraperitonial administration, (**B**) Saline solution with free FITC - intravenous administration, and(**C**) PAMAM dendrimer-FITC (green) - intravenous administration**.**

CHAPTER 3 "PAMAM DENDRIMER-BASED DIAGNOSTIC NANODEVICES FOR IMPROVED DETECTION OF TNF-α CYTOKINE"

3.1 Abstract

A novel dendrimer-based sandwich type enzyme-linked immunosorbent assay (ELISA) kit was developed for the detection of recombinant human tumor necrosis factor-alpha (TNF-α). Hydroxyl terminated generation four poly(amidoamine) dendrimer (PAMAM-OH) was used for the development of a solid phase bio-sensing platform. The surface of the ELISA plate was modified with polyethylene-glycol (PEG) by reacting PEG-maleimide and PEG-hydroxy to get maleimide reactive surface groups. A thiol functionalized PAMAM-OH was synthesized and immobilized on the PEG-functionalized assay plate and the remaining thiol groups of dendrimer were converted to hydrazide groups. A capture antibody was oxidized and covalently immobilized onto dendrimer-modified ELISA plate which gives antibody favorable orientation for the antigen binding sites toward the analyte. The dendrimer modified plate showed enhanced sensitivity and the detection limit for TNF-α was found to be 0.48 pg/mL, which is significantly better than the commercially available ELISA kit. The selectivity of the dendrimer-modified ELISA plate was examined by studying TNF-α in a mixture of cytokines which gave similar results. Dendrimer-modified ELISA plate provides a greater opportunity for the detection of a wide range of cytokines and biomarkers.

3.2 Introduction

One of the greatest challenges faced by modern perinatal medicine is preterm birth (PTB) and perinatal morbidity. Intra-amniotic infection/inflammation (IAI) is one of the most important causes of preterm birth. The relationship between IAI and preterm labor has been well established.[68] It accounts for 75% of perinatal mortality and 50% of perinatal morbidity.[69,70] Early detection of the infection is also challenged by the sub-clinical nature of the disease.[71,72] Fever, uterine tenderness and fetal tachycardia occur late in pregnancy and present in small portion (12.5%) of the women with microbiological evidence of infection.[73,74] An elevated level of pro-inflammatory cytokines (TNF-α, IL-6, IL-1β, and MMP-8) are found in infected intra-amniotic fluid, which are biomarkers for early detection.[75,76] The development of sensitive and specific diagnostic device which will enable an early detection and treatment to prevent fetal damage would be of great interest. The importance of detection of these cytokines is also enhanced by their association with pulmonary and neurodegenerative diseases. There are plenty evidence to prove the presence of an elevated level of TNF-α in the patients suffering from Alzheimer's disease[77], Parkinson's disease[78], Multiple Sclerosis[79] and Chronic Obstructive Pulmonary disease (COPD)[80].

TNF-α is a pro-inflammatory cytokine that regulates the immune system inducing inflammation and apoptosis in many organs of the body. In the brain, overexpression of TNF-α in microglia cells causes neural death which is linked with neurological disorders. An increased level of TNF-α is also associated with pre-term birth and cerebral palsy.[81] Therefore, determining the level of TNF-α in amniotic fluid is essential for an understanding of the mechanism of pre-term birth and its prevention. Enzyme-linked immunosorbent assay (ELISA) is the most

common method used to determine the concentration of TNF-α. In literature, beside the ELISA, various methods have been reported for determination of TNF-α concentration. These methods include radioimmunoassays (RIA),[82] bioassays,[83] chemiluminescence[84] and chemiluminescence imaging[85], matrix-assisted laser desorption/ionization mass spectrometry (MALDI-MS)[86], immuno-PCR[87] and immuno-PCR assay[88], fluorescence immunoassay[89], and electrochemical immunosensor[90]. The detection limits for cytokines of currently used immunosensors are at a much higher level of concentration. Our goal is to develop a diagnostic device that will detect the presence of TNF-α at a lower level by improving its sensitivity and specificity. The solid-liquid interface results in sensitivity, and interaction at the analyte-ligand provides selectivity and stability.[91] In developing an immunosensor, the immobilization of antibodies is a key step. The antibodies should be immobilized onto a substrate at high density with uniform distribution followed by retaining their specific antigen-binding activities, and finally maintaining accessibility to the antigens.[16] The aim is to develop a biosensor which will maximize the biochemical activity and minimize nonspecific protein adsorption. In effort to improve the existing detecting devices, use of dendrimers could play a very important role.

Unlike linear polymers, dendrimers do not form entangled chain but unique in shape with numerous chain ends which can be functionalized. They are stable, can be closely packed on the substrate surface, and have multiple branch ends available for further conjugation.[92,93] Dendrimers have all the specification to be used in next generation of biosensors.[8,94] Dendrimers have been recently reported to significantly increase binding ability and homogeneity in DNA microarray analysis.[11,95,96] Dendrimers are also utilized in electrochemical immunosensor,[13,97] biosensor-based encapsulated Platinum nanoparticles,[9,98] regenerable affinity-sensing surfaces[15]

and surface plasmon resonance biosensor[99]. The application of dendrimer is extended to preparation of metal-dendrimer nanocomposites using PAMAM dendrimers with various terminal groups.[100-101] Carboxyl terminated PAMAM dendrimers have shown to lower the nonspecific cellular protein adsorption and enhancing antibody binding properties.[16]

Recently we have reported a highly sensitive dendrimer-based biosensing platform for IL-6 and IL-1β cytokines detection in which pegylated ELISA plate was modified using amine terminated PAMAM dendrimer.[17] In continuing our effort, we have developed a solid phase biosensing platform using generation four hydroxyl terminated PAMAM dendrimer for TNF- α cytokine detection. The synthesis, characterization, fabrication and functional evaluation of this biosensing platform for TNF-α detection is described in this Chapter. The plate surface was co-immobilized with hydroxyl polyethylene glycol (NH_2-PEG-OH) and maleimide PEG (NH_2-PEG-Mal). Maleimide PEG was covalently linked to PAMAM dendrimers on the surface of the plate leading to controlled dendrimer grafting density which is also responsible for the increased grafting density of the antibody. The modified ELISA plate with long PEG arms and functionalized-dendrimer provides diffusional and conformational flexibility, which gives more favorable antibody-antigen interactions. The resulting dendrimer functionalized plate was employed as template to immobilize the anti-human TNF-α antibody and the performance was evaluated by the detection of TNF-α using TMB detection method. The dendrimer-based assay was compared to commercially available TNF-α kit.

3.3 Materials and Methods

3.3.1 Materials

Hydroxyl terminated generation four poly(amidoamine) dendrimer (G4-OH) was obtained from Dendritech Inc. N-(3-dimethylaminopropyl)-N-ethylcarbodiimide hydrochloride (EDC), 4-(dimethylamino)pyridine (DMAP), *N*-succinimidyl-3-(2-pyridyldithio)-propionate (SPDP), tris(2-carboxyethyl) phosphine (TCEP) and MALDI-TOF mass reference standards were purchased from Sigma-Aldrich. Trifluoroacetic acid (TFA) was obtained from EMD Chemicals. Hydoxyl terminated Polyethylene glycol (NH_2-PEG-OH, 2.0 kDa) and maleimide terminated PEG (NH_2-PEG-Mal, 3.4 kDa) were obtained from JenKem Technology, Beijing, China and Creative PEGworks, Winston Salem, USA respectively. DMSO-d_6 was from Cambridge Isotope Laboratories. Anhydrous DMSO and dichloromethane (DCM) were from Acros Organics, USA. *N*-(ε-maleimidocarproic acid) hydrazide (EMCH) was from Pierce. All other solvents and chemicals used were from Fisher Scientific. Regenerated cellulose (RC) dialysis membrane (molecular weight cut-off 1000 Da) was obtained from Spectrum Laboratories. Recombinant human TNF-α, monoclonal TNF-α anti-human antibody, biotinylated anti-human TNF-α antibody, streptavidin-HRP (DY998), reagent diluent (DY995), substrate reagent (TMB, DY999), stop solution (DY994) and wash buffer (WA126) were obtained from R&D Systems. ELISA plates were purchased from Corning (high bind plate).

3.3.2 NMR Spectra Analysis

NMR spectra were recorded on a Varian INOVA 400 spectrometer using DMSO-d_6. Proton chemical shifts are reported in ppm (δ) and tetramethylsilane (TMS) used for internal standard.

3.3.3 MALDI-TOF Mass

Matrix-assisted laser desorption ionization-time of flight (MALDI-TOF) mass spectra were recorded on a Bruker Ultraflex system. Cytochrome C (MW 12,361 g/mol), and Apomyoglobin (MW 16,952 g/mol) were used as external standards. A dendrimer solution was prepared by dissolving 2 mg of dendrimer in 1 mL of DMSO. The matrix solution was prepared by dissolving 20 mg of trans-3-indoleacrylic acid matrix in 1 mL of the 1:1 mixture of deionized water and acetonitrile (0.1% TFA). Analytical samples were prepared by mixing 10 μL of dendrimer solution with 100 μL of matrix solution, followed by deposition of 1 μL of sample mixture onto a 384-well aluminum plate. This mixture was allowed to air dry at room temperature. All data processing was performed using Bruker Daltonics flexAnalysis software.

3.3.4 HPLC

High performance liquid chromatography (HPLC) characterization was carried out using Waters HPLC instrument. Two pumps, an auto-sampler and dual UV detector are interfaced to Breeze software. The HPLC chromatogram was monitored at 210 and 238 nm simultaneously using the dual UV absorbance detector. H_2O:ACN (0.14% TFA) was used as mobile phase. Both phases were freshly prepared, filtered, and degassed prior to use. Symmetry300 C_{18} reverse-phase column (5 µm particle size, 25 cm × 4.6 mm length × I.D.) equipped with a Supelguard Cartridges (5 µm particle size, 2.0 cm ×3.9 mm length × I.D.) was used for characterization of the conjugates. HPLC analysis was done using 90:10 to 30:70 (H_2O:ACN) gradient flow in 30 minutes with flow rate of 1 mL/min.

3.3.5 Synthesis of Bifunctional G4 PAMAM-OH-PDP Dendrimer

The reaction scheme for the preparation of the bifunctional G4 PAMAM-OH-PDP is outlined in Figure 22. The 5-(Boc-amino)valeric acid (228.2 mg, 1.0504 mmole) was dissolved in DMSO (10 mL), then EDC (603.8 mg, 3.15 mmole) and DMAP (12.0 mg, 0.0982 mmole) were added under nitrogen atmosphere. The mixture was allowed to stir for 1 hour at room temperature and PAMAM G4-OH (500.0 mg, 0.0350 mmole) dissolved in DMSO (5 mL) was added to the reaction mixture. The reaction was stirred for 48 hours at room temperature. The resulting solution was dialyzed extensively with DMSO (dialysis membrane of molecular weight cutoff = 1000 Da) for 24 hours and with deionized water for 6 hours. The obtained reaction mixture was then lyophilized yielding 445.0 mg (0.0242 mmole) of G4-OH-Link-Boc intermediate. This intermediate contains Boc protected amino groups on the surface. ^{1}H NMR (DMSO-d_6, 400 MHz): δ (ppm) 8.04 (bs, CO-NH, Boc), 7.92 (bs, CO-NH, G4-OH), 7.77 (bs, CO-NH, G4-OH), 4.69 (bs, OH, G4-OH), 3.96 (m, CH_2OCO), 3.37-2.18 (986H, m, aliphatic protons of G4-OH and CH_2 of linker), 2.01 (m, CH_2, methylene protons of linker), 1.45 (m, 2 × CH_2, methylene protons of linker), 1.34 (s, 3 × CH_3, methyl groups of Boc).
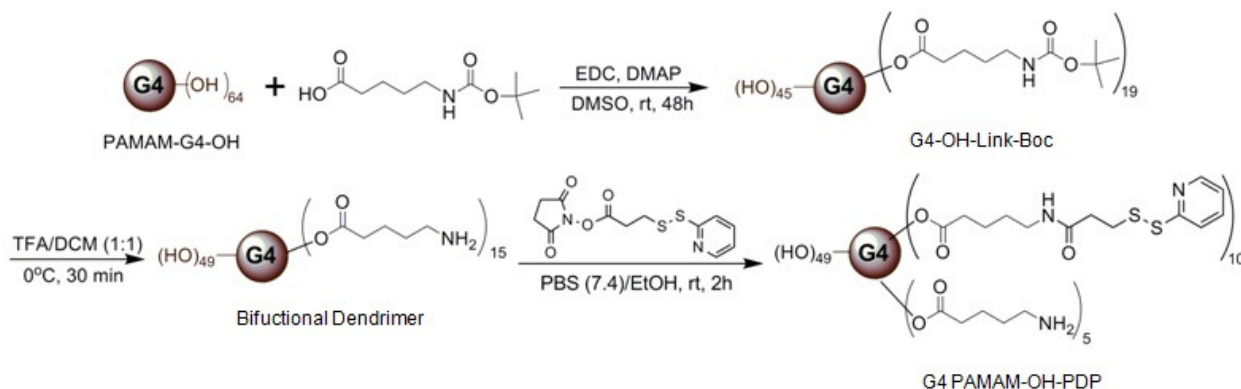
Figure 22. Synthesis of G4 PAMAM-OH-PDP dendrimer .

The deprotection of Boc protected amino groups was done by adding 6.0 mL of TFA:DCM (1:1) to 445.0 mg of G4-OH-Link-Boc in a round bottom flask at 0°C. The reaction was carried out for 1 hour at 0 °C, and then the solvent was removed at reduced pressure. The mixture was re-dissolved in DMSO and dialyzed with DMSO for 24 hours and deionized water for 6 hours. The reaction mixture was then lyophilized yielding 298 mg of bifunctional dendrimer. ^{1}H NMR (DMSO-d_6, 400 MHz): δ (ppm) 7.92 (bs, CO-NH, G4-OH), 7.77 (bs, CO-NH, G4-OH), 4.69 (bs, OH, G4-OH), 3.99 (t, CH_2OCO), 3.40-2.47 (986 H, m, aliphatic protons of G4-OH and CH_2 of linker), 2.31 (m, CH_2, methylene protons of linker), 1.53 (m, 2 × CH_2, methylene protons of linker). Then the bifunctional dendrimer (150.0 mg, 0.00937 mmole) was dissolved in 9 mL of PBS, pH=7.4. To this SPDP (87.0 mg, 0.2798 mmole) in 3.5 mL ethanol was added. The reaction mixture left to react for 2 hours at room temperature. The resulting solution was dialyzed extensively with water (dialysis membrane of molecular weight cutoff = 1000 Da) for 24 hours. The obtained reaction mixture was then lyophilized yielding 90.0 mg (0.00529 mmole) of G4 PAMAM-OH-PDP dendrimer conjugate. The conjugate was characterized by proton NMR. ^{1}H NMR (DMSO-d_6, 400 MHz): δ (ppm) 8.43 (d, 1H, pyridyl H), 8.12 (bs, CO-NH, linker, G4-OH), 7.98 (bs, CO-NH, G4-OH), 7.81 and 7.73 (m, pyridyl Hs), 7.22 (t, 1H, pyridyl H), 4.75 (bs, OH, G4-OH), 3.98 (m, CH_2OCO), 3.51-2.08 (m, 990H, aliphatic protons of G4-OH, CH_2 of linker, and CH_2 of PDP.), 2.04 (m, CH_2, methylene protons of linker), 1.48 (m, CH_2, methylene protons of linker), 1.36 (m, CH_2, methylene protons of linker). MALDI-TOF (pos) m/z 17141.1.

3.3.6 Synthesis of EMCH Functionalized G4 PAMAM-OH-PDP Dendrimer

The reaction scheme of EMCH functionalized G4 PAMAM-OH-PDP synthesis is shown in Figure 23. The G4 PAMAM-OH-PDP dendrimer (2.4 mg, 140 nmole) was dissolved in 1 mL of PBS/EDTA buffer (pH 7.4, 5 mmole EDTA). To this solution, 0.80 mg of TCEP (2.80 µmole, 20 equiv.) in 1mL of PBS/EDTA buffer (pH 7.4, 5 mmole EDTA) was added. The reaction mixture was evacuated, flushed with N_2 and the reaction mixture was stirred for 15 minutes at room temperature under N_2 to get the free thiolated conjugate. Then the reaction mixture was cool down to 0°C and 0.72 mg of EMCH (2.10 µmole, 15 equiv.) in 1 mL of PBS buffer was added. The reaction mixture was reacted for 3 hours at room temperature under N_2. The reaction mixture was extensively dialyzed with water (dialysis membrane of molecular weight cutoff = 1000 Da) for 24 hours and lyophilized to give EMCH functionalized G4 PAMAM-OH-PDP conjugate as a pale yellow oily solid. The EMCH functionalized G4 PAMAM-OH-PDP conjugate was characterized by proton NMR. ^{1}H NMR (DMSO-d_6, 400 MHz): δ (ppm) 8.90 (s, 1H, hydrazide amide NH), 7.94 (bs, CO-NH, linker, G4-OH), 7.82 (bs, CO-NH, G4-OH), 4.8 (bs, OH, G4-OH), 3.95 (m, CH_2OCO), 3.50-2.00 (m, 997H, aliphatic protons of G4-OH, CH_2 of linker, CH_2CH_2S CH CH_2, NCH_2, and NH_2), 1.89 (m, CH_2, methylene protons of linker, and CH_2NHNH$_2$), 1.58-1.32 (m, CH_2, methylene protons of linker, and CH_2NHNH$_2$ of EMCH), 1.30-1.05 (m, CH_2, methylene protons of linker, and of EMCH).
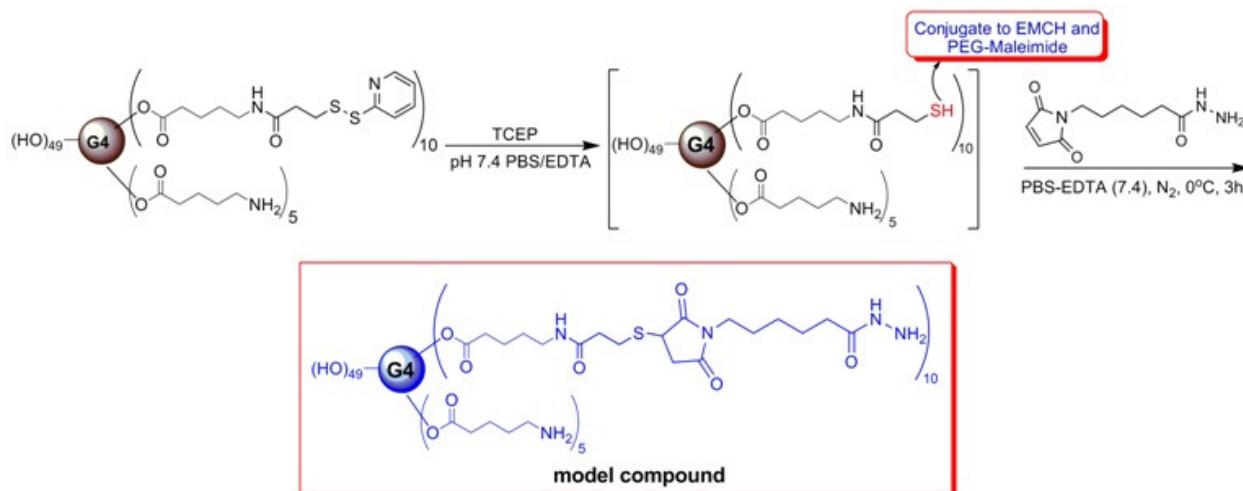
Figure 23. Synthesis of EMCH functionalized G4 PAMAM-OH-PDP as a model compound.

3.3.7 Modification of ELISA Plate with PEG

The solutions of EDC and HOBt in MES buffer (pH 6.5), 1mg/mL, were prepared. The amounts of 75 μL of EDC solution and 60 μL of HOBt solution were added to each well of ELISA plate (391 nmol of each per well). Then 10 μL of NH$_2$-PEG-MeI (MW=3.4 kDa) in MES buffer (pH 6.5), 12.52 μg/mL, was added to each well (7.4 pmole/well) and incubated for 30 minutes at room temperature. To each well 30 μL of NH$_2$-PEG-OH (MW=2 kDa) was added, 5.81 mg/well. The plate covered with aluminum foil and left to incubate for 8 hours at room temperature with constant shaking. Then ELISA plate was washed with PBS buffer (pH 7.4) three times and with deionized water three times, dried under nitrogen, and stored at -20 ˚C.

3.3.8 Conjugation of G4 PAMAM-OH-PDP Dendrimer to Pegylated ELISA Plate

G4 PAMAM-OH-PDP dendrimer (1.2 mg, 70 nmole) was dissolved in 1 mL of PBS/EDTA buffer (pH 7.4, 5 mmole EDTA). To this solution, 0.4 mg of TCEP (1.4 μmole, 20 equiv.) in 0.5 mL of PBS/EDTA buffer (pH 7.4, 5 mmole EDTA) was added. The reaction mixture was evacuated, flushed with N$_2$ and the reaction mixture was stirred for 15 minutes at

room temperature under N_2 to get the free thiolated conjugate. Then the reaction mixture was transferred in glove box and cooled down to 0°C. To this 0.16 mg of EMCH (0.49 µmole, 7 equiv.) in 0.5 ml of PBS buffer was added and incubated for 20 minutes at 0°C. The amount of 10 µL of this reaction mixture was diluted to 31.5 mL with PBS buffer (pH 7.4) and 270 µL of diluted solution was added to each well of pegylated ELISA plate (3 pmole/well). The plate was sealed and incubated for 3 hours at room temperature in glove box with constant shaking. Then 10 µL of 2-mercaptoethanol in PBS (pH 7.4) was added to each well (1 µL of 2-mercaptoethanol/well) and incubated for 1 hour at room temperature. The ELISA plate was washed with PBS buffer (pH 7.4) four times and with deionized water four times, dried under nitrogen, and stored at -20 °C.

3.3.9 Oxidation of Monoclonal Anti-Human TNF-α/TNFSF1 Antibody (MAB610) and Its Immobilization to Dendrimer Modified ELISA Plate

The oxidation was done by using sodium periodate. 500 µg of MAB610 was dissolved in 1 mL of PBS (pH 7) buffer. To this 100 µL of $NaIO_4$ solution in PBS (pH 7) added at 4°C (5 µg $NaIO_4$ per 50 µg MAB610). The reaction mixture left to react for 15 min at 4°C protected from light. Then the reaction mixture was transferred to Amicon centrifuge filter tube and was centrifuged for 30 min, at 4°C, and 2500 rpm. The concentrated sample, approximately 60 µL was diluted with PBS buffer (pH 7.4) to 1 mL and loaded to PD-10 column. The column was equilibrated with PBS (pH 7.4) according the spin protocol. Then the column was centrifuged at 1000 G, and 4°C for 2 min. The concentrated antibody was diluted to 11 mL with PBS buffer (pH 8), and 270 µL added to each well of dendrimer modified ELISA plate (3 µg/well). The ELISA plate was sealed and incubated for 3 hours at 4°C with continuous shaking. Then 10 µL

of NaCNBH$_3$ solution in PBS buffer (pH 8) (1mg NaCNBH$_3$ per 1 mL buffer) was added to each well and incubated for 1 hour at 4°C with continuous shaking. After 10 µL of ethanolamine solution in PBS buffer (pH 8) (1µL ethanolamine per 1 mL buffer) was added to each well and incubated for 30 min at 4°C with continuous shaking. Antibody immobilized dendrimer modified ELISA plate then washed with wash buffer (WA126) seven times to make sure that there are no chemicals left. The plate dried by blotting it against clean paper towels. Then 300 µL of reagent diluents added to each well. The plate was sealed, covered by aluminum foil and left overnight at 4°C. Then the plate was washed again with wash buffer, dried in the same way as above and made ready for assay to be performed, which has to be done immediately.

3.3.10 Assay Procedure

The ELISA plate was washed with wash buffer seven times (300 µl per well). Twelve different dilutions (concentrations from 460-0 pg/mL) of TNF-α standard in reagent diluents were prepared. 100 µL of each dilution were added per well in triplicate. The plate was sealed and incubated for 2 hours at room temperature. Then each well was washed with 300 µL wash buffer seven times. After the plate was dried by blotting it against clean paper towels, 100 µL of biotinylated antihuman TNF-a detection antibody (BAF 210, 1 µg/mL in reagent diluents) was added to each well. The plate was sealed and incubated for 2 hours at room temperature. The plate was washed and dried again in the same way as above and 100 µL of streptavidin-horseradish peroxidase conjugate in reagent diluents was added to each well. The plate was incubated for 30 min at room temperature avoiding light and washed again with wash buffer. Then 100 µL of substrate solution was added to each well and incubated 30 min in the dark at room temperature. To stop the color reaction 50 µl of stop solution (2N sulfuric acid) was added

to each well without washing the plate. The absorbance was measured immediately using a plate reader (Molecular Devices, SpectraMax M2) set at 450 and 570 nm.

3.4 Results and Disscusion

3.4.1 Synthesis of Bifunctional G4 PAMAM-OH-PDP Dendrimer

Previously published results indicate that many commercially available ELISA plates have problem due to nonspecific protein adsorption.[103] In order to reduce the non-specific protein adsorption and to improve the specificity and sensitivity of immunoassay technique, the hydroxyl-terminated G4-PAMAM dendrimer was used to prepare an assay platform for TNF-α cytokine detection. A bifunctional dendrimer was prepared by modifying few hydroxyl terminal groups of generation four PAMAM dendrimer (G4-OH) to reactive amine for this platform. The detailed synthetic procedure for this modification was reported by our group previously.[104] In brief, the G4-OH was reacted with 5-Boc-amino-valeric acid to get Boc protected amine groups followed by deprotection with trifluoroacetic acid to generate a bifunctional dendrimer (**2**) having free amine groups on the surface. To be able to immobilize dendrimer on pegylated ELISA plate, the resulting bifunctional dendrimer was conjugated with linker N-succinimidyl 3-(2-pyridyldithio)-propionate (SPDP) through amide bond (Figure 22). SPDP provides a protected thiol in the form of a disulfide bond. The conjugate was characterized by HPLC, proton NMR, and MALDI-TOF mass. HPLC gave very broad peak at 9.55 min due to large size and low polarity compared to starting dendrimers (Figure 24). The number of attached PDP groups to dendrimer was determined by NMR (Figure 25) by integrating peaks related to dendrimer amide and pyridyl hydrogens at 8.43 (d, 1H), 7.81 and 7.73 (m), and 7.22 (t, 1H) ppm. The integration revealed that 10 molecules of PDP were attached to the surface of the dendrimer. This is in a

good agreement with MALDI-TOF MS (Figure 26) which increased molecular weight indicates also that 10 molecules of PDP were added to dendrimer.

$$Number\ of\ PDP\ link = \frac{Mw\ (G4-OH-link-PDP)-Mw\ (G4-OH)}{Mw\ (link-PDP)} = \frac{17141.1-13949.9}{297} = 10.74$$
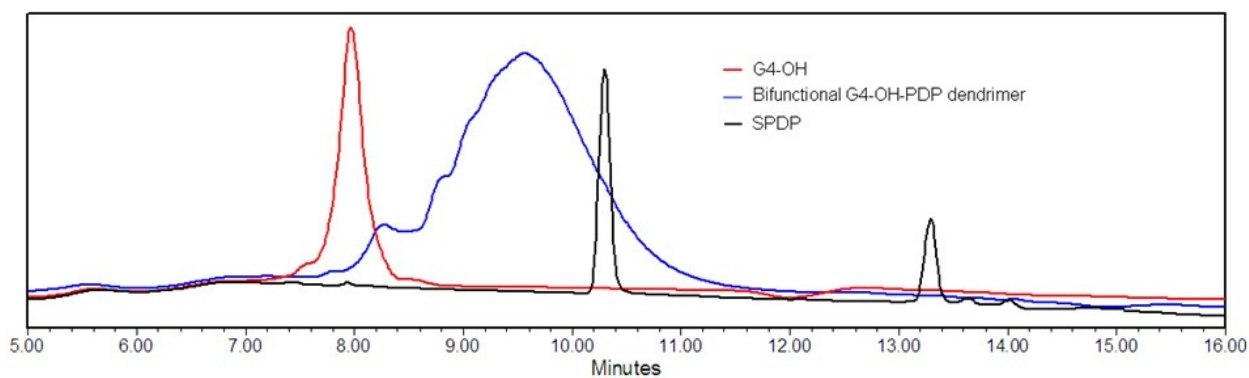
Figure 24. HPLC chromatograms of G4-OH, bifunctional G4-OH-PDP dendrimer, and SPDP at 210 nm.
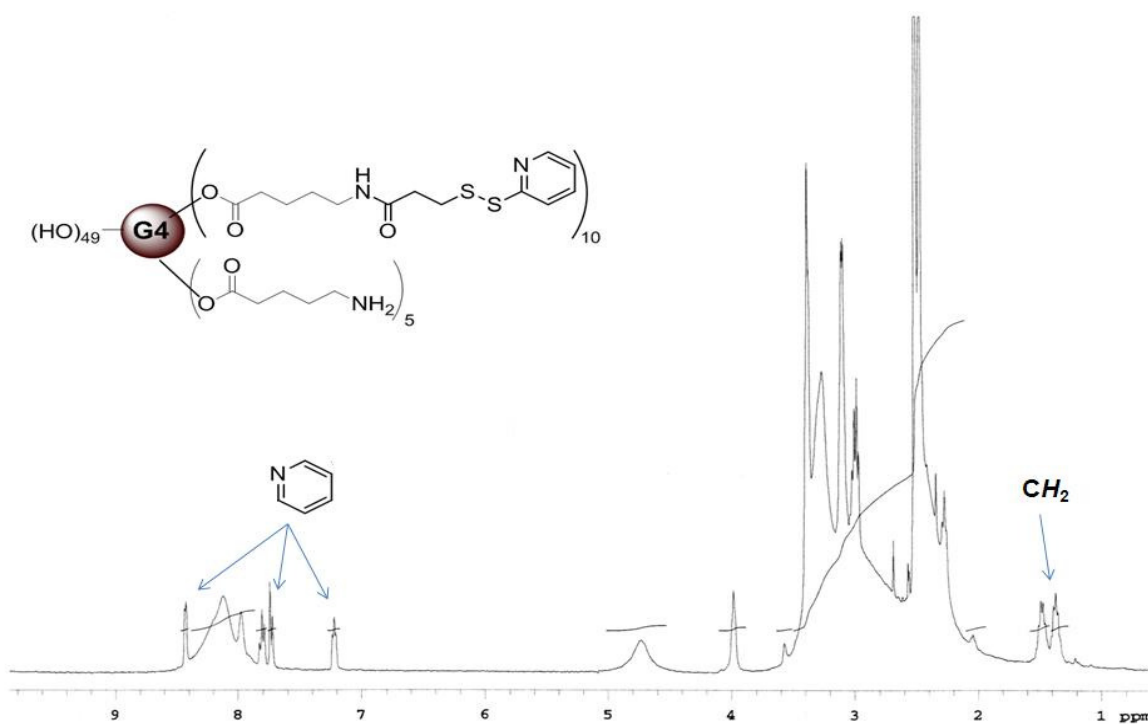
Figure 25. Proton NMR spectrum of G4 PAMAM-OH-PDP dendrimer in DMSO-d_6.
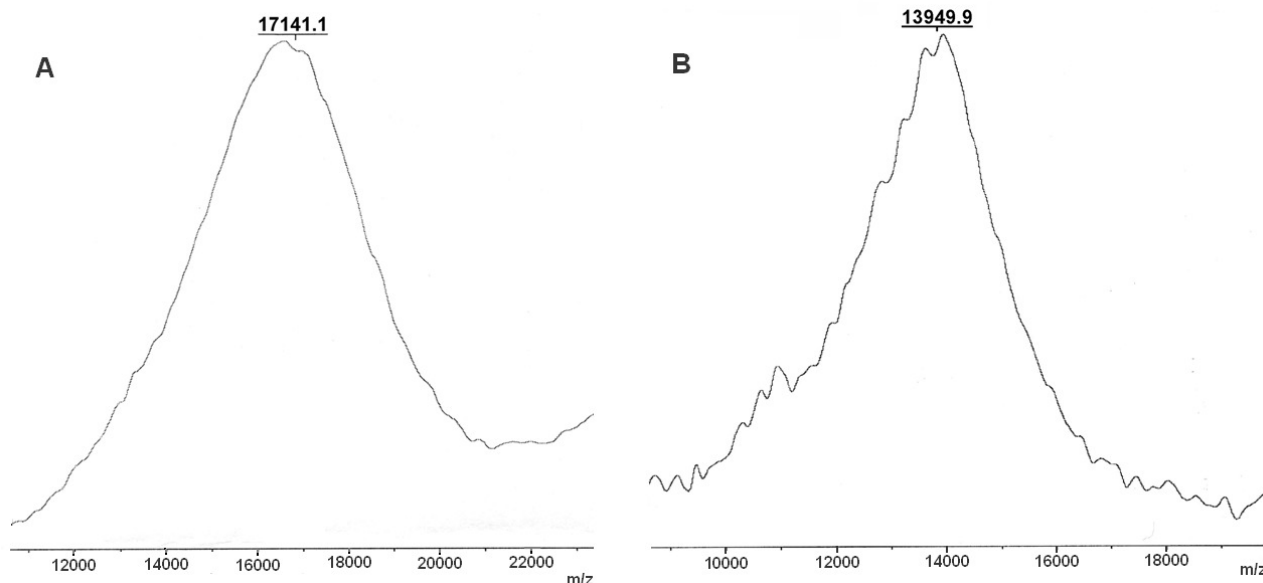
Figure 26. MALDI-TOF mass spectra of (**A**) bifunctional G4 PAMAM-OH-PDP dendrimer, and (**B**) G4-OH dendrimer.

The disulfide bond of PDP linker was reduced by tris(2-carboxyethyl) phosphine (TCEP) to thiol groups quantitatively.[105] The resulting conjugate having free thiol groups was used *in situ* without purification and reacted with seven equivalence of *N*-(ε-maleimidocarproic acid)hydrazide (EMCH) which is going to be used for antibody capturing. The remaining thiol groups were required for dendrimer immobilization onto PEG-ELISA plate by conjugation to maleimide groups. In order to prove that thiol-maleimide conjugation reaction went through, a model reaction was performed (Figure 23). Therefore, all the thiol groups were conjugated with EMCH to give hydrazide functionalized dendrimer. To prevent possible side reaction, the thiol-maleimide conjugation reaction was carried out at 0°C. The structure of of EMCH functionalized G4 PAMAM-OH-PDP conjugate was confirmed by ^{1}H NMR (Figure 27), which shows characteristic hydrazide amide proton, N*H*NH$_2$(C=O), at 8.90 ppm and no pyridyl hydrogens from PDP.
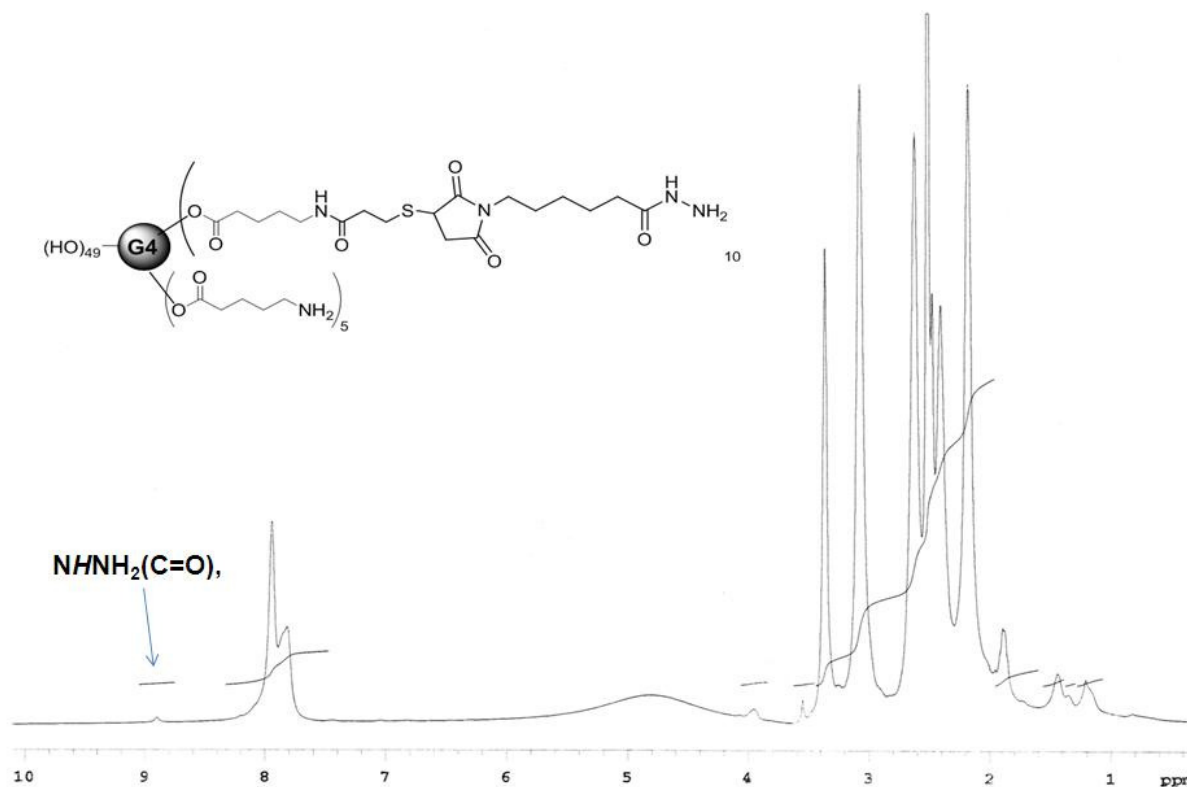
Figure 27. Proton NMR spectrum of EMCH functionalized G4 PAMAM-OH-PDP dendrimer**.**

3.4.2 Surface Modification of ELISA Plate with PEG and Dendrimer Immobilization

Due to nonspecific protein adsorption by commercially available ELISA plates, we modified our plates with polyethylene glycol (PEG). It is found that the nonspecific adsorption of proteins on the plate's surface decreases with the increasing molecular weight of PEG chain. On the other hand, by increasing PEG molecular weight the tethered chain density decreases due to the exclusion volume of each chain on the surface.[106] The ELISA plates were modified according to the procedure reported in our previous study.[17] PEG was linked to the carboxylic acid functionalized 96 well polystyrene plates. The functionalization of polystyrene plate with PEG was carried out under mild conditions to minimize ring opening side reaction. Carboxylic acid groups of polystyrene plate were activated by EDC and 1-hydroxybenzotriazole hydrate

(HOBt), Figure 28. The resulting HOBt activated carboxylic groups could be hydrolyzed under desired mild conditions which minimized the ring-opening side reaction of the NH$_2$-PEG-Mal.[107] PEG-maleimide (NH$_2$-PEG-Mal, MW 3.4k Da) and PEG-hydroxyl (NH$_2$-PEG-OH, MW 2k Da) were co-immobilized to improve the nonfouling character of the surface and also cover the 'defects' on the polystyrene plate.[103] NH$_2$-PEG-Mal groups were used for immobilization of dendrimer. Two equivalents of NH$_2$-PEG-Mal were reacted with activated carboxylic groups, based on the calculated dendrimer grafting density, considering the yield of the amidation reaction and the reduced reactivity of thiol-maleimide conjugation reaction in the presence of TCEP.[105] Thus, NH$_2$-PEG-Mal grafting density reflects the dendrimer graft density on the surface.
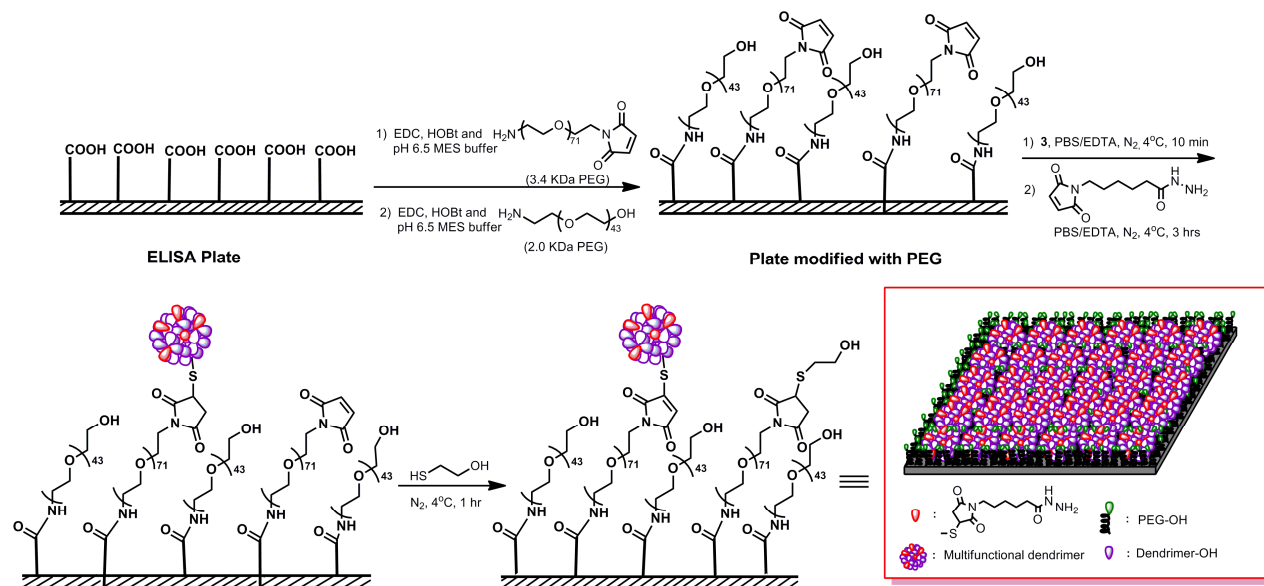
Figure 28. Schematic representation of ELISA plate modification with PEG and immobilization of G4 PAMAM-OH-PDP dendrimer on PEG layer.

Dendrimer immobilization was carried out inside the glove bag under the constant flow of nitrogen at 4°C for 3 hours. Then 2-thioethanol was added to react with unreacted maleimide

groups. The dendrimer modified plates were washed, dried, and stored at -20°C. They can be stable for several months with no signs of reduced reactivity, suggesting that the dendrimer-modified plates are stable and have an appreciable life time.

3.4.3 Antibody Immobilization onto Dendrimer Modified ELISA Plate

Antibodies play a key role in diagnostic methods; therefore the way in which they are immobilized is very important. Antibodies are proteins, also called immunoglobulins (Ig), because they are related to the immunological system. Basically they are glycoproteins having carbohydrate chains added to some of their amino acid residues. The amounts of carbohydrates can vary (3-12%) depending on the type of antibody and they are attached to the protein through N-linked glycosylation site. Most glycosylation sites are located in constant region (Fc) of the heavy chain. Glycosylation of these sites has little if any effect on binding activity of antibodies.[108] The studies showed that steric-hindrance, denaturation of antibody, and its random orientation lead to reduction of binding activity of an antibody.[109] By controlling the orientation of immobilized antibodies on the sensor surface and with decreasing steric-hindrance effects, specificity and sensitivity of an immunosensor can be increased.

The efficacious antigen binding depends on antibody immobilization method. Currently available methods often have disadvantages such as reduced antibody-antigen binding activity mostly due to random antibody orientation, denaturation, or steric-hindrance.[110] The easiest method of antibody immobilization is adsorption on a solid surface. However, adsorbed antibodies are randomly oriented and their antigen binding activity can be reduced due to denaturation. The most common method for antibody immobilization is covalent coupling using amino groups on antibody surface. The disadvantage of this method is random orientation that

leads to nonspecific binding. Some methods employ chemical immobilization of the antibodies by chemically modifying the carbohydrates on the Fc region of an antibody or selectively reducing disulfide bond of the cysteine residue in the hinge region of the antibody. Other methods use protein G and protein A for orientated immobilization that specifically bind to the Fc region of an antibody. These methods are less stable than covalent methods.

Mouse anti-human TNF-α antibodies were immobilized by their oligosaccharide moieties in the constant region to dendrimer hydrazide linker of modified ELISA plate following similar procedure that we used for IL-6 and IL-1β immobilization (Figure 29).[17]
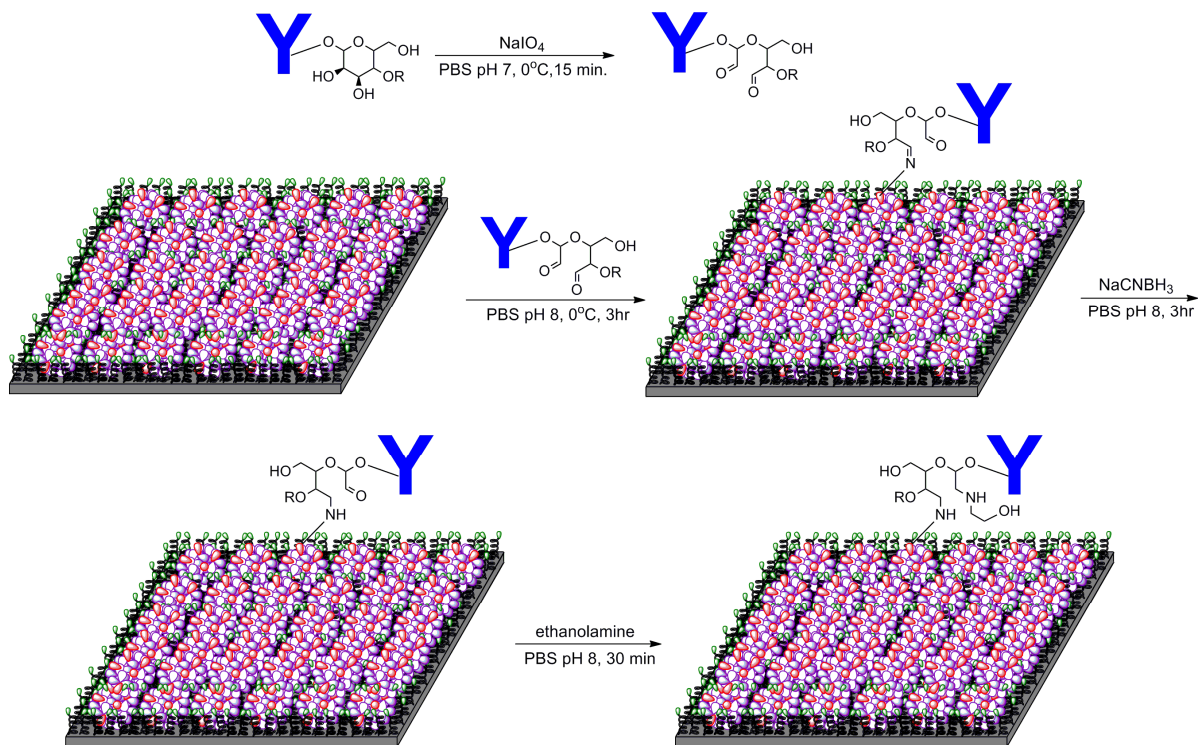
Figure 29. Schematic representation of antibody immobilization on the ELISA plate modified with multifunctional dendrimer.

First, carbohydrate vicinal hydroxyl groups in the constant region of antibody were oxidized by sodium periodate in PBS buffer (pH 7) to aldehyde groups. The number of oxidized sites

generated by NaIO$_4$ depends on pH, temperature, reaction time and the concentration of the oxidizing reagent.[111] Using Purpald test with formaldehyde as a calibrator, we examined the degree of antibody oxidation (Figure 30).[112] Mild oxidation conditions were chosen to preserve the immunoreactivity of the antibody: 50 µg of MAB610 antibody in PBS pH 6.8 was oxidized by 0.1 mg NaIO$_4$ (0.47 mM) for 15 minutes at 4°C in the dark. According to Purpald test, under these conditions, approximately 8 aldehyde groups per antibody were obtained.

$$2.94 \cdot 10^{-9}\, mole/mL \cdot \frac{150{,}000\, g/mole}{50 \cdot 10^{-6}\, g/mL} = 8.81\, mole/mole$$
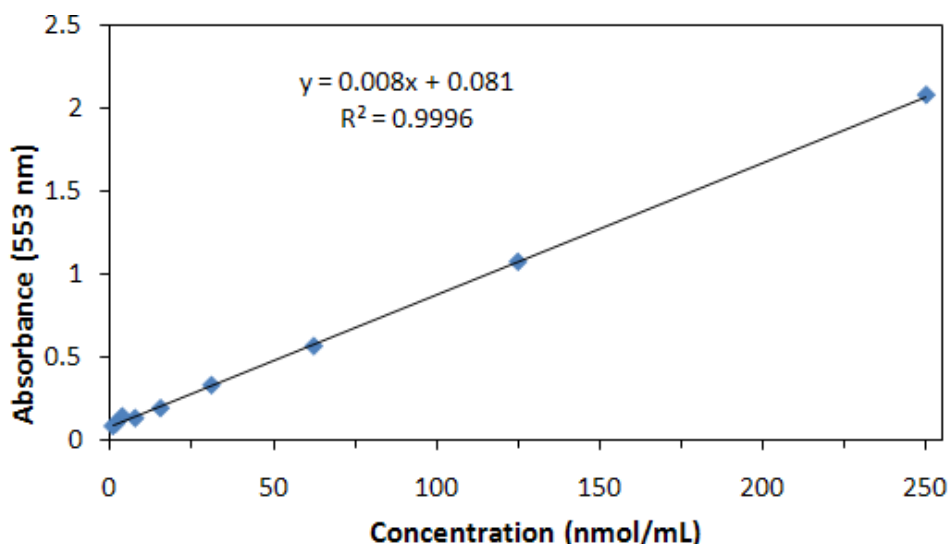
Figure 30. Standard curve of formaldehyde purpald test.

The aldehyde groups are required for the reaction with dendrimer hydrazide end group to form hydrazone linkage. After oxidation, antibody was quickly separated from the oxidizing reagent by the Amicon® centrifugal filter tube, and gel filtration with concomitant buffer exchange. The purified oxidized antibody was dissolved in PBS buffer pH 8 and allowed to react with dendrimer on ELISA plate at 4°C for 3 hours, where hydrazone Schiff base was obtained.

Because Schiff base is unstable, *in situ* reductive amination with sodium cyanoborohydride in PBS buffer pH 8 was performed and hydrazone linkage was transformed into a stable secondary amine linkage.[113] The reaction was completed by adding ethanolamine to block unreacted aldehyde groups.

3.4.4 ELISA evaluation of dendrimer-modified surface

To evaluate the diagnostic performance of the dendrimer-based assay, recombinant human TNF-α were assayed by the sandwich ELISA format using biotinylated goat anti-human TNF-α as detection antibodies, streptavidin-HRP as a reporter and substrate tetramethylbenzidine (TMB), Figure 31. Various known standard concentrations of TNF-α in the range of 0-250 pg/mL were assayed and typical dose-response curve was acquired. The reaction time between antibodies on the sensor and the cytokines was 2 hours, and was the same as that for the kit plate. These data were compared with commercially available TNF-α ELISA kit, and a plate coated with mouse anti-human TNF-α capture antibodies, which were attached by physical adsorption (Figure 32).

The linear regression equation for dendrimer plate for TNF-α was $A = 0.1502 + 0.0037*C_{[TNF-α]}$, with the linear regression coefficient R = 0.996. The sensitivity of dendrimer plate for TNF-α detection (TMB) was determined to be 0.48 pg/mL (Table 3). Various methods have been developed for determination of TNF-α level including ELISA, RIA,[82] bioassays,[83] chemiluminescence[84] and chemiluminescence imaging,[85] MALDI-MS,[86] immuno-PCR[87] and immuno-PCR assay,[88] fluorescence immunoassay,[89] and electrochemical immunosensor[90]. Dendrimer based assay in present study has a detection limit superior to that of other previously reported TNF-α assay except that obtained by Hun et al. which used fluoroimmunoassay method.
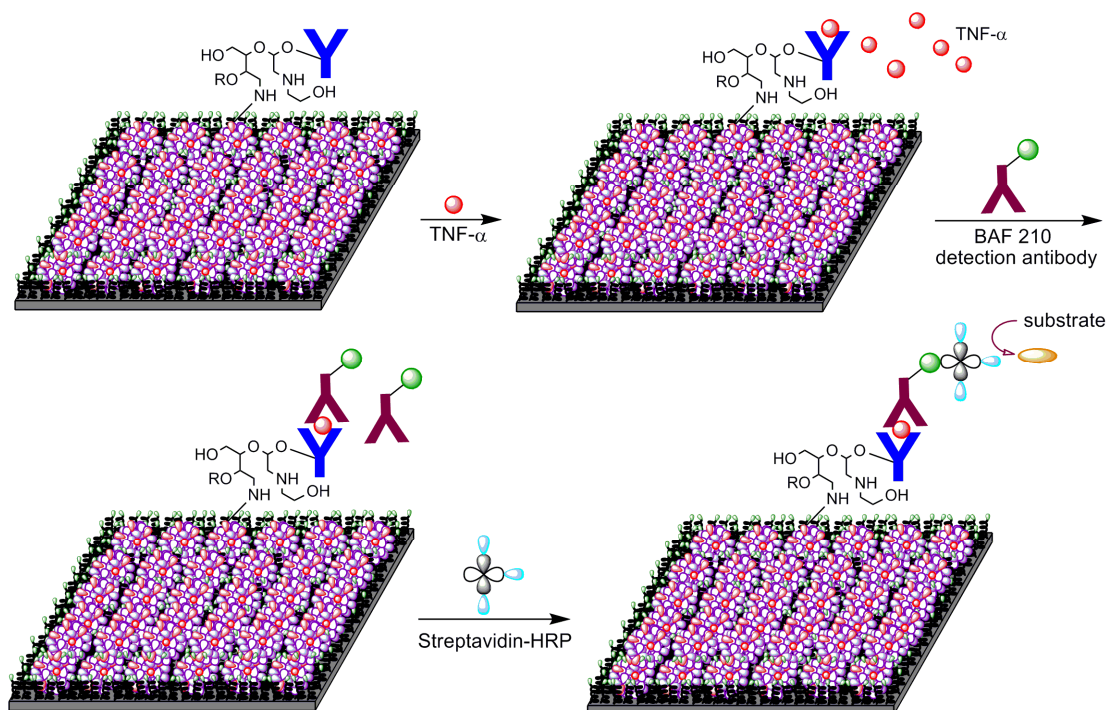
Figure 31. Schematic representation of TNF-α assay using dendrimer modified ELISA plate.
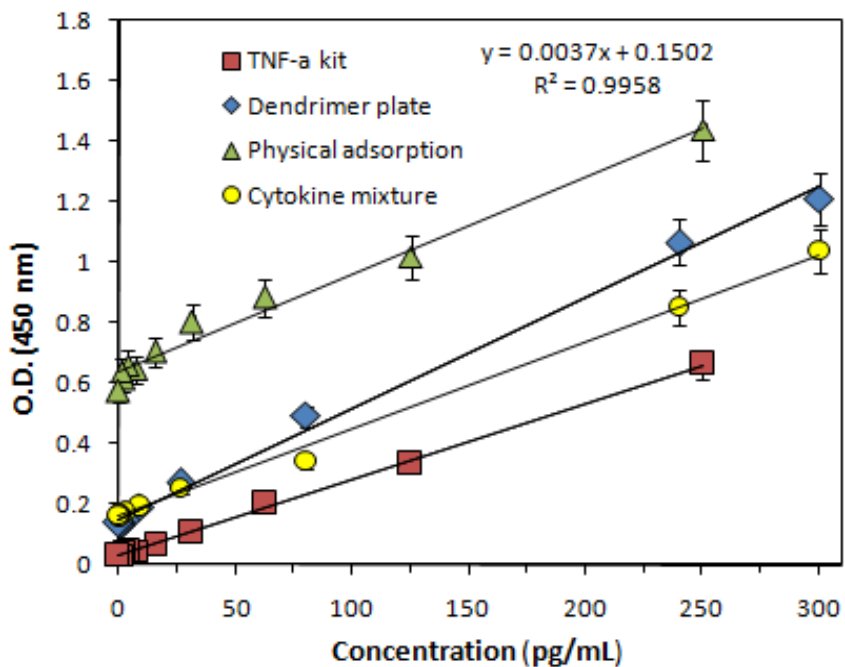
Figure 32. Standard curves for TNF-α ELISA measured with the dendrimer plate, TNF-α kit plate, and the plate prepared by physical adsorption of antihuman TNF-α antibody.

Dendrimer modified plate showed ~3 fold improvements on the detection limit compare to kit plate for TMB detection (0.48 pg/mL vs. 1.28 pg/mL). This result suggests that dendrimer conjugation reactions to the antibody preserved the activity of the antibody and the dendrimer-based assay performed better than the commercially available ELISA kit for TNF-α. Compared to physical adsorption, the dendrimer plate showed significant improvement in detection limit (0.48 pg/mL vs 8.00 pg/mL) which is 17 times better (Table 3).

Table 3. TNF-α ELISA data obtained from dendrimer plate, and plate prepared by physical adsorption, TMB detection

TNF-α Conc. (pg ml^{-1})	Dendrimer Plate (O.D.)	TNF-α Conc. (Cytok. mix.) (pg ml^{-1})	Dendrimer Plate (O.D.)	TNF-α Conc. (pg ml^{-1})	Physical Adsorption (O.D.)	TNF-α Kit (O.D.)
300	1.213	300	1.048	500	1.928	1.287
240	1.067	240	0.800	250	1.440	0.6625
80	0.493	80	0.423	125	1.018	0.3335
26.6	0.270	26.6	0.262	62.5	0.884	0.2045
8.88	0.192	8.88	0.188	31.2	0.804	0.107
2.96	0.151	2.96	0.171	15.6	0.705	0.0655
0.98	0.137	0.98	0.164	7.5	0.646	0.047
0.32	0.143	0.32	0.169	3.75	0.662	0.042
0.11	0.141	0.11	0.158	1.87	0.618	0.035
0.037	0.136	0.037	0.160	0.94	0.640	0.0335
0	0.138	0	0.164	0	0	0.0315
R²	0.996		0.995		0.980	0.998
LLD[a]	0.15		0.17		0.68	0.034
Sensitivity (pg ml^{-1})	<0.48		<1.14		<8	<1.28

[a] The lower limit of detection (LLD) of TNF-α was determined by adding two STD to the mean OD of three zero standard replicates and calculate the corresponding concentration from the standard curve.

The sensitivity was obtained from standard curves (Figure 32) as a slope versus concentration. Compared to kit plate the slope of the dose–response curve for dendrimer plate (0.0037 versus 0.0027) was steeper, which can be explained by the enhanced binding efficiency

of the antibodies immobilized on the dendrimer plate. We also performed chemiluminescence assay (data not shown) for both dendrimer plate and ELISA kit for TNF-α and we found that the sensitivity was similar to colorimetric assay. This is in an agreement with literature data that the chemiluminescence method may not give improved sensitivity for every cytokine.[114]

To assess the overall specificity of the dendrimer-based immunosensors toward TNF-α detection, the mixture of cytokines was prepared and studied with the dendrimer-modified ELISA plate. The standard solution containing 300 pg/mL of each of the following: TNF- α, IL-1α, and IL-6 was used to prepare dilutions in the range of 0-250 pg/mL. The selectivity of the dendrimer modified ELISA plate was examined. No significant difference of OD was observed in comparison with the result obtained in the presence of only TNF-α (Figure 32).

The precision and reproducibility of the dendrimer plate was determined by calculating the relative standard deviation (RSD) for three zero standard replicates and coefficient of variation (CV) for both intra-assay and inter-assay variability, respectively. For immunoassays such as ELISA, intra- or inter-assay variability should be lower that 8–15 % to be considered precise enough for its use. In our case the plate had good precision with RSD of 5.4 %. CV for intra-assay variability was calculated between OD values of triplicates within each run of two independent assay runs, for each dilution concentration, and it ranged between 0.09 and 13.0 %. The inter-assay variability was determined by calculating the CV between OD values obtained from two triplicates of independent assay runs, and it ranged between 2.08 and 13.39 %. This indicates that the assays on dendrimer modified plates are reproducible.

3.5 Conclusions

TNF-α is important cytokine in a variety of inflammatory diseases, and is a marker for chorioaminionitis. The ability to measure accurately and precisely very low concentrations of TNF-α is very important. In this work the dendrimer based biosensor platform was used for detection of TNF-α cytokine. Thiol functionalized G4-OH dendrimers were covalently immobilized onto maleimide-terminated PEG ELISA plate. The dendrimer modified ELISA plate was reacted to oxidized antibody by coupling the hydrazide groups of dendrimer and aldehyde groups of oxidized antibody. In this way the capture antibody has favorable orientation of the antigen binding sites toward the analyte phase. The dendrimer-based capture of TNF-α shows a detection limit of 0.48 pg/mL for TMB detection, which is significantly better than the commercial ELISA kit for TNF-α. The dendrimer based diagnostic nanodevice proved to have improved sensitivity and specificity and can be used for the detection of a wide range of cytokines and biomarkers.

3.6 Future Work

3.6.1 Detection of Pro-inflammatory Cytokines in Human Samples

An elevated level of pro-inflammatory cytokines such as TNF-α, IL-6, IL-1β, and MMP-8 are found in infected intra-amniotic fluid of a pregnant woman. Early detection of these cytokines is very important to prevent preterm labor. In order to assess the accuracy and applicability of dendrimer-based assays the cytokine detection can be done using human serum samples from normal (nonpregnant) and infected women and compared to commercially available kits.

CHAPTER 4 "SYNTHESIS AND CHARECTERIZATION OF DENDRIMER-PROGESTERON METABOLITE CONJUGATES FOR TRAUMATIC BRAIN INJURY TREATMENT"

4.1 Abstract

Progesterone, a steroid hormone, and its metabolite allopregnanolone are potential neuroprotective agents following traumatic brain injury (TBI). The therapeutic use of progesterone is limited due to its poor solubility and stability. This can be much improved using dendrimers as delivery vehicles. In this study poly(amidoamine) (PAMAM) dendrimer-allopregnanolone nanodevices are designed for TBI treatment. Two conjugates have been synthesized, dendrimer-allopregnanolone and dendrimer-allopregnanolone isomer, and characterized by proton NMR, HPLC and MALDI-TOF mass spectroscopy. Release study of dendrimer-allopregnanolone isomer showed no drug release in PBS buffers with varios pH (7.4, 4.6, and 1.4) due to short spacer between the drug and dendrimer. Based on this, dendrimer-allopregnanolone conjugate was prepared by putting longer spacer between drug and dendrimer. Allopregannaolone released from the conjugate in PBS buffer pH 2.1 in a sustained manner. The realase was evaluated by reverse phase HPLC (RP-HPLC) analysis, and 90% of drug payload was released within 9 days. In future study, the pharmacological activity of dendrimer-allopregnanolone conjugate, by measuring the inhibition of prostaglandin secretion, will be evaluated *in vitro* using A 549 lung epithelial cells.

4.2 Introduction

Traumatic brain injury (TBI) occurs when an external force traumatically injures the brain. It is a significant public health problem that affects nearly 1.5 million Americans each year resulting in more than 50,000 deaths.[115] Initially TBI causes ionic imbalances, oxidative damage, microglial activation, immune cell invasion, and cytokine release.[116,117] This can result in cerebral edema, inflammation, tissue necrosis, apoptosis, etc. No matter which factors initiate the injury cascade, the inhibition of inflammation may reduce cell death, gliosis, and edema.[118,119] Currently there are no treatments that improve clinical outcome measures. The research findings have shown that the progesterone and its reduced metabolite allopregnanolone, (5α -pregnane-3α-ol, 20-one or 5α -tetrahydroprogesterone) may be promising therapeutics for TBI treatment (Figure 33).[120,121] Progesterone is a steroid hormone involved in female menstrual cycle, pregnancy, and embryogenesis of humans and other species. It belongs to the group of neurosteroids. Progesterone is produced by the adrenal glands, the corpus luteum, as well by neurons and glial cells within the central and peripheral nervous system.[122] Progesterone showed several different modes of neuroprotection following TBI, including the reduction of cerebral edema,[123] the reduction of lipid peroxidation and oxidative stress,[124] anti-inflammatory effects,[118] reduction of cellular apoptosis,[125] inhibition of excitotoxicity,[126] and helps myelin repairement.[122,127] Progesterone has also neuroactive properties that can modulate neuronal excitability and seizure activity.[128,129] There are two mechanisms engaged in neuroprotective effects of progestrone: binding to progesterone receptors (PRs) and its metabolite to GABA-A receptor modulating neurosteroids.[131,133] Progesterone binding to cytoplasmic PRs of target cells leads to the formation of the hormone-nuclear receptor complexes to translocate to the cell

nucleus where they activate or stop the transcription of downstream gene networks, therefore affect the physiological response of progesterone-responsive target cells.[131] However, numerous studies have showed that the antiseizure effects of progesterone do not directly result from interactions with classical PR. These studies support the idea that 5α-reduced metabolites of progesterone, predominantly allopregnanolone, are responsible for the seizure protection.[128,130,131] Allopregnanolone is synthesized from progesterone via two sequential A-ring reductions both in peripheral tissues and in the brain. It binds to a steroid-binding site on the GABA-type A (GABA$_A$) receptor, and potentiates its function leading antiseizures effects. It is assumed that GABA-A receptors are pentameric with five protein subunits that form the chloride ion channel pore. GABA-A receptors are mostly composed of α, β and γ or δ subunits. Allopregnanolone has unique binding site on GABA-A receptors. Even though that binding of allopregnanolone to PRs is poor, it could indirectly activate PRs by re-conversion to dihydroprogesterone that is a moderately potent PR agonist. Progesterone and neurosteroids also affect GABA-A receptor expression. Therefore, there may be an interaction between genomic and non-genomic actions of progesterone that are involved in seizure protection. [131] Allopregnanolone plays a variety of neurprotective roles during gestation. It also showed improved seizure control in women suffering from catamenial epilepsy.[128,131]

Progesterone   **Allopregnanolone**
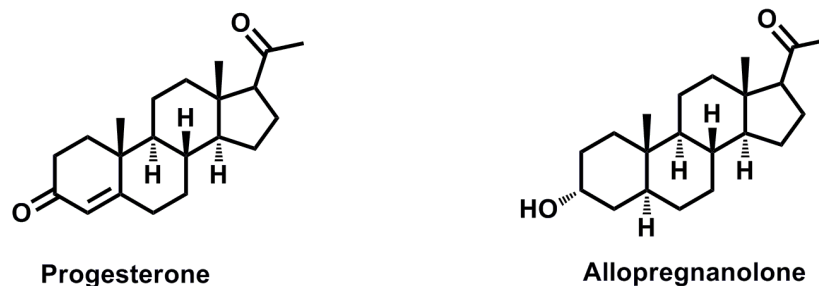
Figure 33. Chemical structures of progesterone and its metabolite allopregnanolone.

Due to their exceptional properties dendrimers are emerging as potential nanoscale delivery vehicles. They are nearly monodisperse, tree-like polymers with a large density of tailorable, functional end groups. Dendrimers have ability of conjugation, complexation, and encapsulation of multifunctional moieties.[2] In this study hydroxyl terminated PAMAM dendrimers are being explored as drug delivery vehicles for TBI treatment. Two conjugate nanodevices were synthesized: PAMAM dendrimer-allopregnanolone 3β,5β-isomer and PAMAM dendrime-allopregnanolone. The isomer of allopregnanolone has been modified to its succinate by reacting to succinic anhydride and conjugated directly to poly(amidoamine) dendrimer (PAMAM) through an ester bond. However the allopregnanolone was modified to allopregnanolone succinate and conjugated to bifuctional dendrimer through and amide bond. Bifuctional dendrimer was prepared by reaction of hydroxyl-terminated poly(amidoamine) dendrimer (G4-OH) to a protected amine linker followed by deprotection. The role of the linker on the dendrimer is to help the drug release in a resonable manner. Coupling the drugs to dendrimer the solubility and stability limitations of progesterone, as well as multistep enzymatic synthesis of allopregnanolone will be avoided. This approach will allow for dose reduction leading to fewer side effects and based on targeting ability of dendrimers the efficacy of the drug is expecting to be increased.

4.3 Materials and Methods

4.3.1 Materials

Hydroxyl terminated G4-PAMAM dendrimer (G4-OH) was purchased from Dendritech®, Inc. (Midland, MI). DMSO-d_6 and $CDCl_3$ was purchased from Cambridge Isotope Laboratories. Benzotriazol-1-yl-oxytripyrrolidinophosphonium hexafluorophosphate (PyBOP), K-Selectride

1M in THF, 5-(tert-butoxycarbonyl-amino)butyric acid, sodium borohydride, succinic anhydride, pyridine, diisoprophylethylamine (DIEA), and MALDI-MS reference standards were purchased from Sigma-Aldrich. Triethylamine (TEA) and ethylene diamine (EDA) were purchased from Thermo Scientific. Palladium, 5% on calcium carbonate, was obtained from Alfa Aesar, MA, USA. Sodium hydroxide was obtained from Fisher Scientific. Trifluoroacetic acid (TFA) was purchased from EMD. Anhydrous DMSO, dichloromethane (DCM), and tetrahydrofuran (THF) were purchased from Acros Organics, USA. All other solvents and chemicals used were purchased from Fisher Scientific. Regenerated cellulose (RC) dialysis membrane with molecular weight cut-off of 1000 Da was obtained from Spectrum Laboratories.

4.3.2 Characterization

NMR spectra were recorded on a Varian INOVA 400 spectrometer using commercially available deuterated solvents. Proton chemical shifts are reported in ppm (δ) and tetramethylsilane (TMS) used for internal standard. ESI mass spectra were recorded on Waters Micromass ZQ spectrometer. Matrix-assisted laser desorption ionization-time of flight (MALDI-TOF) mass spectra were recorded on a Bruker Ultraflex system equipped with a pulsed nitrogen laser (337 nm), operating in positive ion reflector mode, using 19 kV acceleration voltage and a matrix of 2,5-dihydroxybenzoic acid. Cytochrome C (MW 12,361 g/mol), and Apomyoglobin (MW 16,952 g/mol) were used as external standards. A dendrimer solution was prepared by dissolving 2 mg of dendrimer in 1 mL of DMSO. The matrix solution was prepared by dissolving 20 mg of matrix in 1 mL of the 1:1 mixture of deionized water and acetonitrile (0.1% TFA). Analytical samples were prepared by mixing 10 μL of dendrimer solution with 100 μL of

matrix solution, followed by deposition of 1 μL of sample mixture onto a 384-well aluminum plate. This mixture was allowed to air dry at room temperature.

4.3.3 High performance liquid chromatography (HPLC)

HPLC characterization was carried out using Waters HPLC instrument equipped with dual pumps, an auto-sampler and dual UV detector interfaced to Breeze software. The HPLC chromatogram was monitored at 210 and 205 nm simultaneously using the dual UV absorbance detector. H_2O:ACN (0.14 % TFA) was used as mobile phase. Both phases were freshly prepared, filtered, and degassed prior to use. Symmetry300 C_{18} reverse-phase column (5 μm particle size, 25 cm × 4.6 mm length × I.D.) equipped with a Supelguard Cartridges (5 μm particle size, 2.0 cm ×3.9 mm length × I.D.) was used for characterization of the conjugates. HPLC analysis was done using 90:10 to 10:90 (H_2O:ACN) gradient flow in 30 minutes with flow rate of 1 mL/min.

4.3.4 Release Study Protocol

The release studies were performed in 0.1M PBS buffer solution pH 7.4, 0.1 M citrate buffer pH 4.6, and 0.1 M hydrochloric acid buffer pH 2.1. The conjugates were added into 3 mL preheated buffer solutions in triplicates. All the release solutions containing 3.0 mg/mL dendrimer drug conjugates were stirred continuously and maintained at 37ºC. At appropriate time intervals samples were withdrawn and immediately analyzed by HPLC to determine the drug concentrations.

4.3.5 Synthesis

4.3.5.1 5β Reduction Product of Progesterone

The reaction scheme is outlined in Figure 34. Progesteron (1.00 g, 3.18 mmole) was dissolved in 66 mL absolute ethanol in a round bottom flask, and KOH (0.180 g) and 5%

Pd/CaCO$_3$ (0.090 g) were added. The flask was evacuated, flushed with hydrogen and the reaction mixture stirred for 1 hour. The ethanol was removed and the residue was redissolved in ether and washed with water. The water layer was extracted with ether twice. The aqueous layer was then acidified to pH<3 with 1M HCl and extracted with ether. The organic layers were combined, dried, filtered, and concentrated to give crude 5β reduction product. The pure 5β reduction product was isolated by flash column chromatography on silica gel using ethyl acetate/hexanes (1:5) as mobile phase (0.60 g, yield 60%); Rf = 0.16 (1:5 ethylacetate /hexanes), and it was characterized by proton NMR. ^{1}H NMR (CDCl$_3$) δ 2.66 (t, 1H, J = 15 Hz), 2.53 (t, 1H, J = 9.0 Hz), 2.34 (dt, 1H, J 14.4, 5.4 Hz), 2.21-1.09 (m, 20H), 2.12 (s, 3H), 1.02 (s, 3H), 0.64 (s, 3H). ESI MS (*m/z*): calcd for C$_{21}$H$_{32}$NO$_2$ [M+H]$^+$ 317.2481, found 317.2471.
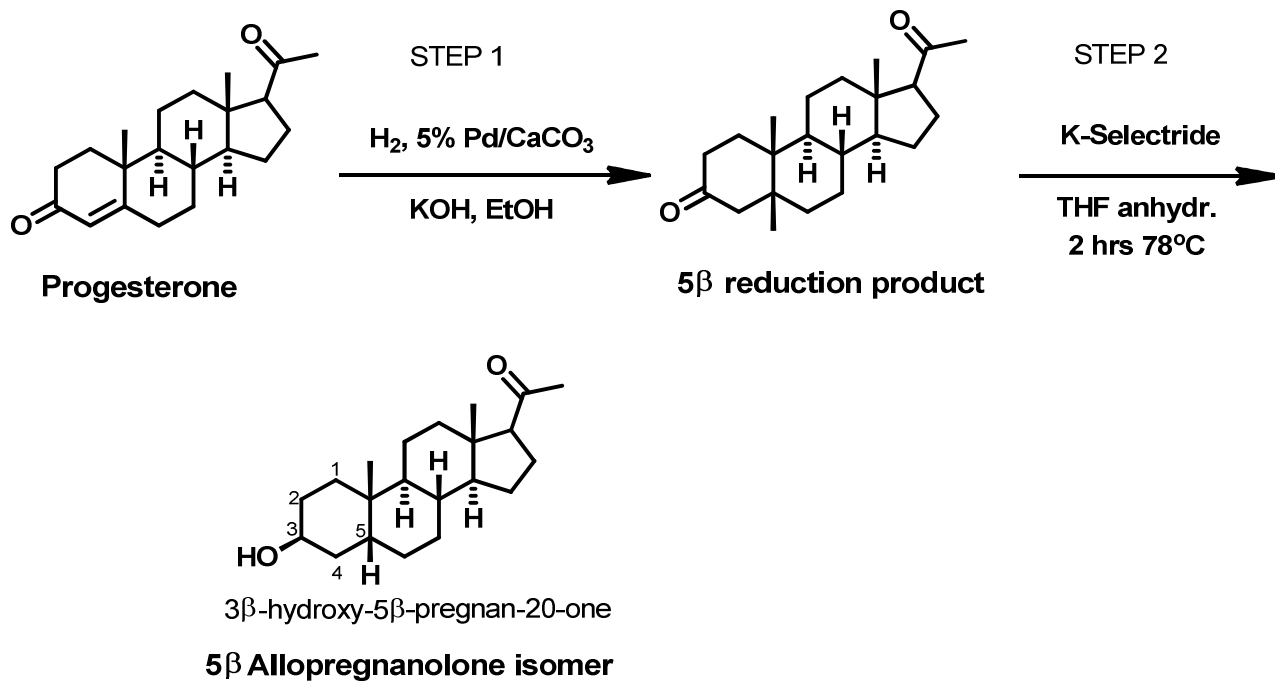
Figure 34. Synthesis of 3β,5β allopregnanolone isomer from progesterone.

4.3.5.2 Allopregnanolone Isomer

The reaction pathway is shown in Figure 34. The pure 5β reduction product (0.849 g, 2.68 mmole) dissolved in dry THF (5 mL) under nitrogen atmosphere and cooled down to 78°C. To this 3.22 mL of K-Selectride was added. The reaction mixture was stirred for 1.5 hours at 78°C, and 1 hour at 0°C. Then 7 mL of 10% NaOH and 5 mL of 30% H_2O_2 added followed by overnight stirring at room temperature. The product was extracted by ethylacetate three times. Organic layers combined and washed with water two times, sodium bisulfate two times and brine two times, dried over $NaSO_4$ and evaporated under reduced pressure. The pure product, of 3β, 5β-tetrahydroprogesterone was isolated by flash column chromatography on silica gel using ethylacetate/hexanes (1:3) as mobile phase (0.765 g, yield 90%); Rf = 0.28 (1:3 ethyl acetate /hexanes), and it was characterized by proton NMR. ^1H NMR ($CDCl_3$) δ 4.091 (t, 1H), 2.499 (t, 1H), 2.200 - 1.000 (m, 23H), 2.081 (s, 3H), 0.930 (s, 3H), 0.568 (s, 3H). ESI MS (*m/z*): calcd for $C_{21}H_{35}O_2$ [M+H]$^+$ 319.2637, found 319.2630..

4.3.5.3 Allopregnanolone Isomer Succinate (3β, 5β-tetrahydroprogesterone Succinate)

The reaction scheme is shown in Figure 35. Succinic anhydride (383.95 mg, 3.8364 mmole) and DMAP (78.08 mg, 0.6394 mmole) added to a solution of 3α, 5β-tetrahydroprogesterone (203.00 mg, 0.6394 mmole) in pyridine. The reaction mixture stirred under N_2 and 45°C and monitored by TLC plate until its completion. After 24 hours the reaction stopped, and the solvent was evaporated. The crude product was redissolved in dichloromethane and washed with water. The water layer was washed three times with dichloromethane. Organic layers combined and washed with water and brine, dried over $NaSO_4$ and evaporated under reduced pressure. The pure product was isolated by flash column chromatography on silica gel

using ethylacetate/hexanes (2:3) as mobile phase (214 mg, yield 80%); Rf = 0.35 (2:3 ethyl acetate /hexanes), and it was characterized by proton NMR. ^{1}H NMR (CDCl$_3$) δ 5.092 (t, 1H), 2.556-2.700 (m, 4H linker), 2.087 (s, 3H), 2.000-1.000(m, 23H), 0.934 (s, 3H), 0.576 (s, 3H). ESI MS (*m/z*): calcd for C$_{21}$H$_{37}$O$_5$ [M-H]$^+$ 417.2641, found 417.2652.

allopreglanone isomer succinate

Dendrimer-Allopregnanolone isomer conjugate
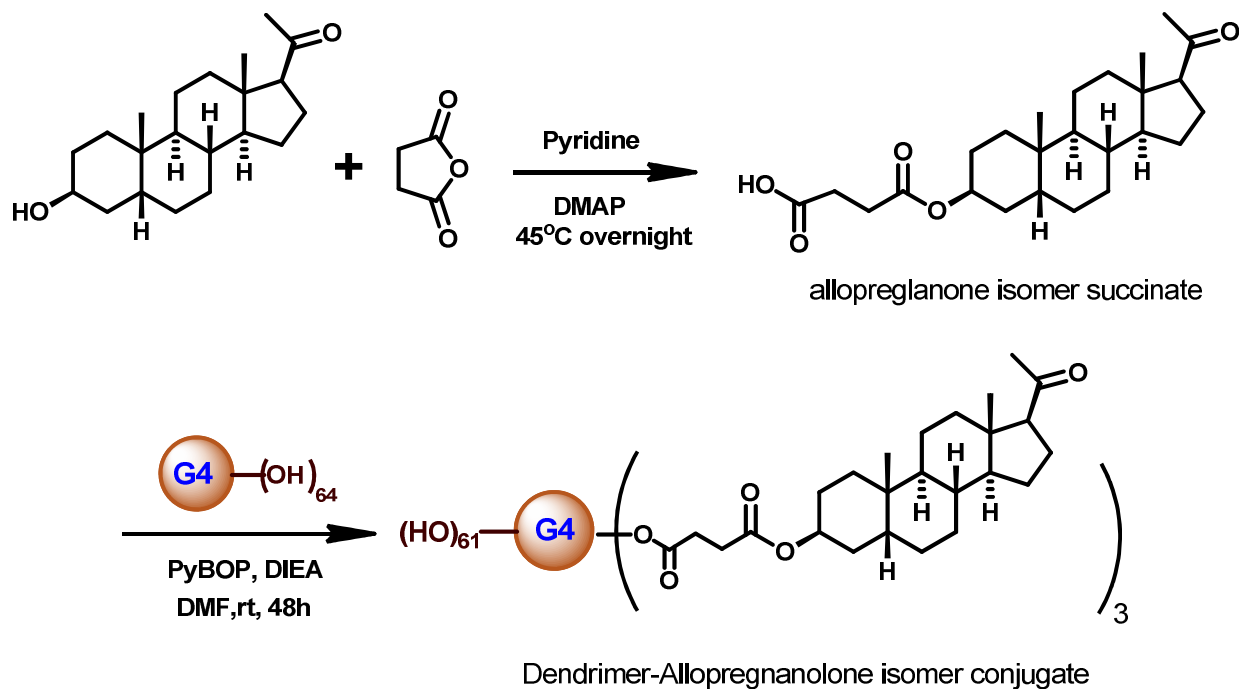
Figure 35. Synthesis of G4-OH PAMAM – allopregananolone isomer nanodevice.

4.3.5.4 Allopregnanolone Succinate (3α, 5α-tetrahydroprogesterone Succinate)

Allopregnanolone succinate was prepared in the same way as allopregananolone isomer succinate. Pure product was isolated by flash column chromatography and characterized by proton NMR . ^{1}H NMR (CDCl$_3$) δ 5.027 (t, 1H), 2.600-2.700 (m, 4H linker), 2.505 (t, 1H), 2.124 (m, 1H), 2.095 (s, 3H), 1.970 (m,1H) 1.750-1.080(m, 19H), 0.926 (m, 1H), 0.766 (m, 1H) 0.766 (s, 3H), 0.582 (s, 3H).

4.3.5.5 G4-OH PAMAM – Allopregnanolone Isomer Nanodevice

The reaction scheme for the preparation of the conjugate is outlined in Figure 35. The allopregnanolone isomer-succinate (52.0 mg, 0.1242 mmole) dissolved in DMF (1 mL) and cooled down to 0°C using ice water bath. To this PyBOP (96.0 mg, 0.1863 mmole) dissolved in DMF (1 mL) and DIEA (32.54 μL, 0.1863 mmole) added under nitrogen atmosphere. Ice water bath removed and the mixture stirred for 1 hour at room temperature. Then PAMAM G4-OH (113.0 mg, 0.0079 mmole) dissolved in DMF (2 mL) added to the reaction mixture. The reaction stirred for 48 hours at room temperature. The resulting solution dialyzed extensively with DMF (dialysis membrane of molecular weight cutoff = 1000 Da) for 24 h. The obtained reaction mixture lyophilized yielding G4-OH PAMAM-allopregnanolone isomer conjugate with ester linker. The conjugate was characterized by proton NMR. ^{1}H NMR (DMSO-d_6, 400 MHz): δ (ppm) 8.048 (bs, CO-N*H*, linker), 7.939 (bs, CO-N*H*, G4-OH), 7.783 (bs, CO-N*H*, G4-OH), 4.298 (t, 1 H, Allo-iso), 4.715 (bs, O*H*, G4-OH), 3.989 (m, C*H$_2$*OCO, G4-OH), 3.37-2.16 (m, 984 H aliphatic protons, G4-OH; 4 H C*H$_2$*, linker; 28 H, Allo-iso), 2.034 (s, 3 H, Allo-iso-C*H$_3$*) 2.000-1.000 (m, 23H, Allo-iso), 0.895 (s, 3H, Allo-iso-C*H$_3$*), 0.482 (s, 3 H, Allo-C*H$_3$*).

4.3.5.6 G4-OH PAMAM – Allopregnanolone Nanodevice

The reaction scheme is shown in Figure 36. Allopregnanolone-succinate (22.0 mg, 0.0526 mmole) dissolved in DMF (1 mL) and cooled down to 0°C using ice water bath. To this PyBOP (41.0 mg, 0.0788 mmole) dissolved in DMF (1 mL) and DIEA (15.0 μL, 0.0788 mmole) added under nitrogen atmosphere. Ice water bath removed and the mixture stirred for 1 hour at room temperature. Then bifuctional PAMAM dendrimer (100.0 mg, 0.0066 mmole) dissolved in DMF (2 mL) added to the reaction mixture. The reaction stirred for 48 hours at room

temperature. The resulting solution dialyzed extensively with DMF (dialysis membrane of molecular weight cutoff = 1000 Da) for 24 h. The obtained reaction mixture lyophilized yielding G4-OH PAMAM-link-allopregnanolone conjugate. The conjugate was characterized by proton NMR. ^{1}H NMR (DMSO-d_6, 400 MHz): δ (ppm) 8.042 (bs, CO-NH, linker), 7.931 (bs, CO-NH, G4-OH), 7.770 (bs, CO-NH, G4-OH), 4.853 (t, 1 H, All), 4.705 (bs, OH, G4-OH), 3.977 (m, CH_2OCO, G4-OH), 3.40-1.90 (m, 984 H aliphatic protons, G4-OH; 4 H CH_2, linker; 6 H, Allo), 1.750-1.080 (m, 19 H, Allo), 0.833 (m, 1 H, Allo), 0.727 (s, 3H, Allo-CH_3), 0.482 (s, 3 H, Allo-CH_3).
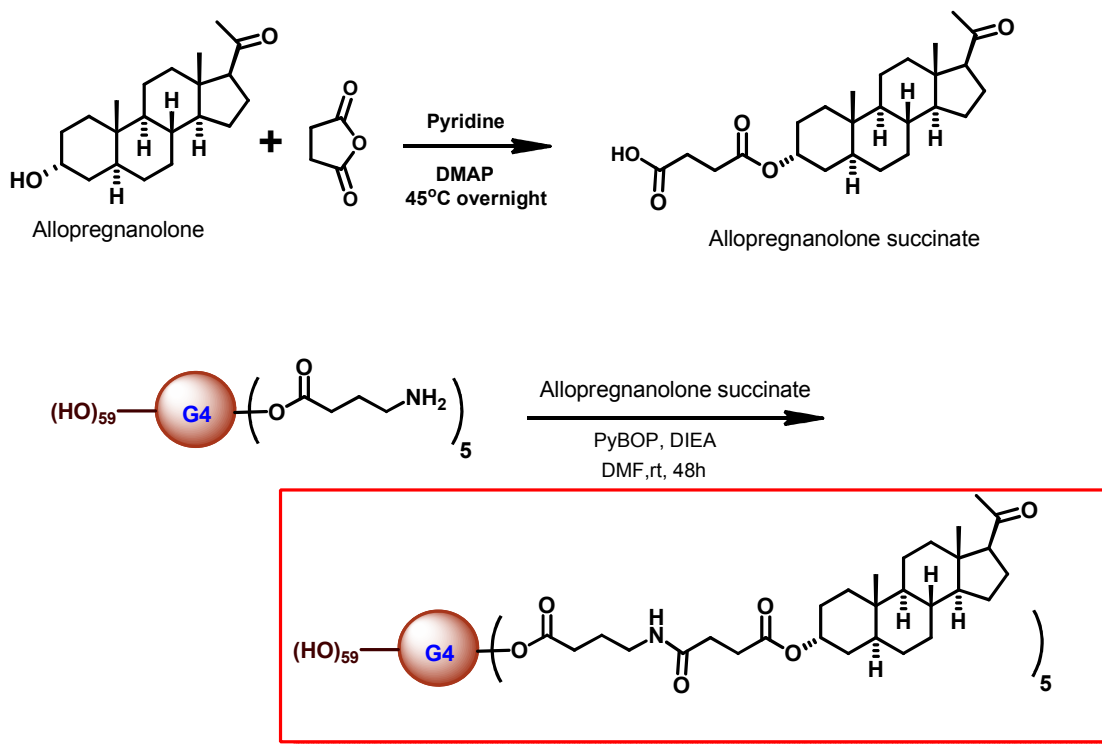
Figure 36. Synthesis of dendrimer-allopregananolone nanodevice.

4.4 Results

4.4.1 Synthesis of Nanodevices

G4-OH-Allopregnanolone Isomer Nanodevice. The nanodevice was prepared by coupling reaction of G4-OH dendrimer with allopregnanolone isomer succinate. Since allopregnanolone is a quite expensive compound (Sigma – Aldrich sells 10 mg for $159.50), for preliminary studies the isomer of allopregnanolone was synthesized from progesterone following already published procedures (Figure 34).[134,135] Hydrogenation of progesterone in the presence of hydroxides is known to provide 5β reduction product. Treatment of 5β reduction product with K-Selectride in dry THF leads to selective reduction of the C-3 carbonyl in the presence of the C-20 ketone giving allopregnanolone isomer (or 3β, 5β-tetrahydroprogesterone) product. Then reaction of allopregnanolone isomer with succinic anhydride produces a succinate having a carboxylic group required for the coupling reaction to dendrimer. All three compounds are charectirized by mass, proton NMR, and HPLC. The HPLC chromatograms showed that the retention times for allopregananolone isomer, 5β reduction product of progesterone, and allopregnanolone isomer succinate were 25.50, 26.00 and 26.23 min respectively (Figure 37). The allopregnanolone isomer succinate was conjugated to dendrimer using an ester link for '*slow drug release*'. The specific steps of the synthesis of allopregnanolone isomer-dendrimer nanodevices, is shown in Figure 35. Brifely, the nanodevices was obtained by coupling hydroxyl terminated generation 4 PAMAM dendrimer with allopregnanolone isomer succinate using PyBOP (as a coupling agent) in the presence of catalytic amount of DIEA in DMF. The resulting conjugate was purified by dialysis in DMF, lyophilized, and charectirized using NMR, MALDI-TOF MS, and HPLC.
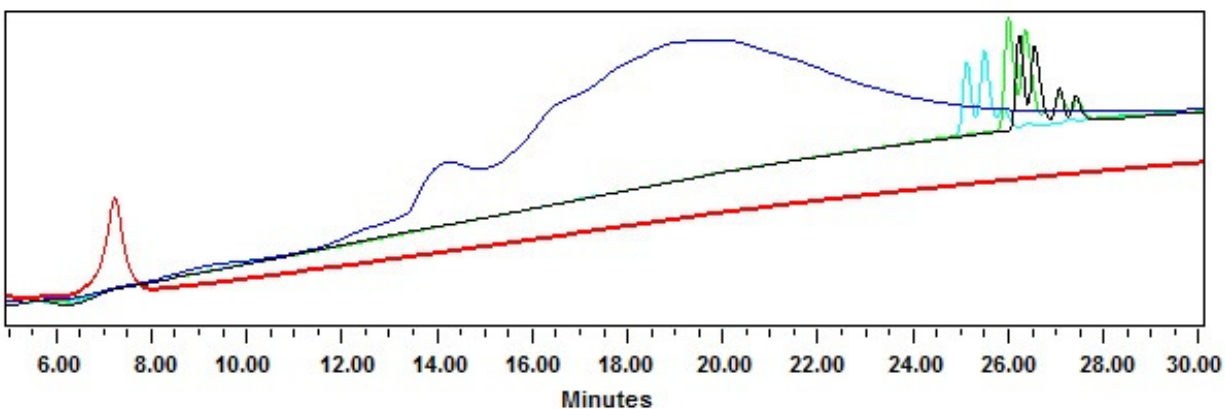
Figure 37. HPLC chromatograms of G4-OH (red), G4-OH-allopregnanolone isomer conjugate (blue), allopregananolone isomer (light blue), 5β reduction product of progesterone (green), and allopregnanolone isomer succinate (black)

The HPLC spectra showed that the conjugate G4-OH-allopregnanolone isomer gave very distinct broad peak at 18.9 min compared to G4-OH dendrimer that gave a peak at 7.2 min (Figure 37). The proton NMR of G4-OH-allopregnanolone isomer conjugate is shown in Figure 38. Comparison of the integration of amide peaks of dendrimer and methyl groups of allopregnanolone revealed that three molecules of allopregnanolone isomer were attached to the surface of the dendrimer.

MALDI-TOF MS spectra of G4-OH-allopregnanolone isomer conjugate is shown in Figure 39. The obtained molecular weight of G4-OH-allopregnanolone isomer (15,686.4) compared with G4-OH (13,949.5) suggests that a payload of approximately three to four molecules of allopregnanolone isomer was achieved. This represents a drug payload in the conjugate of ~8% by weight. The conjugate was soluble in PBS buffer pH 7.4, compared to the free allopregnanolone isomer which is not.
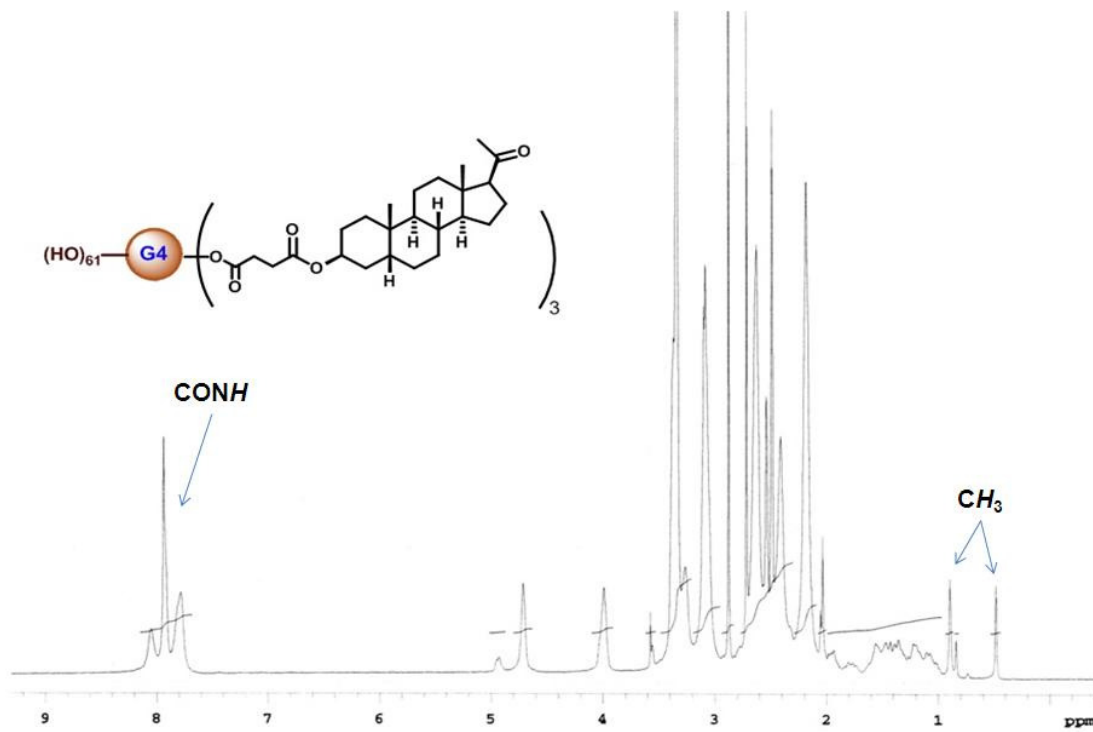
Figure 38. Proton NMR spectrum of dendrimer-allopregnanolone isomer conjugate in DMSO-d_6.
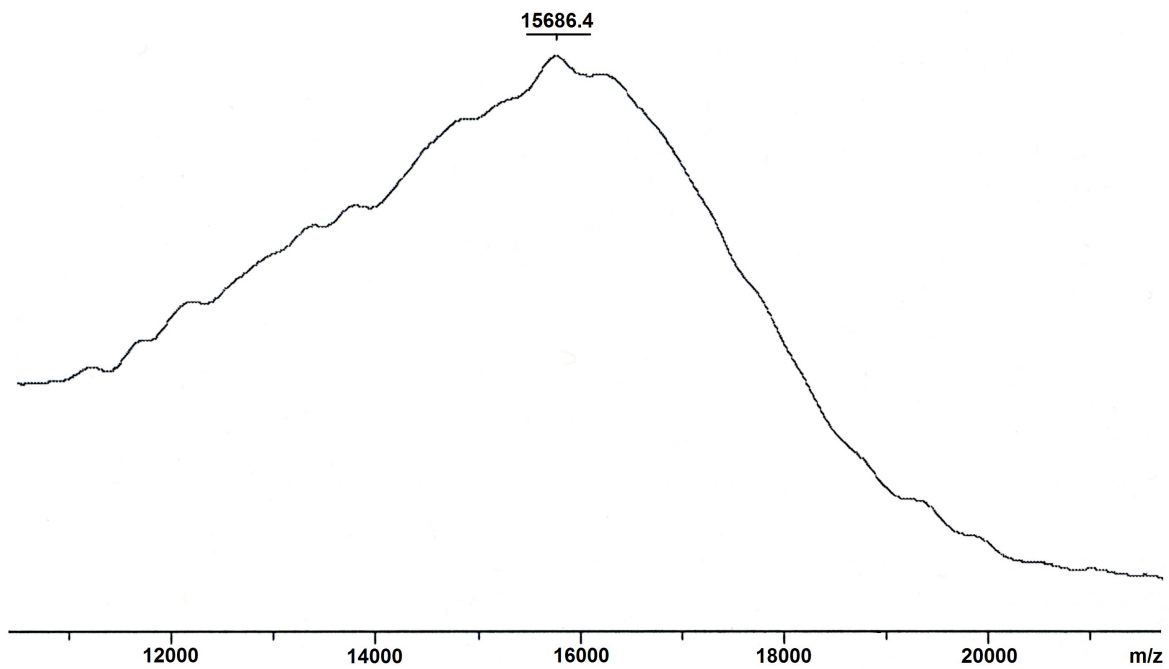
Figure 39. MALDI-TOF MS spectra of G4-OH PAMAM-allopregananolone isomer conjugate.

G4-OH-Link-Allopregnanolone Nanodevice. For the synthesis of this nanodevice a bifuctional dendrimer was used to improve the drug release from dendrimer by putting an additional spacer between drug and dendrimer, Figure 36. The bifunctional dendrimer was prepared by reacting 4-Boc-amino-butyric acid, as a linker to provide protected NH_2 groups, and G4-OH hydroxyl terminated dendrimer followed by deprotection of Boc protected amine groups. Based on proton NMR and and MALDI-TOF mass (not shown here) there are approximately 5-6 amine groups added. Then bifuctional dendrimer was reacting to allopregnanolone succinate to obtain G4-OH-link-allopregnanononolone conjugate. The conjugate was thoroughly characterized by proton NMR (Figure 40), HPLC (Figure 41), and MALDI-TOF mass (Figure 42). Based on proton NMR and MALDI-TOF mass analyses five molecules of allopregnanolone were attached to dendrimer giving the drug payload ~10% by weight.
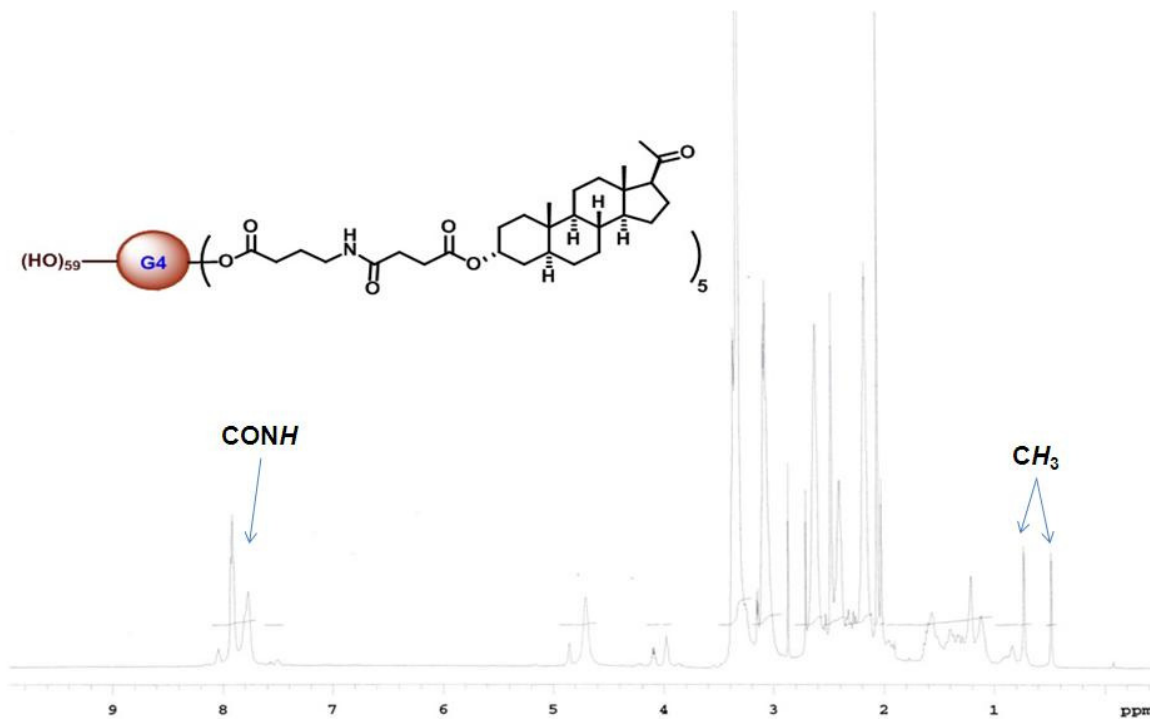
Figure 40. Proton NMR spectrum of dendrimer-allopregnanolone conjugate in DMSO-d_6.
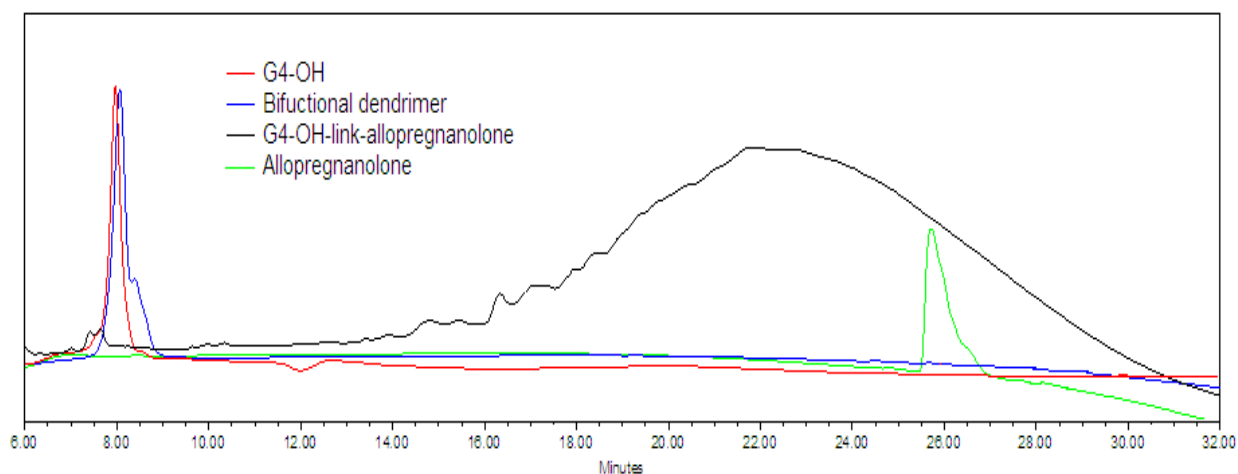
Figure 41. HPLC chromatograms of G4-OH, bifuctional dendrimer, G4-OH-link-allopregnanolone conjugate, and allopregnanolone at 205 nm.
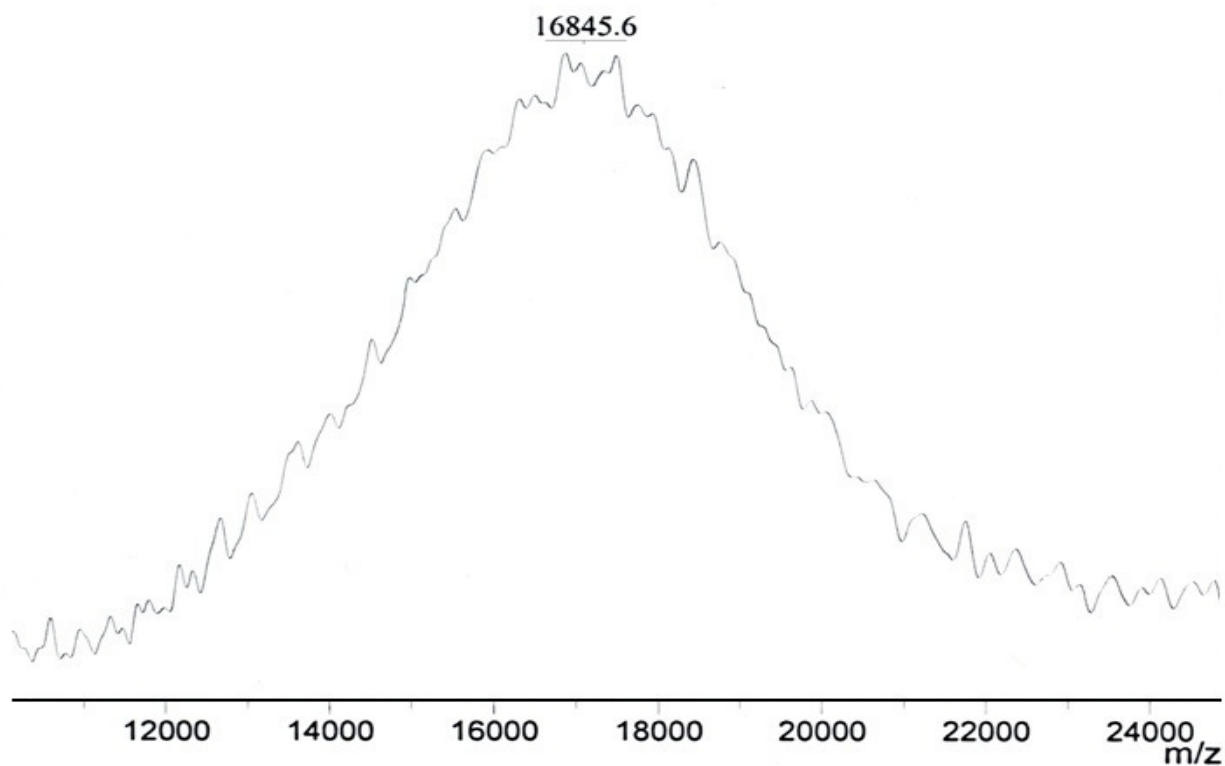
Figure 42. MALDI-TOF MS spectra of G4-OH PAMAM-allopregananolone conjugate.

4.4.2 Release Studies

In vitro drug release rate from dendrimer-drug nanodevices were carried out at various pH values at 37°C and analyzed by HPLC at 205 nm. The drug release rate of G4-OH-allopregananolone isomer nanodevice was studied at pH 2.1, 4.6, and 7.4 and HPLC analysis showed no drug release from conjugate. The stability of ester linkages of the G4-OH-allopregananolone isomer nanodevice could be attributed to the size and chemical structure of the spacer between the drug and dendrimer as well as steric effect caused by dendrimer structure. To increase the drug release kinetics, G4-OH-link-allopregnanolone nanodevice was designed. The design consisted of the conjugation of allopregnanolone having succinic acid linker with bifuctional dendrimer (G4-OH dendrimer having several linkers with end amine groups) giving G4-OH-link-allopregnanolone nanodevice. In this case the spacer was longer and had peptide link and resulted in successful drug release from dendrimer. The drug release rate of this nanodevice was studied in hydrochloric acid buffer pH 2.1 and HPLC analysis showed that the nanodevice was susceptible to hydrolysis and about 90% of the drug was released within 9 days (Figure 43). HPLC chromathogram cleary showed the appereance of the drug peak and peak of the bifuctional dendrimer with the time (not shown here). This indicates that the hydrolytic cleavage of ester bond on the dendrimer's side is quite stable. The release rate of allopregnanolone appears to be following first order reaction kinetics. The logarithmic equation was fitted to the release profile as shown in Figure 43. The equation fits fairly well and this indicates that the release of the drug from nanodevice depends on the concentration of the drug.
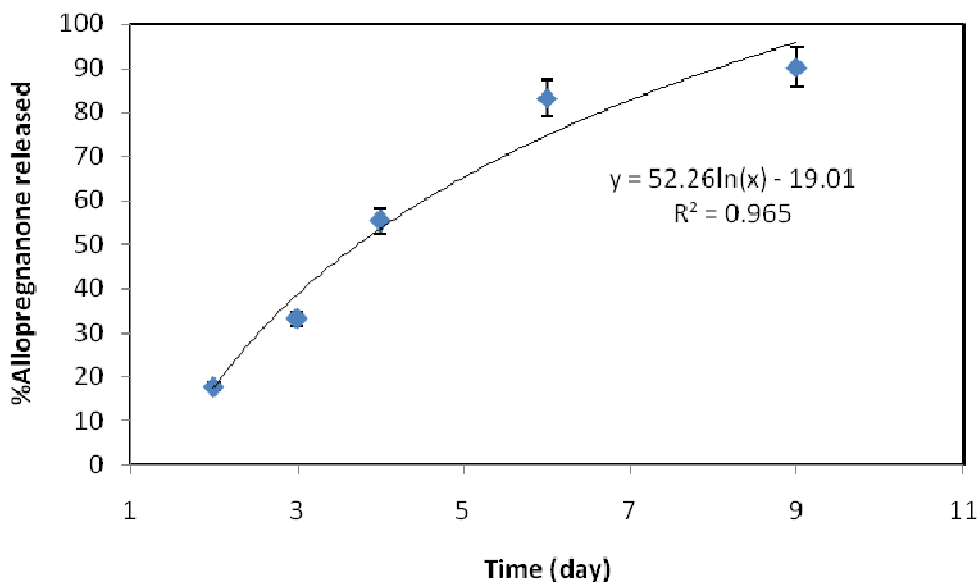
Figure 43. Drug release profile of G4-OH-link-allopregnanolone nanodevice at pH 2.1.

4.5 Discussion

TBI is a significant public health problem throughout the world. It can cause cerebral edema, inflammation, tissue necrosis, programmed cell death, etc. The research findings have shown that the progesterone may be a promising therapeutic drug for the treatment of TBI. Progesterone belongs to the group of neurosteroids. It has a variety of neurprotective roles during gestation, and it has also been linked to several different modes of neuroprotection following TBI, including the attenuation of cerebral edema, the reduction of lipid peroxidation and oxidative stress, anti-inflammatory effects, reduction of cellular apoptosis, inhibition of excitotoxicity, and assisting in the repair of myelin. However, the poor aqueous solubility of progesterone limits its potential use as a therapeutic. It is known that the protective effects of progesterone in the brain arise largely from its conversion to 5α-reduced metabolites such as allopregnanolone (5α -pregnane-3α ol, 20-one or 5α -tetrahydroprogesterone). Allopregnanolone binds to a steroid-binding site on the $GABA_A$ receptor complex, and by increasing chloride flux

thereby increase GABAergic receptor activity and decrease the excitability of the central nervous system.

In this study allopregnanolone and allopregnanolone isomer were conjugated to generation 4 hydroxyl PAMAM dendrimer as a drug carrier with a longer and shorter spacer respectively. Since release study of G4-OH-allopregnanolone isomer at pH 7.4, 4.6, and 2.1 showed no drug release from conjugate, allopregnanolone was reacted first to succinic anhydride to obtaine an acid group required for conjugation raction with the dendrimer and then conjugated to bifuctional dendrimer that is G4-OH dendrimer having several linker moieties terminated with amine groups. The spacer between drug and dendrimer had a peptide link and because it was longer moved drug molecules a little bit further from dendrimer reducing the steric effect and resulted in effective drug release in acidic conditions. Around 90% of allopregnanolone was successfully released in 9 days from the dendrimer-drug nanodevice at 2.1 pH. Future study will involve *in vitro* determination of pharmacological activity of dendrimer-allopregnanolone nanodevices, by measuring the inhibition of prostaglandin secretion in LPS pretreated A 549 lung epithelial cells.

4.6 Future Work

4.6.1 Pharmacological Activity of Dendrimer-Allopregnanolone Nanodevice

Prostaglandins (PGs) play a key role in the generation of the inflammatory response. Their concentration is elevated in inflamed tissue and can lead to acute inflammation. To evaluate the therapeutic potential of dendrimer-allopregnanolone nanodevices, in inhibiting the prostaglandin synthesis, an *in vitro* study can be demonstrated using A549 human lung epithelial carcinoma cell lines. The pretreated cells with lipopolysaccharide induce prostaglandin synthesis.

The inhibition of prostaglandin synthesis by dendrimer-allopregnanolone nanodevices would be the measure of anti-inflammatory activity of the nanodevices.

APPENDIX

Selected ^{1}H ans ESI MS Spectra
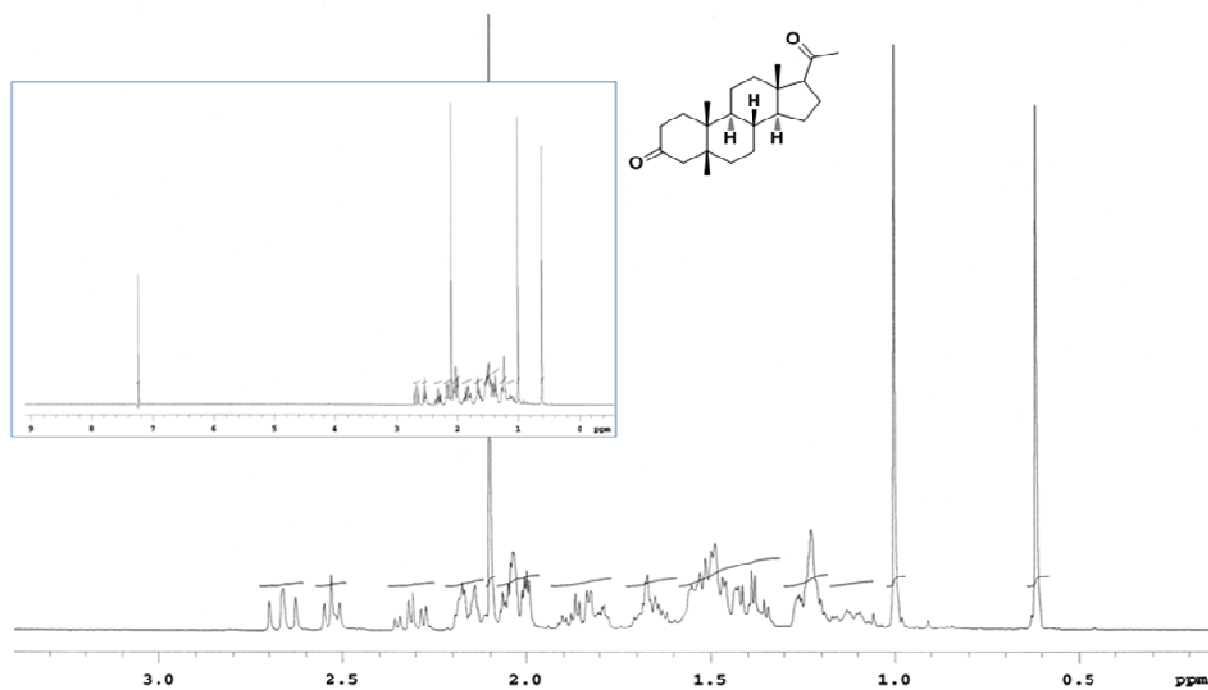
Proton NMR of 5β Reduction Product
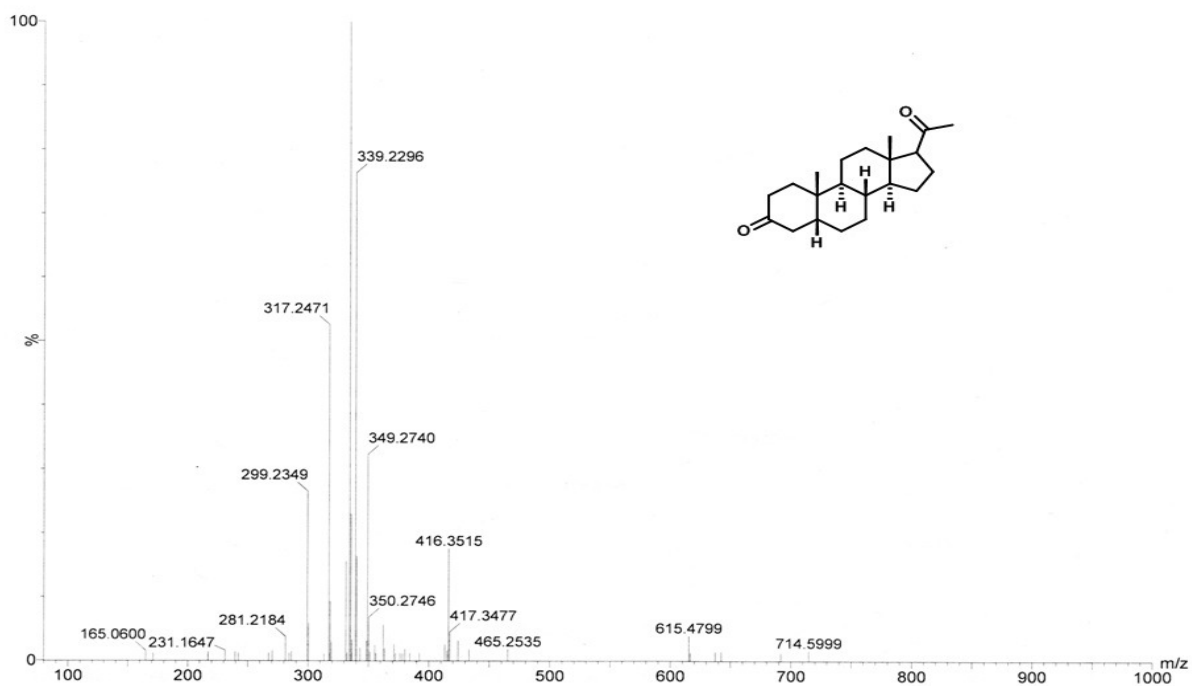
ESI MS of of 5β Reduction Product,
(*m/z*): calc. for $C_{21}H_{32}O_2$ [M+H]$^+$ 317.2481, found 317.2471
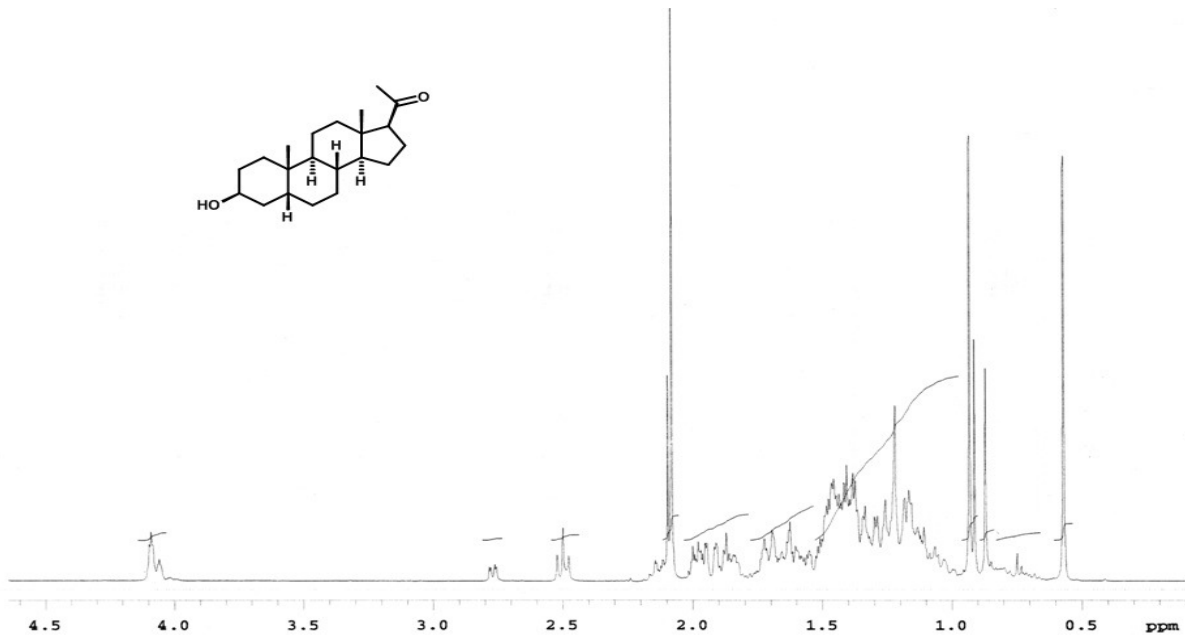
Proton NMR of Allopregnanolone Isomer.
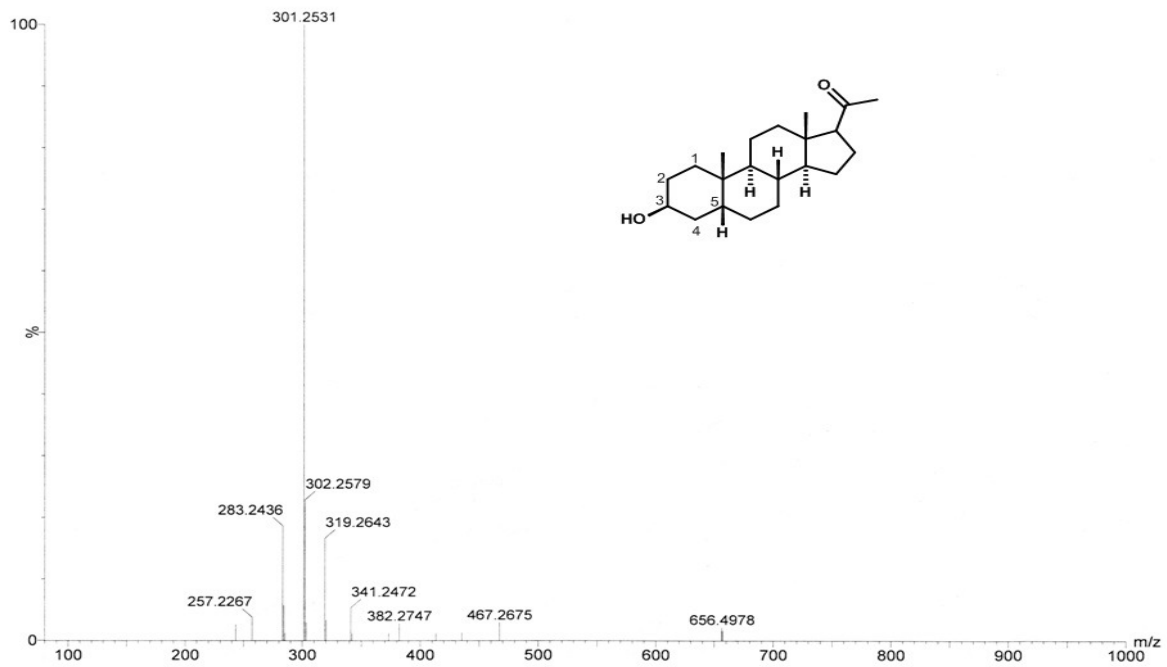
ESI MS Allopregnanolone Isomer
(*m/z*): calc. for $C_{21}H_{35}O_2$ [M+H]$^+$ 319.2637, found 319.2630
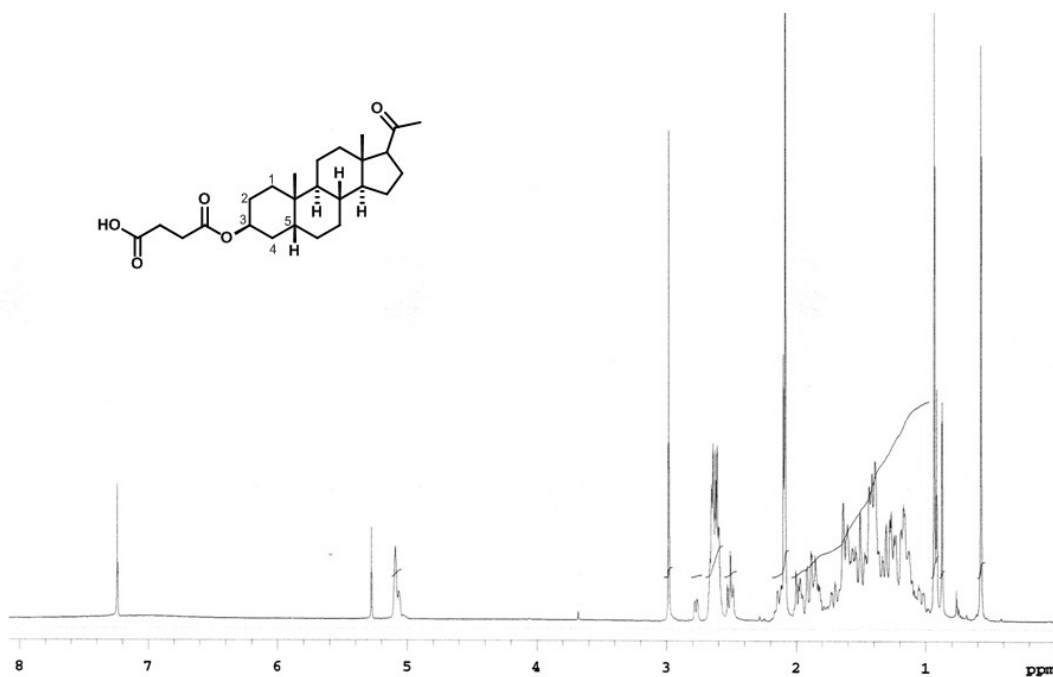
Proton NMR of Allopregnanolone Isomer Succinate.
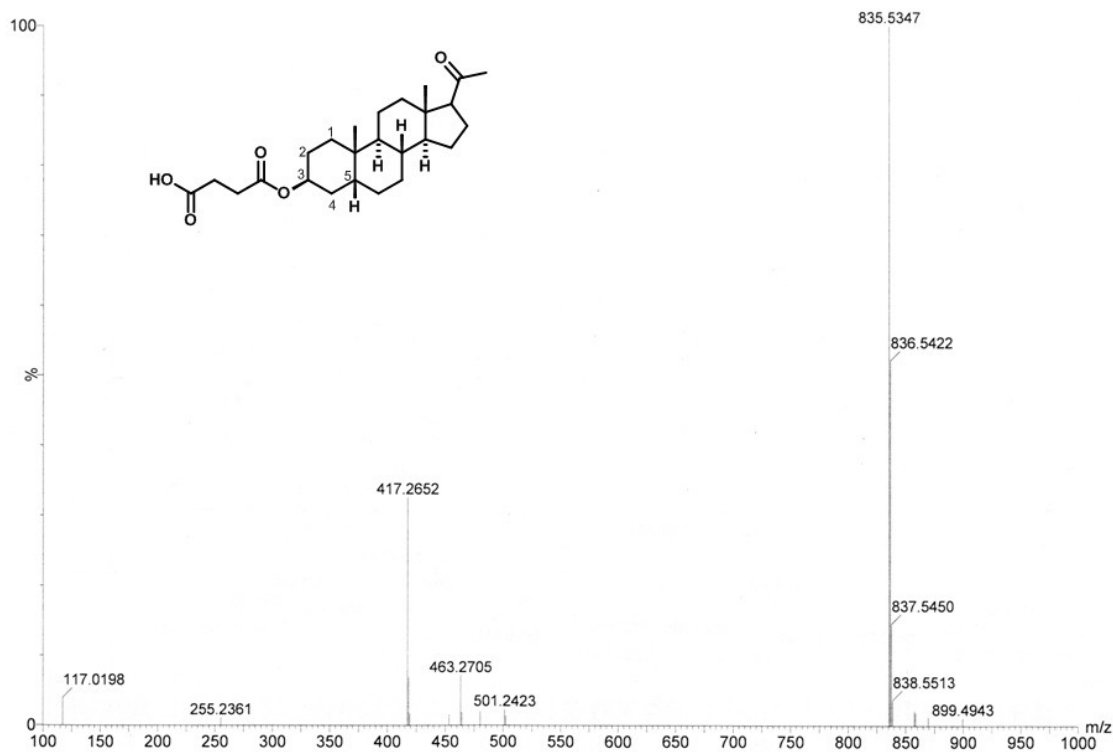
ESI MS of Allopregnanolone Isomer Succinate
(*m/z*): calc. for $C_{21}H_{37}O_5$ [M-H]$^+$ 417.2641, found 417.2652

Proton NMR of Allopregnanolone Succinate
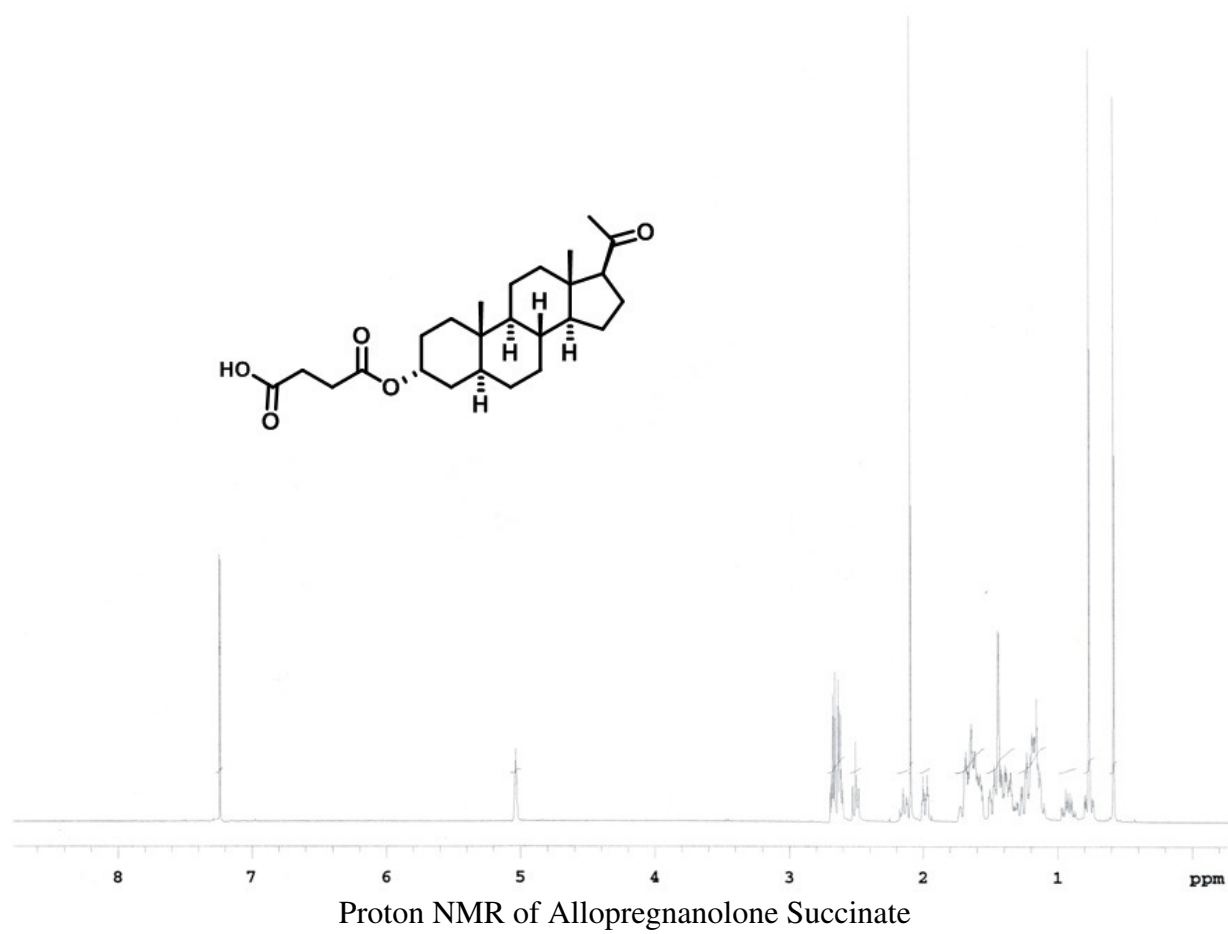
REFERENCES

1. Tomalia, D.A., Reyna, L.A., Svenson, S., 2007. Dendrimers as multi-purpose nanodevices for oncology drug delivery and diagnostic imaging. *Biochem. Soc. T. 35*, 61-67.

2. Svenson, S., Tomalia, D. A., 2005. Dendrimers in biomedical applications & reflections on the field. *Adv. Drug Deliv. Rev. 57*, 2106-2129.

3. Kobayashi, H., Kawamoto, S., Choyke, P. L., Sato, N., Knopp, M. V., Star, R. A., Waldmann, T. A., Tagaya, Y., Brechbiel, M. W., 2003. Comparison of dendrimer-based macromolecular contrast agents for dynamic micro-magnetic resonance lymphangiography. *Magn. Reson. Med. 50*, 758-766.

4. Talanov, V.S., Regino, C.A.S., Kobayashi. H., Bernardo, M., Choyke, P.L., Brechbiel, M.W., 2006. Dendrimer-based nanoprobe for dual modality magnetic resonance and fluorescence imaging. *Nano Lett. 6*, 1459-1463.

5. Gurdag, S., Khandare, J., Stapels, S., Matherly, L. H., and Kannan, R. M., 2006. Activity of dendrimer-methotrexate conjugates on methotrexate-sensitive and -resistant cell lines. *Bioconjugate Chem. 17*, 275-283.

6. Khandare, J., Kolhe, P., Pillai, O., Kannan, S., Lieh-Lai, M., Kannan, R. M., 2005. Synthesis, cellular transport, and activity of polyamidoamine dendrimer-methylprednisolone conjugates. *Bioconjugate Chem. 16*, 330-337.

7. Kolhe, P., Khandare, J., Pillai, O., Kannan, S., Lieh-Lal, M., and Kannan, R. M., 2006. Preparation, cellular transport, and activity of polyamidoamine-based dendritic nanodevices with a high drug payload. *Biomaterials 27*, 660-669.

8. Yoon, H. C., Hong, M.-Y., Kim, H.-S., 2000. Affinity biosensor for avidin using a double functionalized dendrimer monolayer on a gold electrode. *Anal. Biochem. 282*, 121-128.

9. Zhu, Y., Zhu, H., Yang, X., Xu, L., Li, C., 2007. Sensitive biosensors based on (dendrimer encapsulated Pt nanoparticles)/enzyme multilayers. *Electroanalysis 19*, 698-703.

10. Salazar, R. B., Shovsky, A., Schoenherr, H., Vancso, G. J., 2006. Dip-pen nanolithography on (bio)reactive monolayer and block-copolymer platforms: Deposition of lines of single macromolecules. *Small 2*, 1274-1282.

11. Degenhart, G. H., Dordi, B., Schönherr, H., Vancso, G. J., 2004. Micro and Nanofabrication of Robust Reactive Arrays Based on Covalent Coupling of Dendrimer to Activated Monolayers. *Langmuir 20*, 6216-6224.

12. Le Berre, V., Trévisiol, E., Dagkessamanskaia, A., Sokol, S., Caminade, A.-M., Majoral, J. P., Meunier, B., François, J. 2003. Dendrimeric coating of glass slides for sensitive DNA microarrays analysis. *Nucleic Acid Res. 31*, e88-e88.

13. Selvaraju, T., Das, J., Han, S. W., Yang, H. 2008. Ultrasensitive electrochemical immunosensing using magnetic beads and gold nanocatalysts. *Biosens. Bioelectron. 23*, 932-938.

14. Xu, L., Zhu, Y., Yang, X., Li, C. 2009. Amperometric biosensor based on carbon nanotubes coated with polyaniline/dendrimer-encapsulated Pt nanoparticles for glucose detection. *Materials Science and Engineering: C 29*, 1306-1310.

15. Yoon, H. C., Hong, M.-Y., Kim, H.-S., 2001. Reversible association/dissociation reaction of avidin on the dendrimer monolayer functionalized with a biotin analogue for a regenerable affinity-sensing surface. *Langmuir 17*, 1234-1239.

16. Ajikumar, P. K., Ng, J. K., Tang, Y. C., Lee, J. Y., Stephanopoulos, G., Too, H.-P., 2007. Carboxyl-Terminated Dendrimer-Coated Bioactive Interface for Protein Microarray: High-Sensitivity Detection of Antigen in Complex Biological Samples. *Langmuir 23*, 5670-5677.

17. Han, H. J., Kannan, R. M., Wang, S., Mao, G., Kusanovic, J. P., Romero, R., 2009. Multifunctional dendrimer-templated antibody presentation on biosensor surfaces for improved biomarker detection. *Adv. Funct. Mater, 20,* 171-185.

18. Gillies, E.R., and Fréchet, J.M.J., 2005. Dendrimers and dendritic polymers in drug delivery. *Drug. Discov. Today 10*, 35-43.

19. Alving, R. C., Steckt, A. E., Chapman, L. W., Waits, B. V.,Jr., Hendrickst, D. L., Swartz, M. G, Jr., Hansont, L. I., 1978. Therapy of leishmaniasis: Superior efficacies of liposomeencapsulated drugs. *Proc. Natl. Acad. Sci. U.S.A. 75*, 2959-2963.

20. Patri, K. A., Kukowska-Latallo, F. J., and Baker Jr., J. R. 2005. Targeted drug delivery with dendrimers: Comparison of the release kinetics of covalently conjugated drug and noncovalent drug inclusion complex. *Adv. Drug Delivery Rev. 57*, 2203-2214.

21. Kurtoglu, Y. E., Mishra, M., Kannan, S., Kannan, R. M. 2010. Drug release charecteristics of PAMAM dendrimer-drug conjugates with different linkers. *Int. J. Pharm. 384*, 189-194.

22. Menjoge, A. R., Kannan, R. M., Tomalia, D. A. (2010) Dendrimer-based drug and imaging conjugates: design considerations for nanomedical applications. *Drug. Discov. Today 15*, 171-185.

23. Najlah, M., Freeman, S., Attwood, D., D'Emanuele, A., 2007. In vitro evaluation of dendrimer prodrugs for oral drug delivery. *Int. J. Pharm. 336,* 183–190.

24. Najlah, M., Freeman, S., Attwood, D., D'Emanuele, A., 2006. Synthesis, characterization and stability of dendrimer prodrugs. *Int. J. Pharm. 308,*175–182.

25. Navath, R. S., Kurtoglu, Y. E., B. Wang, B., Kannan, S., Romero, R., Kannan, R.M., 2008. Dendrimer-Drug Conjugates for Tailored Intracellular Drug Release Based on Glutathione Levels. *Bioconjugate Chem. 19,* 2446–2455.

26. Malik, N., Wiwattanapatapee, R., Klopsch, R., Lorenz, K., Frey, H., Weener, J. W., Meijer, E. W., Paulus, W., Duncan, R., 2000. Dendrimers: Relationship between structure and biocompatibility in vitro, and preliminary studies on the biodistribution of ^{125}I-labelled polyamidoamine dendrimers in vivo. *J. Control. Release 65*, 133-148.

27. Lavignac, N., Lazenby, M., Franchini, J., Ferruti, P., Duncan, R., 2005. Synthesis and preliminary evaluation of poly(amidoamine)–melittin conjugates as endosomolytic polymers and/or potential anticancer therapeutics. *Int. J. Pharm. 300*, 102-112.

28. Nanjwade, B.K., Bechra, H. M., Derkar, G. K., Manvi, F.V., Nanjwade, V. K., 2009. Dendrimers: Emerging polymers for drug-delivery systems. *Eur. J. Pharm. Sci. 38*, 185-196.

29. Rolland, O., Turrin, C-O., Caminade, A-M., Majoral, J-P., 2009. Dendrimers and nanomedicine: multivalency in action. *New J. Chem., 33*, 1809–1824.

30. Buhleier, E., Wehner, F., Vögtle, F., 1978. 'Cascade'- and 'nonskid-chain-like' synthesis of molecular cavity topologies. *Synthesis 78*, 155–158.

31. Denkewalter, R.G., Kolc, J., Lukasavage, W.J., 1981. Macromolecular highly branched homogeneous compound based on lysine units. US Patent 4,289,872.

32. Newkome, G. R., Yao, Z., Baker, G. R., Gupta, V. K., 1985. Micelles. Part 1. Cascade molecules: a new approach to micelles. A [27]-arborol. *J.Org. Chem. 50*, 2003-2004.

33. Tomalia, D. A., Baker, H., Dewald, J., Hall, M., Kallos, G., Martin, S., Roeck, J., Ryder, J., Smith, P., 1985. A new class of polymers: starburst-dendritic macromolecules. *Polym. J. (Tokyo, Japan) 17*, 117-132.

34. Tomalia, D. A., 2005. Birth of a new macromolecular architecture: dendrimers as quantized building blocks for nanoscale synthetic polymer chemistry. *Prog. Polym. Sci. 30*, 294–324.

35. Hawker, C. J., Fréchet, J. M. J., 1990. Preparation of Polymers with Controlled Molecular Architecture. A New Convergent Approach to Dendritic Macromolecules. *J. Am. Chem. Soc. 112,* 7638-7647.

36. Esfand, R., Tomalia, D. A., 2001. Poly(amidoamine) (PAMAM) dendrimers: from biomimicry to drug delivery and biomedical applications. *Drug. Discov. Today 6*, 427-436.

37. Yang, H., Lopina, S.T., 2007. Stealth dendrimers for antiarrhythmic quinidine delivery. J. *Mater. Sci. Mater. Med. 18,* 2061–2065.

38. Kobayashi, H., Kawamoto, S., Saga, T., Sato, N., Hiraga, A., Ishimori, T., Konishi, J., Togashi, K., Brechbiel, M.W., 2001. Positive effects of polyethylene glycol conjugation

to generation-4 polyamidoamine dendrimers as macromolecular MR contrast agents. *Magn. Reson. Med. 46*, 781–788.

39. Wang, B., Navath, R. S., Menjoge, A. R., Balakrishnana, B., Bellair, R.,Dai, H., Romero, R., Kannana, S., Kannan, R. M., 2010. Inhibition of bacterial growth and intramniotic infection in a guinea pig model of chorioamnionitis using PAMAM dendrimers. *Int. J. Pharm. 395*, 298–308.

40. Jain, N. K., Gupta, U., 2008. Application of dendrimer-drug complexation in the enhancement of drug solubility and bioavailability. *Expert. Opin. Drug. Metabol. Toxicol. 4*, 1035–1052.

41. Chauhan, A. S., Sridevi, S., Chalasani, K. B., Jain, A. K., Jain, S. K., Jain, N. K., Diwan, P. V., 2003. Dendrimer-mediated transdermal delivery: enhanced bioavailability of indomethacin. *J. Control. Release 90*, 335-343.

42. Dai, H., Navath, R. S., Balakrishnan, B., Guru, B. R., Mishra, M. K., Romero, R., Kannan, R. M., Kannan, S., 2010. Intrinsic targeting of neuroinflammation by polyamidoamine dendrimers in a rabbit model of cerebral palsy. *Fut. Med. Nanomed. 5*, 1317-1329.

43. El-Sayed, M., Ginski, M., Rhodes, C. A., Ghandehari, H., 2003. Influence of surface chemistry of poly(amidoamine) dendrimers on Caco-2 cell monolayers. *J. Bioact. Compat. Pol. 18*, 7-22.

44. Wooley, P. H., Schwarz, E. M., 2004. Aseptic loosening. *Gene Ther.* 11, 402-407.

45. Schwarz, E. M., 2008. What potential biologic treatments are available for osteolysis? *J. Am. Acad. Orthop. Surg. 16*, Suppl.1, S72-75.

46. Pollice, P. F., Rosier, R. N., Looney, R. J., Puzas, J. E., Schwarz, E. M., O'Keefe, R.J., 2001. Oral pentoxifylline inhibits release of tumor necrosis factor-alpha from human peripheral blood monocytes: a potential treatment for aseptic loosening of total joint components. *J. Bone Joint Surg. Am. 83*, 1057-1061.

47. Childs, L. M., Goater, J. J., O'Keefe, R. J., Schwarz, E. M., 2001. Efficacy of etanercept for wear debris-induced osteolysis. *J. Bone Miner. Res. 16*, 338-347.

48. Yatsunami, J., Hayashi, S., 2001. Fourteen-membered ring macrolides as anti-angiogenic compounds. *Anticancer Res. 21*, 4253-4258.

49. Cervin, A., 2001. The anti-inflammatory effect of erythromycin and its derivatives, with special reference to nasal polyposis and chronic sinusitis. *Acta Otolaryngol. 121*, 83-92.

50. Giamarellos-Bourboulis, E. J., 2008. Macrolides beyond the conventional antimicrobials: a class of potent immunomodulators. *Int. J. Antimicrob. Agents 31*,12-20.

51. Dette, G. A., Knothe, H., Kellner, H. M., 1987. Whole body tissue distribution of [14C]-erythromycin in the guinea pig. An autoradiographic study. *Arzneimittelforschung 37*,524-527.

52. Cuffini, A. M., Tullio, V., Cimino, F., Carlone, N. A., 1989. Comparative effects of roxithromycin and erythromycin on cellular immune functions in vitro. 1. Uptake of 3H-macrolides by human macrophages. *Microbios. 57*,167-178.

53. Kudoh, S. 1998. Erythromycin treatment in diffuse panbronchiolitis. *Curr. Opin. Pulm. Med. 4*, 116-121.

54. Kudoh, S., Azuma, A., Yamamoto, M., Izumi, T., Ando, M., 1989. Improvement of survival in patients with diffuse panbronchiolitis treated with low-dose erythromycin. *Am. J. Respir. Crit. Care Med. 157*, 1829-1832.

55. Ren, W. P., Li, X.Y., Chen, B. D., Wooley, P. H., 2004. Erythromycin inhibits wear debris-induced osteoclastogenesis by modulation of murine macrophage NFkB activity. *J. Orthop. Res. 22*, 21-29.

56. Aoki, Y., Kao, P. N., 1999. Erythromycin inhibits transcriptional activation of NF-kappaB, but not NFAT, through calcineurin-independent signaling in T cells. *Antimicrob. Agents Chemother. 43*, 2678-2684.

57. Nakashima, Y., Sun, D. H., Trindade, M. C., Maloney, W. J., Goodman, S. B., Schurman, D. J., Smith, R. L., 1999. Signaling pathways for tumor necrosis factor-alpha and interleukin-6 expression in human macrophages exposed to titanium-alloy particulate debris in vitro. *J. Bone Joint Surg. Am. 81*, 603-615.

58. Shinkai, M., Henke, M. O., Rubin, B. K., 2008. Macrolide antibiotics as immunomodulatory medications: Proposed mechanisms of action. *Pharmacol. Ther. 117*.393-405.

59. Ren, W. P., Bin, W., Mayton, L., Wooley, P. H., 2006. Erythromycin (EM) inhibits wear debris-induced inflammatory osteolysis in a murine model. *J. Orthop. Res. 24*, 280-290.

60. Ren, W. P., Blasier, R., Peng, X., Shi, T., Wooley, P. H., Markel, D. C., 2009. Effect of oral erythromycin therapy in patients with aseptic loosening of joint prostheses. *Bone 44*, 671-677.

61. Markel, D. C., Zhang, R., Shi, T., Hawkins, M., Ren, W. P., 2009. Inhibitory effects of erythromycin on wear debris-induced VEGF/Flt-1 gene production and osteolysis. *Inflamm. Res. 58*, 413-421.

62. Ren, W. P., Markel, D. C., Zhang, R., Peng, X., Wu, B., Monica, H., Wooley, P. H., 2006. Association between UHMWPE particle-induced inflammatory osteoclastogenesis and expression of RANKL, VEGF, and Flt-1 in vivo. *Biomaterials 27*, 5161-5169.

63. Ogura, H., Nagai, S., Takeda, K. A., 1980. Novel reagent (*N*-succinimidyl diphenyl phosphate) for synthesis of active ester and peptide. *Tetrahedron Lett. 21*, 1467-1468.

64. Alvarez-Elcoro, S., Enzler, M. J., 1999. The macrolides: erythromycin, clarithromycin and azithromycin. *Mayo Clin. Proc. 74*, 613-634.

65. Jones, P. H., Baker, E. J., Rowley, E. K., Perun, T. J., 1972. Chemical modifications of erythromycin antibiotics. 3. Synthesis of 4" and 11 esters of erythromycin A and B. *J. Med. Chem. 15*, 631-634.

66. Lewis, C. A., Miller, S. J., 2006. Site-selective derivatization and remodeling of erythromycin A by using simple peptide-based chiral catalysts. *Angew. Chem. Int. Ed. 45*, 5616-5619.

67. Tomalia, D. A., Naylor, A. M., Goddard, W. A., 1990. Starburst dendrimers: molecularlevel control of size, shape, surface chemistry, topology, and flexibility from atoms to macroscopic matter. *Angew. Chem. Int. Edn. Engl. 29*, 138-175.

68. Gotsch, F., Kusanovic, J.P., Mazaki-Tovi, S., Pineles, B.L., Erez, O., Espinoza, J., Hassan, S. S., 2007. The fetal inflammatory response syndrome. *Clin. Obstet. Gynecol. 50*, 652-83.

69. Rüetschi, U., Rosén, Å., Karlsson, G., Zetterberg, H., Rymo, L., Hagberg, H., Jacobsson, B., 2005. Proteomic Analysis Using Protein Chips to Detect Biomarkers in Cervical and Amniotic Fluid in Women with Intra-Amniotic Inflammation. *J. Proteome. Res. 4*, 2236-2242.

70. Slattery, M.M., Morrison, J.J., 2002. Preterm delivery. *The Lancet 360*, 1489-1497.

71. Romero, R., Espinoza, J., Gonçalves, L.F., Kusanovic, J.P., Friel, L.A., Nien, J.K., 2006. Inflammation in preterm and term labour and delivery. *Seminar in Fetal and Neonatal Med. 11*, 317-26.

72. McIntire, D.D, Leveno, K.J., 2008. Neonatal Mortality and Morbidity Rates in Late Preterm Births Compared With Births at Term. *Obstet. Gynecol. 111*, 35-41.

73. Romero, R., Sirtori, M., Oyarzun, E., Avila, C., Mazor, M., Callahan, R., Sabo, V., Athanassiadis, A.P., Hobbins, J.C., 1989. Infection and labor. V: Prevalence, microbiology, and clinical significance of intraamniotic infection in women with preterm labor and intact membranes. *Am. J. Obstet. Gynecol. 161*, 817–824.

74. Harirah, H., Donia, S.E., Hsu, C.-D., 2002. Amniotic Fluid Matrix Metalloproteinase-9 and Interleukin-6 in Predicting Intra-Amniotic Infection. *Obstet. Gynecol*. 99, 80-84.

75. Romero, R., Mazor, M., 1988. Infection and preterm labor. *Clin. Obstet. Gynecol. 31*, 553-584.

76. Romero, R., Chaiworapongsa, T., Espinoza, J. J., 2003. Micronutrients and Intrauterine Infection, Preterm Birth and the Fetal Inflammatory Response Syndrome. *The J. Nutrition 133*, 1688S-1973S.

77. Edward, T., Gross, H., Weinberger, A., Cohen, H., 2006. TNF-alpha Modulation for Treatment of Alzheimer's Disease: A 6-Month Pilot Study. *MedGenMed. 8*, 25.

78. Clarke, D.J., Branton, R.L., 2002. A role for tumor necrosis factor alpha in death of dopaminergic neurons following neural transplantation. *Exp. Neurol. 176*, 154-162.

79. Titelbaum, D.S., Degenhardt, A., Kinkel, R.P., 2005. Anti-Tumor Necrosis Factor Alpha-Associated Multiple Sclerosis. *Am. J. Neuroradiol. 26*, 1548-1550.

80. Sakao, S., Tatsumi, K., Igari, H., Shino, Y., Shirasawa, H., Kuriyama, T., 2001. Association of Tumor Necrosis Factor α Gene Promoter Polymorphism with the Presence of Chronic Obstructive Pulmonary Disease. *Am. J. Respir. Crit. Care Med. 163*, 420-22.

81. Yoon, B., Jun, J., Romero, R., Park, K., Gomez, R., Choi, J., Kim, I., 1997. Amniotic fluid inflammatory cytokines (interleukin-6, interleukin-1β, and tumor necrosis factor-α), neonatal brain white matter lesions, and cerebral palsy. *Am. J. Obstet. Gynecol. 177.* 19-26.

82. Teppo, A.M., Maury, C.P., 1987. Radioimmunoassay of tumor necrosis factor in serum. *Clin. Chem. 33*, 2024-2027.

83. Jones, L.J., Singer, V.L., 2001. Fluorescence microplate-based assay for tumor necrosis factor activity using SYTOX Green stain. *Anal. Biochem. 293*, 8-15.

84. Berthier, F., Lambert, C., Genin, C., Bienvenu, J., 1999. Evaluation of an Automated Method for Cytokine Measurement Using the Immulite[®] Immunoassay System. *Clin. Chem. Lab. Med. 37*, 593–599.

85. Luo, L., Zhang, Z., Ma, L., 2005. Determination of recombinant human tumor necrosis factor-α in serum by chemiluminescence imaging. *Anal. Chim. Acta. 539*, 277-282.

86. Hurst, G.B., Buchanan, M.V., Foote, L.J., Kennel, S.J., 1999. Analysis for TNF-α using solid-phase affinity capture with radiolabel and MALDI-MS detection. *Anal. Chem. 71*, 4727-4733.

87. Saito, K., Kobayashi, D., Komatsu, M., Yajima, T., Yagihashi, A., Ishikawa, Y., Minami, R., Watanabe, N., 2000. A sensitive assay of tumor necrosis factor α in sera from Duchenne muscular dystrophy patients. *Clin. Chem. 46*, 1703-1704.

88. Saito, K., Kobayashi, D., Sasaki, M., Araake, H., Kida, T., Yagihashi, A., Yajima, T.,Kameshima, H., Watanabe, N., 1999. Detection of human serum tumor necrosis factor-α in healthy donors, using a highly sensitive immuno-PCR assay. *Clin. Chem. 45*, 665-669.

89. Hun, X., Zhang, Z., 2007. Fluoroimmunoassay for tumor necrosis factor-α in human serum using Ru(bpy)$_3$Cl$_2$-doped fluorescent silica nanoparticles as labels. *Talanta 73*, 366-371.

90. Wang, J., Liu, G., Engelhard, M.H., Lin, Y., 2006. Sensitive immunoassay of a biomarker tumor necrosis factor-α based on poly(guanine)-functionalized silica nanoparticle label. *Anal. Chem. 78*, 6974-6979.

91. Liu, Z., Amiridis, M.D., 2005. Quantitative FT-IRRAS Spectroscopic Studies of the Interaction of Avidin with Biotin on Functionalized Quartz Surfaces. *J. Phys. Chem. B 109*, 16866-16872.

92. Bosman, A.W., Janssen, H.M., Meijer, E.W., 1999. About Dendrimers: Structure, Physical Properties, and Applications. *Chem. Rev. 99*, 1665-1688.

93. Fréchet, J.M.J., Tomalia, D.A., 2001. *Dendrimers and Other Dendritic Polymers*; Wiley: Chichester.

94. Sayed-Sweet, Y., Hedstrand, D.M., Spinder, R. Tomalia, D.A., 1997. Hydrophobically modified poly(amidoamine) (PAMAM) dendrimers: their properties at the air–water interface and use as nanoscopic container molecules *J. Mater. Chem. 7*, 1199-1205.

95. Benters, R., Niemeyer, C.M., Drutschmann, D., Blohm, D., Wöhrle, D., 2002. DNA microarrays with PAMAM dendritic linker systems. *Nucleic Acid Research* 30, e10.

96. Benters, R., Niemeyer, C. M., Wöhrle, D., 2001. Dendrimer-Activated Solid Supports for Nucleic Acid and Protein Microarrays. *Chem. Biochem. 2*, 686-694.

97. Das, J., Aziz, M.A., Yang, H., 2006. A Nanocatalyst-Based Assay for Proteins: DNA-Free Ultrasensitive Electrochemical Detection Using Catalytic Reduction of *p*-Nitrophenol by Gold-Nanoparticle Labels. *J. Am. Chem. Soc. 128*, 16022-16023.

98. Bustos, E.B., Ma Jiménez, G.G., Díaz-Sánchez, B.R., Juaristi, E., Chapmam, T.W., Godínez, L.A., 2007. Glassy carbon electrodes modified with composites of starburst-PAMAM dendrimers containing metal nanoparticles for amperometric detection of dopamine in urine. *Talanta 72*, 1586-1592.

99. Mark, S.S., Sandhyarani, N., Zhu, C., Campagnolo, C., Batt, C.A., 2004. Dendrimer-Functionalized Self-Assembled Monolayers as a Surface Plasmon Resonance Sensor Surface. *Langmuir 20*, 6808-6817.

100. Crooks, R.M., Zhao, M., Sun, L., Chechik, V., Yeung, L.K., 2001. Dendrimer-Encapsulated Metal Nanoparticles: Synthesis, Characterization, and Applications to Catalysis. *Acc. Chem. Res. 34*,181-190.

101. Gröhn, F., Bauer, B.J., Akpalu, Y.A., Jackson, C.L., Amis, E.J., 2000. Dendrimer Templates for the Formation of Gold Nanoclusters. *Macromolecules 13*, 6042-6050.

102. Esumi, K., Akiyama, S., Yoshimura, T., 2003. Multilayer Formation Using Oppositely Charged Gold- and Silver-Dendrimer Nanocomposites. *Langmuir 19*, 7679-7681.

103. Rebeski, D. E., Winger, E. M., Shin, Y.-K., Lelenta, M., Robinson, M. M., Varecka, R., Crowther, J. R., 1999. Identification of unacceptable background caused by non-specific protein adsorption to the plastic surface of 96-well immunoassay plates using a standardized enzyme-linked immunosorbent assay procedure. *J. Immunol. Methods 226*, 85-92.

104. Bosnjakovic, A.; Mishra, M. K.; Ren, W.; Kurtoglu, Y. E.; Shi, T.; Fan, D.; Kannan, R. M., 2011. Poly(amidoamine) dendrimer-erythromycin conjugates for drug delivery to macrophages involved in periprosthetic inflammation. *Nanomed.-Nanotechnol.7*, 284-294.

105. Getz, E. B., Xiao, M., Chakrabarty, T., Cook, R., Selvin, P. R.,1999. A Comparison between the eulfhydryl reductants tris(2-carboxyethyl)phosphine and dithiothreitol for use in protein biochemistry. *Anal. Biochem.273,* 73-80.

106. Nagasaki, Y., Kobayashi, H., Katsuyama,Y., Jomura, T., Sakura, T., 2007. Enhanced immunoresponse of antibody/mixed-PEG co-immobilized surface construction of high-performance immunomagnetic ELISA system. *J. Colloid Interface Sci. 309,* 524-530.

107. Nie, T., Baldwin, A., Yamaguchi, N., Kiick, K., 2007. Production of heparin-functionalized hydrogels for the development of responsive and controlled growth factor delivery systems. *J. Controlled Release, 122,* 287-296.

108. Donadel, G., Calabro, A., Sigounas, G., Hascall, V. C., Notkins, A. L., Harindranath, N., 1994. Human polyreactive and monoreactive antibodies: effect of glycosylation antigen binding. *Glycobiology 4***,** 491-496.

109. Jung, Y., Kang, H. J., Lee, J. M., Jung, S. O., Yun, W. S., Chung, S. J., Chung, B. H., 2008. Controlled antibody immobilization onto immunoanalytical platforms by synthetic peptide. *Anal. Biochem. 374,* 99-105.

110. Jung, Y., Jeong, J. Y., Chung, B. H., 2008. Recent advances in immobilization methods of antibodies on solid supports. *Analyst 133*, 697–701.

111. Abraham, R., Moller, D., Gabel, D., Senter, P., Hellström, I., Hellström, K. E., 1991. The influence of periodate oxidation on monoclonal antibody avidity and immunoreactivity. *J. Immunol. Methods* 144, 77-86.

112. Jacobsen, N. W., Dickinson R. G., 1974. Spectrometric assay of aldehydes as 6-mercapto-3-substituted-s-trizolo(4,3-b)-tetrazines. *Anal. Chem. 46*, 298–299.

113. Roberts, J. C., Adams, Y. E., Tomalia, D., Mercer-Smith, J. A., Lavallee, D. K., 1990. Using starburst dendrimers as linker molecules to radiolabel antibodies. *Bioconjugate Chem. 1*, 305-308.

114. Samineni, S., Parvataneni, S., Kelly, C., Gangur, V., Karmaus, W., Brooks, K., 2006. Optimization, comparison, and application of colorimetric vs. chemiluminescence based

indirect sandwich ELISA for measurement of human IL-23. *J. Immunoass. Immunoch.27*, 183-193.

115. Langlois, J. A., Rutland-Brown, W., Thomas, K. E., 2006. Traumatic Brain Injury in the United States: Emergency Department Visits, Hospitalizations, and Deaths; Centers for Disease Control and Prevention, National Center for Injury Prevention and Control: Atlanta.

116. Arvin, B., Neville, L. F., Barone, F. C., Feuerstein, G. Z., 1996. The role of inflammation and cytokines in brain injury, *Neurosci. Biobehav. Rev. 20*, 445–452.

117. Holmin, S., Mathiesen, T., 1999. Long-term intracerebral inflammatory response after experimental focal brain injury in rat, *Neuro. Report 10*, 1889– 1891.

118. Pettus, E.H., Wright, D. W., Stein, D. G., Hoffman, S. W., 2005. Progesterone treatment inhibits the inflammatory agents that accompany traumatic brain injury. *Brain Res. 1049*, 112–119.

119. Cekic, M., Stein, D. G., 2010. Traumatic Brain Injury and Aging: Is a Combination of Progesterone and Vitamin D Hormone a Simple Solution to a Complex Problem? *Neurotherapeutics 7*, 81-90.

120. Gibson, C.L., Gray, L.J., Bath, P.M.W.,Murphy, S.P., 2008. Progesterone for the treatment of experimental brain injury; a systematic review. *Brain 131*, 318–328.

121. Roof, R. L., Duvdevani, R., Stein, D.G., 1993. Gender influences outcome of brain injury: progesterone plays a protective role. *Brain Res. 607*, 333–336.

122. Schumacher, M., Guennoun, R., Stein, D. G., De Nicola, A. F., 2007. Progesterone: therapeutic opportunities for neuroprotection and myelin repair. *Pharmacol. Ther. 116*, 77–106.

123. Pan, D. S.Liu, W. G., Yang, X. F., Cao, F., 2007. Inhibitory effect of on inflammatory factors after experimental traumatic brain injury. *Biomedical and Environmental Sciences 20*, 432-438.

124. Roof, R. L., Hoffman, S. W., Stein, D. G. 1997. Progesterone protects against lipid peroxidation following traumatic brain injury in rats, *Mol. Chem. Neuropathol. 31*, 1 – 11.

125. Djebaili, M., Guo, Q., Pettus, E. H., Hoffman, S. W., Stein D. G., 2005. The neurosteroids progesterone and allopregnanolone reduce cell death, gliosis, and functional deficits after traumatic brain injury in rats. J. Neurotrauma 22, 106 –118.

126. Mani, S. K., 2006. Signaling mechanisms in progesterone neurotransmitter interactions. *Neuroscience 138*, 773–781.

127. Ghoumari, A. M., Ibanez, C., el-Etr, M., Leclerc, P., Eychenne, B., O'Malley, B.W., 2003. Progesterone and its metabolites increase myelin basic protein expression in organotypic slice cultures of rat cerebellum. *J. Neurochem. 86*, 848–859.

128. Herzog, A. G., Frye, C. A., 2003. Seizure exacerbation associated with inhibition of progesterone metabolism. *Ann. Neurol. 53*, 390–391.

129. Singh, S., Hota, D., Prakash, A., Khanduja, K. L., Arora, S. K., Chakrabarti, A., 2010. Allopregnanolone, the active metabolite of progesterone protects against neuronal

damage in picrotoxin-induced seizure model in mice. *Pharmacol. Biochem. Be. 94*, 416–422.

130. Yawno, T., Hirst, J. J., Castillo-Melendez, M., Walker, D. W., 2009. Role of neurosteroids in regulating cell death and proliferation in the late gestation fetal brain. *Neuroscience 163*, 838–847.

131. Reddy, D.S., 2009. The role of neurosteroids in the pathophysiology and treatment of catamenial epilepsy. *Epilepsy Res. 85*, 1-30.

132. Majewska M. D., Harrison, N. L., Schwartz, R. D., Barker, J. L., Paul, S. M., 1986. Steroid hormone metabolites are barbiturate-like modulators of the GABA receptor. *Science 232*, 1004–1007.

133. Singh, M., 2006. Progesterone-induced neuroprotection. *Endocrine 29*, 271–274.

134. MacNevin, C. J., Atif, F., Sayeed, I., Stein, D. G., Liotta, D. C., 2009. Development and Screening of Water-Soluble Analogues of Progesterone and Allopregnanolone in Models of Brain Injury. *J. Med. Chem. 52*, 6012–6023.

135. Fortunato, J. M., Ganem, B., 1976. Lithium and potassium trialkylborohydrides. Reagents for direct reduction of α,β-unsaturated carbonyl compounds to synthetically versatile enolate anions. *J. Org. Chem. 41*, 2194–2200.

ABSTRACT

PAMAM DENDRIMER-BASED THERAPEUTIC AND DIAGNOSTIC NANODEVICES

by

ADMIRA BOSNJAKOVIC

December 2011

Advisor: Dr. Rangaramanujam M. Kannan

Major: Materials Science and Engineering

Degree: Doctor of Philosophy

Dendrimers are ideal materials to be used in the emerging field of nanomedicine. Their nanoscale size and high density of functional groups on their peripheries allow them to be used for various biomedical applications. This work exploits dendrimers as drug delivery vehicles and a versatile platform for capturing biomarkers with improved sensitivity and specificity. Hydroxyl terminated poly(amidoamine) dendrimer (PAMAM-OH) was modified with a linker having amine group at the end and conjugated to two drugs, erythromycin (EM) and allopregnanonolne, respectively and evaluated *in vitro*. Both drugs were provided with a linker having carboxylic group required for conjugation reaction with dendrimer. The release rate of the drugs from the conjugates in PBS buffers at pH 7.4 for EM and pH 2.1 for allopregnanolone were evaluated by reverse phase HPLC (RP-HPLC) analysis. EM released quite fast, about 90% of the drug was released within 10 hours and completed within 20 hours, while allopregnanolone released in slower manner, about 90% of the drug was released within 9 days. Dendrimer-EM conjugate was not cytotoxic and was significantly efficacious in inhibiting the nitrite production compared to free drug. The inhibition of bacterial growth by dendrimer-EM conjugate was comparable to free

EM. Combined with the intinsinic properties of dendrimers, these nanodevices could lead to improved *in vivo* efficacy. PAMAM-OH was successfully used for the development of a solid phase bio-sensing platform. The ELISA plate was modified first with polyethylene-glycol (PEG) and then PAMAM-OH was immobilized. A capture antibody was oxidized and covalently attached to dendrimer-modified ELISA plate which gives antibody favorable orientation for the antigen binding sites toward the analyte. The dendrimer modified plate showed enhanced sensitivity and the detection limit for TNF-α was found to be 0.48 pg/mL, which is significantly better than the commercially available ELISA kit. The selectivity of the dendrimer-modified ELISA plate was examined by studying TNF-α in a mixture of cytokines which gave similar results. Dendrimer-modified ELISA plate provides a greater opportunity for the detection of a wide range of cytokines and biomarkers.

AUTOBIOGRAPHICAL STATEMENT

ADMIRA BOSNJAKOVIC

BIRTH: November 27, 1968, Gradacac, Bosnia & Herzegovina

EDUCATION: Ph.D. in Materials Science and Engineering, expected December 2011, Wayne State University, Detroit, MI

               MA in Chemistry, May 2009, Wayne State University, Detroit, MI

               MS in Chemistry, May 2004, University of Detroit Mercy, Detroit, MI

               BS in Chemical Technology, November 1996, University of Tuzla, Tuzla, Bosnia & Herzegovina

AWARDS:

Thomas C. Rumble University Graduate Fellowship for 2009-2010, Wayne State University, Detroit, MI.

Certificate for exceptional service as Graduate Teaching Assistant in 2006, Wayne State University, Detroit, MI.

SELECTED PUBLICATIONS:

1. **Bosnjakovic, A.**, Mishra, M. K., Kannan, R.M., 2011. PAMA dendrimer-allopregnanolone conjugates as a potential therapeutic nanodevices for traumatic brain injury treatment (manuscript in preparation).

2. **Bosnjakovic, A.**, Mishra, M. K., Han, H. J., Romero, R., Kannan, R.M., 2011. A dendrimer-based immunosensor for improved capture and detection of tumor necrosis factor-α cytokine. *Analytica Chimica Acta* (submitted).

3. **Bosnjakovic, A.**, Mishra, M. K., Ren, W., Kurtoglu, Y. E., Shi, T., Fan, D., Kannan, R. M., 2011. Poly(amidoamine) dendrimer-erythromycin conjugates for drug delivery to macrophages involved in periprosthetic inflammation. *Nanomed.-Nanotechnol.7*, 284-294.

4. Danilczuk, M.; **Bosnjakovic, A.**; Kadirov, M. K**;** Schlick, S. "Direct ESR and spin trapping methods for the detection and identification of radical fragments in Nafion membranes and model compounds exposed to oxygen radicals" *Journal of Power Sources* **2007**, *172*, 78-82.

5. **Bosnjakovic, A.;** Schlick, S. "Spin Trapping by 5,5-Dimethylpyrroline-N-oxide in Fenton Media in the Presence of Nafion Perfluorinated Membranes: Limitations and Potential" *J. Phys. Chem. B.* **2006**, *110*, 10720-10728.

6. Kadirov, M. K.; **Bosnjakovic, A.**; Schlick, S. "Membrane-Derived Fluorinated Radicals Detected by Electron Spin Resonance in UV-Irradiated Nafion and Dow Ionomers: Effect of Counterions and H_2O_2" *J. Phys. Chem. B.* **2005**, *109*, 7664-7670.

7. **Bosnjakovic, A.**; Schlick, S. "Nafion Perfluorinated Membranes Treated in Fenton Media: Radical Species Detected by ESR Spectroscopy" *J. Phys. Chem. B* **2004**, 108, 4332-4337.